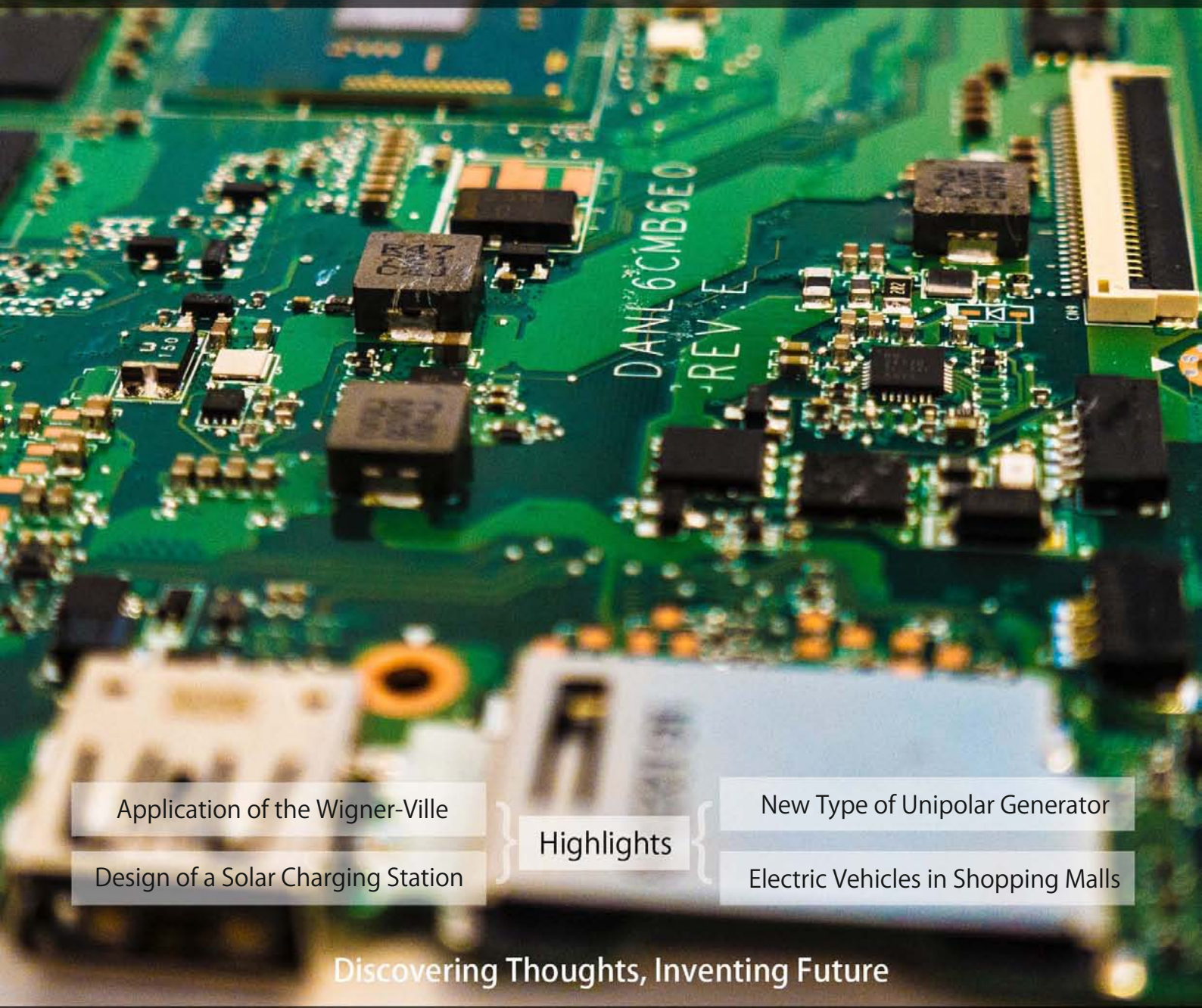# GLOBAL JOURNAL
OF RESEARCHES IN ENGINEERING: F

Electrical and Electronic Engineering

Application of the Wigner-Ville

Design of a Solar Charging Station

Highlights

New Type of Unipolar Generator

Electric Vehicles in Shopping Malls

Discovering Thoughts, Inventing Future

GLOBAL JOURNAL OF RESEARCHES IN ENGINEERING: F
ELECTRICAL AND ELECTRONICS ENGINEERING

Global Journals Inc.

Publisher's Headquarters office

Global Journals® Headquarters
945th Concord Streets,
Framingham Massachusetts Pin: 01701,
United States of America
USA Toll Free: +001-888-839-7392
USA Toll Free Fax: +001-888-839-7392

Offset Typesetting

Global Journals Incorporated
2nd, Lansdowne, Lansdowne Rd., Croydon-Surrey,
Pin: CR9 2ER, United Kingdom

Packaging & Continental Dispatching

Global Journals Pvt Ltd
E-3130 Sudama Nagar, Near Gopur Square,
Indore, M.P., Pin:452009, India

Find a correspondence nodal officer near you

To find nodal officer of your country, please
email us at *local@globaljournals.org*

eContacts

Press Inquiries: *press@globaljournals.org*
Investor Inquiries: *investors@globaljournals.org*
Technical Support: *technology@globaljournals.org*
Media & Releases: *media@globaljournals.org*

Pricing (Excluding Air Parcel Charges):

Yearly Subscription (Personal & Institutional)
250 USD (B/W) & 350 USD (Color)

Dr. Sofoklis S. Makridis

B.Sc(Hons), M.Eng, Ph.D. Professor Department of Mechanical Engineering University of Western Macedonia, Greece

Dr. Steffen Lehmann

Faculty of Creative and Cultural Industries Ph.D., AA Dip University of Portsmouth United Kingdom

Dr. Wenfang Xie

Ph.D., Department of Electrical Engineering, Hong Kong Polytechnic University, Department of Automatic Control, Beijing University of Aeronautics and Astronautics China

Dr. Hai-Wen Li

Ph.D., Materials Engineering, Kyushu University, Fukuoka, Guest Professor at Aarhus University, Japan

Dr. Saeed Chehreh Chelgani

Ph.D. in Mineral Processing University of Western Ontario, Adjunct professor, Mining engineering and Mineral processing, University of Michigan United States

Belen Riveiro

Ph.D., School of Industrial Engineering, University of Vigo Spain

Dr. Adel Al Jumaily

Ph.D. Electrical Engineering (AI), Faculty of Engineering and IT, University of Technology, Sydney

Dr. Maciej Gucma

Assistant Professor, Maritime Univeristy of Szczecin Szczecin, Ph.D.. Eng. Master Mariner, Poland

Dr. M. Meguellati

Department of Electronics, University of Batna, Batna 05000, Algeria

Dr. Haijian Shi

Ph.D. Civil Engineering Structural Engineering Oakland, CA, United States

Dr. Chao Wang

Ph.D. in Computational Mechanics Rosharon, TX, United States

Dr. Joaquim Carneiro

Ph.D. in Mechanical Engineering, Faculty of Engineering, University of Porto (FEUP), University of Minho, Department of Physics Portugal

Dr. Wei-Hsin Chen

Ph.D., National Cheng Kung University, Department of Aeronautics, and Astronautics, Taiwan

Dr. Bin Chen

B.Sc., M.Sc., Ph.D., Xian Jiaotong University, China. State Key Laboratory of Multiphase Flow in Power Engineering Xi?an Jiaotong University, China

Dr. Charles-Darwin Annan

Ph.D., Professor Civil and Water Engineering University Laval, Canada

Dr. Jalal Kafashan

Mechanical Engineering Division of Mechatronics KU Leuven, Belglum

Dr. Alex W. Dawotola

Hydraulic Engineering Section, Delft University of Technology, Stevinweg, Delft, Netherlands

Dr. Shun-Chung Lee

Department of Resources Engineering, National Cheng Kung University, Taiwan

Dr. Gordana Colovic

B.Sc Textile Technology, M.Sc. Technical Science Ph.D. in Industrial Management. The College of Textile? Design, Technology and Management, Belgrade, Serbia

Dr. Philip T Moore

Ph.D., Graduate Master Supervisor School of Information Science and engineering Lanzhou University China

Dr. Giacomo Risitano

Ph.D., Industrial Engineering at University of Perugia (Italy) "Automotive Design" at Engineering Department of Messina University (Messina) Italy

Dr. Cesar M. A. Vasques

Ph.D., Mechanical Engineering, Department of Mechanical Engineering, School of Engineering, Polytechnic of Porto Porto, Portugal

Dr. Maurizio Palesi

Ph.D. in Computer Engineering, University of Catania, Faculty of Engineering and Architecture Italy

Dr. Jun Wang

Ph.D. in Architecture, University of Hong Kong, China Urban Studies City University of Hong Kong, China

Dr. Salvatore Brischetto

Ph.D. in Aerospace Engineering, Polytechnic University of Turin and in Mechanics, Paris West University Nanterre La D?fense Department of Mechanical and Aerospace Engineering, Polytechnic University of Turin, Italy

Dr. Stefano Invernizzi

Ph.D. in Structural Engineering Technical University of Turin, Department of Structural, Geotechnical and Building Engineering, Italy

Dr. Wesam S. Alaloul

B.Sc., M.Sc., Ph.D. in Civil and Environmental Engineering, University Technology Petronas, Malaysia

Dr. Togay Ozbakkaloglu

B.Sc. in Civil Engineering, Ph.D. in Structural Engineering, University of Ottawa, Canada Senior Lecturer University of Adelaide, Australia

Dr. Ananda Kumar Palaniappan

B.Sc., MBA, MED, Ph.D. in Civil and Environmental Engineering, Ph.D. University of Malaya, Malaysia, University of Malaya, Malaysia

Dr. Zhen Yuan

B.E., Ph.D. in Mechanical Engineering University of Sciences and Technology of China, China Professor, Faculty of Health Sciences, University of Macau, China

Dr. Hugo Silva

Associate Professor, University of Minho, Department of Civil Engineering, Ph.D., Civil Engineering, University of Minho Portugal

Dr. Jui-Sheng Chou

Ph.D. University of Texas at Austin, U.S.A. Department of Civil and Construction Engineering National Taiwan University of Science and Technology (Taiwan Tech)

Dr. Fausto Gallucci

Associate Professor, Chemical Process Intensification (SPI), Faculty of Chemical Engineering and Chemistry Assistant Editor, International J. Hydrogen Energy, Netherlands

Dr. Houfa Shen

Ph.D. Manufacturing Engineering, Mechanical Engineering, Structural Engineering, Department of Mechanical Engineering, Tsinghua University, China

Prof. (LU), (UoS) Dr. Miklas Scholz

Cand Ing, BEng (equiv), PgC, MSc, Ph.D., CWEM, CEnv, CSci, CEng, FHEA, FIEMA, FCIWEM, FICE, Fellow of IWA, VINNOVA Fellow, Marie Curie Senior, Fellow, Chair in Civil Engineering (UoS) Wetland Systems, Sustainable Drainage, and Water Quality

Dr. Yudong Zhang

B.S., M.S., Ph.D. Signal and Information Processing, Southeast University Professor School of Information Science and Technology at Nanjing Normal University, China

Dr. Minghua He

Department of Civil Engineering Tsinghua University Beijing, 100084, China

Dr. Philip G. Moscoso

Technology and Operations Management IESE Business School, University of Navarra Ph.D. in Industrial Engineering and Management, ETH Zurich M.Sc. in Chemical Engineering, ETH Zurich, Spain

Dr. Stefano Mariani

Associate Professor, Structural Mechanics, Department of Civil and Environmental Engineering, Ph.D., in Structural Engineering Polytechnic University of Milan Italy

Dr. Ciprian Lapusan

Ph. D in Mechanical Engineering Technical University of Cluj-Napoca Cluj-Napoca (Romania)

Dr. Francesco Tornabene

Ph.D. in Structural Mechanics, University of Bologna Professor Department of Civil, Chemical, Environmental and Materials Engineering University of Bologna, Italy

Dr. Kitipong Jaojaruek

B. Eng, M. Eng, D. Eng (Energy Technology, Asian Institute of Technology). Kasetsart University Kamphaeng Saen (KPS) Campus Energy Research Laboratory of Mechanical Engineering

Dr. Burcin Becerik-Gerber

University of Southern Californi Ph.D. in Civil Engineering Ddes, from Harvard University M.S. from University of California, Berkeley M.S. from Istanbul, Technical University

Hiroshi Sekimoto

Professor Emeritus Tokyo Institute of Technology Japan Ph.D., University of California Berkeley

Dr. Shaoping Xiao

BS, MS Ph.D. Mechanical Engineering, Northwestern University The University of Iowa, Department of Mechanical and Industrial Engineering Center for Computer-Aided Design

Dr. A. Stegou-Sagia

Ph.D., Mechanical Engineering, Environmental Engineering School of Mechanical Engineering, National Technical University of Athens, Greece

Diego Gonzalez-Aguilera

Ph.D. Dep. Cartographic and Land Engineering, University of Salamanca, Avilla, Spain

Dr. Maria Daniela

Ph.D in Aerospace Science and Technologies Second University of Naples, Research Fellow University of Naples Federico II, Italy

Dr. Omid Gohardani

Ph.D. Senior Aerospace/Mechanical/ Aeronautical, Engineering professional M.Sc. Mechanical Engineering, M.Sc. Aeronautical Engineering B.Sc. Vehicle Engineering Orange County, California, US

Dr. Paolo Veronesi

Ph.D., Materials Engineering, Institute of Electronics, Italy President of the master Degree in Materials Engineering Dept. of Engineering, Italy

CONTENTS OF THE ISSUE

Implementation of an Associative Memory using a Restricted Hopfield Network

By Tet Yeap

University of Ottawa

Abstract- A trainable analog restricted Hopfield Network is presented in this paper. It consists of two layers of nodes, visible and hidden nodes, connected by weighted directional paths forming a bipartite graph with no intralayer connection. An energy or Lyapunov function was derived to show that the proposed network will converge to stable states. The proposed network can be trained using either the modified SPSA or BPTT algorithms to ensure that all the weights are symmetric. Simulation results show that the presence of hidden nodes increases the network's memory capacity. Using EXOR as an example, the network can be trained to be a dynamic classifier. Using A, U, T, S as training characters, the network was trained to be an associative memory. Simulation results show that the network can perform perfect re-creation of noisy images. Its recreation performance has higher noise tolerance than the standard Hopfield Network and the Restricted Boltzmann Machine. Simulation results also illustrate the importance of feedback iteration in implementing associative memory to re-create from noisy images.

Keywords: hopfield network, restricted boltzmann machine, energy function, lyapunov function, restricted hopfield network, trainable networks, hidden nodes, basin of attraction, attractors.

IMPLEMENTATIONOFANASSOCIATIVEMEMORYUSINGARESTRICTEDHOPFIELDNETWORK

Strictly as per the compliance and regulations of:

Implementation of an Associative Memory using a Restricted Hopfield Network

Tet Yeap

Abstract- A trainable analog restricted Hopfield Network is presented in this paper. It consists of two layers of nodes, visible and hidden nodes, connected by weighted directional paths forming a bipartite graph with no intralayer connection. An energy or Lyapunov function was derived to show that the proposed network will converge to stable states. The proposed network can be trained using either the modified SPSA or BPTT algorithms to ensure that all the weights are symmetric. Simulation results show that the presence of hidden nodes increases the network's memory capacity. Using EXOR as an example, the network can be trained to be a dynamic classifier. Using A, U, T, S as training characters, the network was trained to be an associative memory. Simulation results show that the network can perform perfect re-creation of noisy images. Its recreation performance has higher noise tolerance than the standard Hopfield Network and the Restricted Boltzmann Machine. Simulation results also illustrate the importance of feedback iteration in implementing associative memory to re-create from noisy images.

Keywords: hopfield network, restricted boltzmann machine, energy function, lyapunov function, restricted hopfield network, trainable networks, hidden nodes, basin of attraction, attractors.

I. Introduction

In 1982, based on his studies of collective dynamical computation in neural networks, Hopfield [1, 2, 3] proposed an influential recurrent neural network with many potential applications such as content addressable memory and optimization engine for the traveling-salesman problem. He formulated an Energy function for the network using the Lyapunov Direct Method showing that the network converges to a stable state if it has symmetric weights. Each network node does not have self-feedback.

Hopfield network comes in two forms: analog or discrete. However, in either format, the network can only be programmed to memorize patterns using the Hebbian Rule and has a limited memory capacity to store 0.15N patterns where N is the network's number of nodes. Many have tried to improve the network's memory capacity problem and trainability issue [4, 5]. For example, instead of trying to memorize the patterns in one presentation cycle, Gardner [6, 7, 8] improved the network by presenting the training patterns repeatedly and using the perceptron convergence procedure to train each node to generate the correct state given the

states of all the other nodes for a particular training vector.

A Boltzmann machine is a stochastic recurrent neural network with interconnected visible and hidden nodes introduced by Hinton [9, 10]. Like a Hopfield network, a Boltzmann has a similar energy function when the weights are symmetric and converges to a stable state when an input vector is presented to the visible nodes. A Boltzmann machine takes a long time to train. As a result, a restricted Boltzmann machine (RBM) was introduced [11, 12, 13]. It consists of two layers of nodes, L visible and M hidden nodes, connected by symmetric weights with no intralayer connection. Each node makes probabilistic decisions to be either on or off. The connection restriction allows for more efficient training algorithms, notably the gradient-based contrastive divergence algorithm, to be developed. The network is capable of learning the probabilistic pattern of a set of inputs.

An analog restricted Hopfield network (RHN) is proposed in this paper to solve the memory capacity and the trainability issue of the Hopfield network. Like an RBM, the architecture consists of two layers of nodes, visible and hidden nodes, connected by directional weighted connection paths. The network is a fully-connected bipartite graph and has no intralayer connection. The visible nodes are classified into either input or output nodes to manage the flow of information to/from the visible nodes. An energy or Lyapunov function was derived to prove that the proposed network always converges to stable states when an input vector is presented. The proposed network iterates, sending signals back and forth between the two layers until all its nodes reach an equilibrium state based on the corresponding basin of attraction, generating the desired output vector.

Two training algorithms were used to train the proposed network: Simultaneous Perturbation Stochastic Approximation (SPSA) [14, 15] and Back propagation Through Time (BPTT) [16, 17]. The SPSA algorithm was introduced by Spall and is simple to implement. It can estimate the gradient of the error function using only two final error values of the function. Therefore, the merit of this training rule was demonstrated to train the proposed network. The BPTT algorithm, on the other hand, is based on the fact that the temporal operation of an RHN may be unfolded into

Author: School of Electrical Engineering and Computer Science University of Ottawa. e-mail: tyeap@uottawa.ca

a multilayer perceptron so that a standard back propagation algorithm could be applied.

Simulation results show that the proposed network can be trained to implement a dynamic classifier implementing an EXOR function. Using A, U, T, S as training characters, the network was trained to be an associative memory. Simulation results show that the network performs perfect re-creation of these images even when the input image is noisy. The results also show that the proposed network performs better than the standard Hopfield Network and RBM.

The paper is organized as follows. Section 2 presents the background work on Hopfield Network and Restricted Boltzmann Machine. An RHN with hidden nodes function is presented in section 3. In section 4, two algorithms to train the network are introduced. Section 5 presents some simulation results on the performance of the RHN.

II.   Background

a) Hopfield Network

An analog Hopfield network consists of fully interconnected nodes modeled as amplifiers, in conjunction with feedback circuits comprises of wires, resistors, and capacitors, as shown in Figure 1.
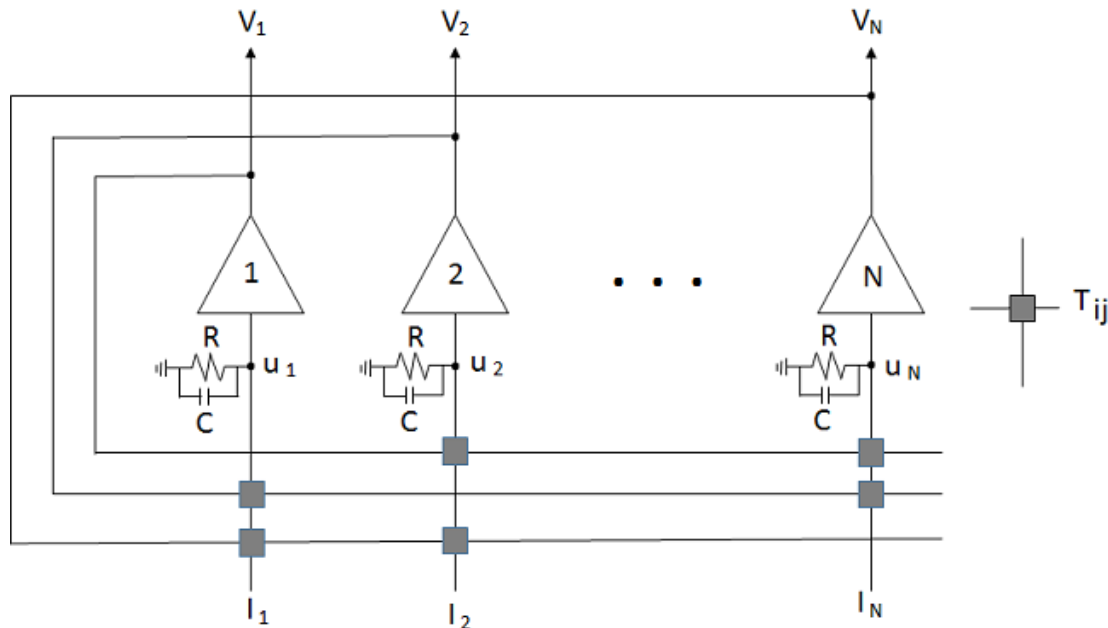
Figure 1: An analog Hopfield network

The dynamics of the network can be described by the following differential equations:

$$\frac{du_i}{dt} = \sum_{j=1}^{N} T_{ij} v_j - \frac{u_i}{\tau} + I_i \qquad (1)$$

$$\tau = RC$$

$$V_i = g(u_i)$$

Where N is the number of nodes in the network, u_i is the input voltage of the amplifier, T_{ij} is the weight or conductance connecting the output of node j to the input of node i, V_j is the output of node j, RC is the time constant of the network, I_i is the input to node i, and $g()$ is the output function of a node.

The following energy function for the network was derived by Hopfield using the Lyapunov Direct Method if the network has symmetric weights and each network node does not have self-feedback. For the initial-value problem, I_i input is applied to node i at $t = 0$ and then allow the network to evolve. The integration of the above differential equations provides the network states' evolution. With the energy function's existence, the network will always converge to a stable state.

$$E = -\frac{1}{2} \sum_{i=1}^{N} \sum_{j=1}^{N} T_{ij} V_i V_j - \sum_{i=1}^{N} V_i \frac{u_i}{\tau} - \sum_{i=1}^{N} V_i I_i \ (2)$$

Hopfield networks can only be programmed to memorize patterns using the Hebbian Rule. When the output function $g()$ is a sigmoid function, the network transforms the initial input vector it- eratively and continuously into the output vector in the range [0, 1]. To program the network to memorize specific binary input vectors ($S(p)$, $p = 1 \ldots P$), the weight or conductance T_{ij} is deter- mined by the following formula:

$$T_{ij} = \sum_{p=1}^{P} (2S_i(p) - 1)(2S_j(p) - 1) \qquad (3)$$

When the output function $g()$ is a hyperbolic tangent function, the network transforms the initial input vector

iteratively and continuously into the output vector in the range [1, 1]. To program the network to memorize specific binary input vectors ($S(p)$, $p = 1 \ldots P$), the weight or conductance T_{ij} is determined by the following formula:

$$T_{ij} = \sum_{p=1}^{P} S_i(p)S_j(p) \qquad (4)$$

b) Restricted Boltzmann Machine (RBM)

A restricted Boltzmann machine (RBM) is a stochastic recurrent neural network [4, 9, 10] consisting of two layers of nodes, L visible and M hidden nodes, connected by symmetric weights with no intralayer connection. Each node makes probabilistic decisions to be either on or off. The network is capable of learning the probabilistic pattern of a set of inputs.

The following differential equations can describe the dynamics of the network:
In the forward path:

$$sum_i^H = \sum_{j=1}^{L} w_{ij}^H V_j^V + \theta_i^H \qquad (5)$$

$$V_i^H = g(sum_i^H)$$

Where sum_i^H is the sum of all inputs to the hidden node i, w_{ij}^H is the weight connecting the output of visible node j to the input of hidden node i, V_j^v is the output of visible node j, θ_i^H is the threshold of hidden node i, V_i^H is the output of hidden node i, $g()$ is the Sigmoid logistic output function of hidden node i.
In the backward path:

$$sum_j^V = \sum_{i=1}^{M} w_{ji}^V V_i^H + \theta_j^V \qquad (6)$$

$$V_j^V = g(sum_j^V)$$

Where sum_j^v is the sum of all inputs to the visible node i, $w_j i^v$ the weight connecting the output of hidden node i to the input of visible node j, V_i^H is the output of hidden node i, θ_j^V is the threshold of visible node j, V_j^V is the output of visible node j, $g()$ is the Sigmoid logistic output function of hidden node j.

For symmetric weights configuration, the energy or Lyapunov function of an RBM is given by:

$$E = -\sum_{i=1}^{M}\sum_{j=1}^{L} w_{ij}^H V_i^H V_j^V - \sum_{j=1}^{L} \theta_j^V V_j^V - \sum_{i=1}^{M} \theta_i^H V_i^H \qquad (7)$$

With the existence of energy function, the network will always converge to a stable state when an input vector is presented to the visible nodes.

During the training of the network, an input vector p is presented. Let e_{ij}^+ (p) $=V_i^H V_j^v$ denotes the correlation of hidden node i and visible node j in the forward direction, and e_{ij}^- (p) $= V_i^H X_j^V$ denotes the correlation in the backward direction, where X_j^V is the value of visible unit j of pattern p that is estimated by the network. The weight is updated during a training process by:

$$w_{ij}(k+1) = w_{ij}(k) + \beta(e_{ij}^+(p) - e_{ij}^-(p)) \qquad (8)$$

Where β is a small positive number.

III. PROPOSED RESTRICTED HOPFIELD NETWORK(RHN)

An analog restricted Hopfield network (RHN) is proposed to solve the memory capacity and train- ability issues of the Hopfield network. Like an RBM, the architecture consists of two layers of nodes, L visible and M hidden nodes, connected by directional weighted connection paths, as shown in Figure 2. The network is a connected bipartite graph and has no intralayer connection.

Figure 2: A Restricted Hopfield Network

The following differential equations describe the dynamics of the network: In the forward path:

$$\frac{du_i^H}{dt} = \sum_{j=1}^{L} w_{ij}^H V_j^V + \theta_i^H \qquad (9)$$

$$V_i^H = g(u_i)$$

Initial conditions:

$$V_j^V(0) = I_j$$
$$V_i^H(0) = 0$$

Where u_i^H is the sum of all inputs to the hidden nodes, W_{ij}^H is the weight connecting the output of visible node j to the input of hidden node i, V_j^V is the output of visible node j, θ_i^H is the threshold of hidden node i, V_i^H is the output of hidden node i, $g()$ is the output function of hidden node l, and I_j is the initial input presented to the visible node j.

In the backward path:

$$\frac{du_j^V}{dt} = \sum_{i=1}^{M} w_{ji}^V V_i^H + \theta_j^V \qquad (10)$$

$$V_j^V = g(u_j^V)$$

Where u_j^V is the sum of all inputs to the visible nodes, w_{ji}^V is the weight connecting the output of hidden node i to the input of visible node j, V_i^H is the output of hidden node i, θ_j^V is the threshold of output node j, V_j^V is the output of visible node j, and $g()$ is the output function of visible node j.

The network input can be either digital or analog, taking a value between 0 and 1. Using a Sigmoid function as output function $g()$ for all the nodes, the output of all the nodes takes the value between 0 and 1. The proposed network will also work when the hyperbolic tangent function is used as the output function. In such a case, the output of all the nodes takes the value between 1 and 1. The proposed RHN always generates analog outputs between 0 and 1 using the Sigmoid output function or between−1 and 1 using the hyperbolic tangent output function.

Based on the Lyapunov Direct Method, it can be shown that Eqn. 11 is the energy or a Lyapunov function of the proposed network.

$$E = -\frac{1}{2}\sum_{i=1}^{M}\sum_{j=1}^{L} w_{ij}^H V_i^H V_j^H - \frac{1}{2}\sum_{j=1}^{L}\sum_{i=1}^{M} w_{ji}^V V_j^H V_i^V - \sum_{i=1}^{M} V_i^H \theta_i^H - \sum_{i=1}^{L} V_i^V \theta_i^V \qquad (11)$$

Differentiating *E*, we get:

$$\frac{dE}{dt} = -\frac{d}{dt}\left(\frac{1}{2}\sum_{i=1}^{M}\sum_{j=1}^{L} w_{ij}^H V_i^H V_j^H\right) - \frac{d}{dt}\left(\frac{1}{2}\sum_{j=1}^{L}\sum_{i=1}^{M} w_{ji}^V V_j^H V_i^V\right) - \frac{d}{dt}\left(\sum_{i=1}^{M} V_i^H \theta_i^H\right) - \frac{d}{dt}\left(\sum_{i=1}^{L} V_i^V \theta_i^V\right)$$
$$(12)$$

Expanding all the above terms in Eqn. 12, we get:

$$\frac{d}{dt}\left(\frac{1}{2}\sum_{i=1}^{M}\sum_{j=1}^{L} w_{ij}^H V_i^H V_j^H\right) = \frac{1}{2}\sum_{i=1}^{M}\sum_{j=1}^{L} w_{ij}^H \frac{dV_i^H}{dt} V_j^V + \frac{1}{2}\sum_{i=1}^{M}\sum_{j=1}^{L} w_{ij}^H V_i^H \frac{dV_j^V}{dt}$$

$$\frac{d}{dt}\left(\frac{1}{2}\sum_{j=1}^{M} L \sum_{i=1}^{M} w_{ji}^{V} V_{j}^{H} V_{i}^{V}\right) = \frac{1}{2}\sum_{j=1}^{L}\sum_{i=1}^{M} w_{ji}^{V} \frac{dV_{j}^{V}}{dt} V_{i}^{H} + \frac{1}{2}\sum_{j=1}^{L}\sum_{i=1}^{M} w_{ji}^{V} V_{j}^{V} \frac{dV_{i}^{H}}{dt} \qquad (13)$$

$$\frac{d}{dt}\left(\sum_{i=1}^{M} V_{i}^{H}\theta_{i}^{H}\right) = \sum_{i=1}^{M} \frac{dV_{i}^{H}}{dt}\theta_{i}^{H}$$

$$\frac{d}{dt}\left(\sum_{i=1}^{L} V_{i}^{V}\theta_{i}^{V}\right) = \sum_{i=1}^{L} \frac{dV_{i}^{V}}{dt}\theta_{i}^{V}$$

Now consider the forward path:

Because the outputs of visible nodes are constant in the forward path, then:

$$\frac{dV_{i}^{V}}{dt} = 0 \qquad (14)$$

Assume that all the weights are symmetric, then:

$$w_{ij}^{H} = w_{ji}^{V} \qquad (15)$$

Therefore, Equation 12 can be reduced to the following:

$$\frac{dE}{dt} = -\sum_{i=1}^{M}\sum_{j=1}^{L} w_{ij}^{H} \frac{dV_{i}^{H}}{dt} V_{j}^{V} - \sum_{i=1}^{M} \frac{dV_{i}^{H}}{dt}\theta_{i}^{H} \qquad (16)$$

and can be simplified to:

$$\frac{dE}{dt} = -\sum_{i=1}^{M} \frac{dV_{i}^{H}}{dt}\left(\sum_{j=1}^{L} w_{ij}^{H} V_{j}^{V} + \theta_{i}^{H}\right) \qquad (17)$$

Further simplified to:

$$\frac{dE}{dt} = -\sum_{i=1}^{M} \frac{dV_{i}^{H}}{dt}\frac{du_{i}^{H}}{dt} \qquad (18)$$

Using Chain Rule:

$$\frac{dE}{dt} = -\sum_{i=1}^{M} \frac{dV_{i}^{H}}{du_{i}^{H}}\frac{du_{i}^{H}}{dt}\frac{du_{i}^{H}}{dt}$$

$$\frac{dE}{dt} = -\sum_{i=1}^{M} \frac{dV_{i}^{H}}{du_{i}^{H}}\left(\frac{du_{i}^{H}}{dt}\right)^{2} \qquad (19)$$

Since:

$$V_{i}^{H} = g(u_{i}^{H}) \qquad (20)$$

If the output function is a Sigmoid or hyperbolic tangent function, then:

$$\frac{dV_{i}^{H}}{du_{i}^{H}} \; is \; always \; positive$$

Then:

$$\frac{dE}{dt} \; is \; always \; negative \; in \; the \; forward \; path$$

Now consider the backward path:

Because the outputs of hidden nodes are constant in the backward path, then:

$$\frac{dV_{i}^{H}}{dt} = 0 \qquad (21)$$

Assume that all the weights are symmetric, then:

$$w_{ij}^H = w_{ji}^V \tag{22}$$

Therefore, Equation 12 can be reduced to the following:

$$\frac{dE}{dt} = -\sum_{j=1}^{L}\sum_{i=1}^{M} w_{ji}^V \frac{dV_j^V}{dt} V_i^H - \sum_{j=1}^{L} \frac{dV_j^V}{dt}\theta_j^V \tag{23}$$

and can be simplified to:

$$\frac{dE}{dt} = -\sum_{j=1}^{L} \frac{dV_j^V}{dt}\left(\sum_{j=1}^{M} w_{ji}^V V_i^H + \theta_j^V\right) \tag{24}$$

Further simplified to:

$$\frac{dE}{dt} = -\sum_{i=1}^{L} \frac{dV_j^V}{dt}\frac{du_j^V}{dt} \tag{25}$$

Using Chain Rule:

$$\frac{dE}{dt} = -\sum_{j=1}^{L} \frac{dV_j^V}{du_j^V}\frac{du_j^V}{dt}\frac{du_j^V}{dt}$$

$$\frac{dE}{dt} = -\sum_{j=1}^{L} \frac{dV_j^V}{du_j^V}\left(\frac{du_j^V}{dt}\right)^2 \tag{26}$$

Since:

$$V_j^V = g(u_j^V) \tag{27}$$

If the output function is a Sigmoid or hyperbolic tangent function, then:

$$\frac{dV_j^V}{du_j^V} \text{ is always positive}$$

Then:

$$\frac{dE}{dt} \text{ is always negative in the backward path}$$

Therefore, combining the forward and backward path, the energy function E of Eqn.11 is a Lyapunov function if and only if all the weights are symmetric.

The proposed RHN is a dynamic system. Therefore, it has attractors toward which a system tends to evolve for a wide variety of the system's initial conditions. The existence of a basin of attraction for each attractor guarantees that any initial condition in the nearby region will iterate to the attractor. When an input vector in a specific basin of attraction is presented, the proposed network sends signals back and forth between the hidden and visible layers until all the nodes reach an equilibrium state minimizing the energy function above, generating the desired output vector.

The visible nodes can be divided into either A input and B output nodes, as shown in Figure 3. In the forward computation path, each node in the hidden layer receives the weighted output of both the input and output nodes of the visible layer. In the backward computation direction, only the output nodes receive the weighted output of the hidden nodes. Therefore, when an input vector is presented to the input nodes, signals are sent back and forth between the hidden and output nodes until an equilibrium state is reached.
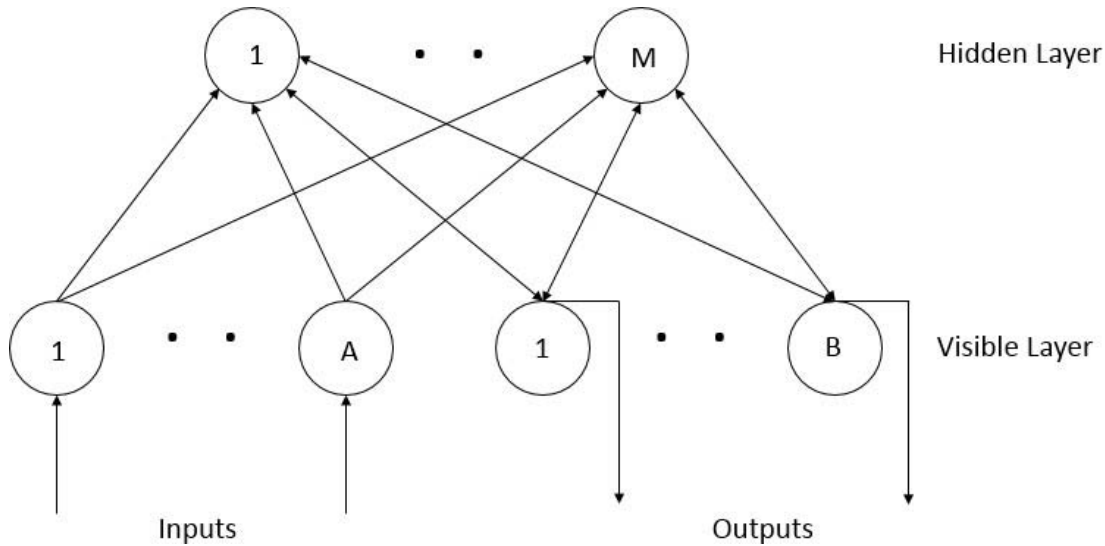
Figure 3: A Restricted Hopfield Network with Inputs and Outputs Nodes

The following differential equations describe the dynamics of the network:

In the forward path:

$$\frac{du_i^H}{dt} = -\sum_{j=1}^{B} w_{ij}^H V_j^O + \sum_{k=1}^{H} w_{ik}^H I_k + \theta_i^H \quad (28)$$

$$V_i^H = g(u_i^H)$$

Initial conditions:

$$V_j^O(0) = 0 \\ V_i^H(0) = 0 \quad (29)$$

Where u_i^H is the sum of all inputs to the hidden nodes, W_{ij}^H is the weight connecting the output of output node j to the input of hidden node i, V_j^O is the output of output node j, W_{ik}^H is the weight connecting the output of input node k to the input of hidden node i, I_k is the output of input node k, θ_i^H is the threshold of hidden node i, V_i^H is the output of hidden node i, and $g()$ is the output function of hidden node i.

In the backward path:

$$\frac{du_j^O}{dt} = \sum_{i=1}^{M} w_{ji}^O V_i^H + \theta_j^O \quad (30)$$

$$V_j^O = g(u_j^O)$$

Where u_j^o is the sum of all inputs to the output nodes, w_{ji}^O is the weight connecting the output of hidden node i to the input of output node j, V_i^H is the output of hidden node i, θ_j^O is the threshold of output node j, V_j^O is the output of output node j, and $g()$ is the output function of output node j.

The proposed RHN always generates analog outputs between 0 and 1 when $g()$ is a sigmoid function or between -1 and 1 when g() is a hyperbolic tangent function.

Using the Lyapunov Direct Method, it can be shown that Eqn. 31 is the energy or Lyapunov functions of the proposed network.

$$E = -\frac{1}{2}\sum_{i=1}^{M}\sum_{j=1}^{B} w_{ij}^H V_i^H V_j^O - \frac{1}{2}\sum_{j=1}^{B}\sum_{i=1}^{M} w_{ji}^O V_j^O V_i^H$$

$$- \sum_{i=1}^{M}\sum_{k=1}^{A} w_{ik}^H V_i^H I_k - \sum_{i=1}^{M} V_i^H \theta_i^H - \sum_{i=1}^{B} V_i^O \theta_i^O \quad (31)$$

Differentiating *E*, we get:

$$\frac{dE}{dt} = -\frac{d}{dt}\left(\frac{1}{2}\sum_{i=1}^{M}\sum_{j=1}^{B} w_{ij}^H V_i^H V_j^O\right) - \frac{d}{dt}\left(\frac{1}{2}\sum_{j=1}^{B}\sum_{i=1}^{M} w_{ji}^O V_j^O V_i^H\right)$$

$$- \frac{d}{dt}\left(\sum_{i=1}^{M}\sum_{k=1}^{A} w_{ik}^H V_i^H I_k\right) - \frac{d}{dt}\left(\sum_{i=1}^{M} V_i^H \theta_i^H\right) - \frac{d}{dt}\left(\sum_{i=1}^{B} V_i^O \theta_i^O\right) \quad (32)$$

Expanding all the above terms in Eqn.32, we get:

$$\frac{d}{dt}\left(\frac{1}{2}\sum_{i=1}^{M}\sum_{j=1}^{B}w_{ij}^{H}V_{i}^{H}V_{j}^{O}\right) = \frac{1}{2}\sum_{i=1}^{M}\sum_{j=1}^{B}w_{ij}^{H}\frac{dV_{i}^{H}}{dt}V_{j}^{O} + \frac{1}{2}\sum_{i=1}^{M}\sum_{j=1}^{B}w_{ij}^{H}V_{i}^{H}\frac{dV_{j}^{O}}{dt}$$

$$\frac{d}{dt}\left(\frac{1}{2}\sum_{j=1}^{B}\sum_{i=1}^{M}w_{ji}^{O}V_{j}^{O}V_{i}^{H}\right) = \frac{1}{2}\sum_{j=1}^{B}\sum_{i=1}^{M}w_{ji}^{O}\frac{dV_{j}^{O}}{dt}V_{i}^{H} + \frac{1}{2}\sum_{j=1}^{B}\sum_{i=1}^{M}w_{ji}^{O}V_{j}^{O}\frac{dV_{i}^{H}}{dt} \tag{33}$$

$$\frac{d}{dt}\left(\sum_{i=1}^{M}\sum_{k=1}^{A}w_{ik}^{H}V_{i}^{H}I_{k}\right) = \sum_{i=1}^{M}\sum_{k=1}^{A}w_{ik}^{H}\frac{dV_{i}^{H}}{dt}I_{k} + \sum_{i=1}^{M}\sum_{k=1}^{A}w_{ik}^{H}V_{i}^{H}\frac{dI_{k}}{dt}$$

For constant input Ik:

$$\frac{dI_{k}}{dt} = 0 \tag{34}$$

Then:

$$\frac{d}{dt}\left(\sum_{i=1}^{M}\sum_{k=1}^{A}w_{ik}^{H}V_{i}^{H}I_{k}\right) = \sum_{i=1}^{M}\sum_{k=1}^{A}w_{ik}^{H}\frac{dV_{i}^{H}}{dt}I_{k} \tag{35}$$

For the rest of the terms, we get:

$$\frac{d}{dt}\sum_{i=1}^{M}V_{i}^{H}\theta_{i}^{H} = \sum_{i=1}^{M}\frac{dV_{i}^{H}}{dt}\theta_{i}^{H}$$

$$\frac{d}{dt}\sum_{i=1}^{B}V_{i}^{O}\theta_{i}^{O} = \sum_{i=1}^{B}\frac{dV_{i}^{O}}{dt}\theta_{i}^{O} \tag{36}$$

Now consider the forward path:
Because the outputs of visible nodes are constant in the backward path, then:

$$\frac{dV_{j}^{O}}{dt} = 0 \tag{37}$$

Assume that all the weights are symmetric, then:

$$w_{ij}^{H} = w_{ji}^{O} \tag{38}$$

Therefore, Equation 32 can be reduced to:

$$\frac{dE}{dt} = -\sum_{i=1}^{M}\sum_{j=1}^{B}w_{ij}^{H}\frac{dV_{i}^{H}}{dt}V_{j}^{O} - \sum_{i=1}^{M}\sum_{k=1}^{A}w_{ik}^{H}\frac{dV_{i}^{H}}{dt}I_{k} - \sum_{i=1}^{M}\frac{dV_{i}^{H}}{dt}\theta_{i}^{H} \tag{39}$$

and can be simplified to:

$$\frac{dE}{dt} = -\sum_{i=1}^{M}\frac{dV_{i}^{H}}{dt}\left(\sum_{j=1}^{B}w_{ij}^{H}V_{j}^{O} + \sum_{k=1}^{A}w_{ik}^{H}I_{k} + \theta_{i}^{H}\right) \tag{40}$$

Further simplified to:

$$\frac{dE}{dt} = -\sum_{i=1}^{M}\frac{dV_{i}^{H}}{dt}\frac{du_{i}^{H}}{dt} \tag{41}$$

Using Chain Rule:

$$\frac{dE}{dt} = -\sum_{i=1}^{M}\frac{dV_{i}^{H}}{du_{i}^{H}}\frac{du_{i}^{H}}{dt}\frac{du_{i}^{H}}{dt}$$

$$\frac{dE}{dt} = -\sum_{i=1}^{M}\frac{dV_{i}^{H}}{du_{i}^{H}}\left(\frac{du_{i}^{H}}{dt}\right)^{2} \tag{42}$$

Since:

$$V_{i}^{H} = g(u_{i}^{H}) \tag{43}$$

If the output function is a sigmoid or hyperbolic tangent function, then:

$$\frac{dV_{i}^{H}}{du_{i}^{H}} \ is\ always\ positive \tag{44}$$

Then:

$$\frac{dE}{dt} \text{ is always negative in the forward path} \tag{45}$$

Now consider the backward path:
Because the outputs of hidden nodes are constant in the backward path, then:

$$\frac{dV_i^H}{dt} = 0 \tag{46}$$

Assume all the weights are symmetric:

$$w_{ji}^O = w_{ij}^H \tag{47}$$

Therefore,

$$\frac{dE}{dt} = -\sum_{j=1}^{B}\sum_{i=1}^{M} w_{ji}^O \frac{dV_j^O}{dt} V_i^H - \sum_{j=1}^{B} \frac{dV_j^O}{dt}\theta_j^O \tag{48}$$

and can be simplified to:

$$\frac{dE}{dt} = -\sum_{j=1}^{B} \frac{dV_j^O}{dt}\left(\sum_{i=1}^{M} w_{ji}^O V_i^H + \theta_j^O\right) \tag{49}$$

Further simplified to:

$$\frac{dE}{dt} = -\sum_{j=1}^{B} \frac{dV_j^O}{dt}\frac{du_j^O}{dt} \tag{50}$$

Using Chain Rule:

$$\frac{dE}{dt} = -\sum_{j=1}^{B} \frac{dV_j^O}{du_j^O}\frac{du_j^O}{dt}\frac{du_j^O}{dt} \tag{51}$$

$$\frac{dE}{dt} = -\sum_{j=1}^{B} \frac{dV_j^O}{du_j^O}\left(\frac{du_j^O}{dt}\right)^2$$

Since:

$$V_j^O = g(u_j^O) \tag{52}$$

If the output function is a sigmoid or hyperbolic tangent function, then:

$$\frac{dV_j^O}{du_j^O} \text{ is always positive} \tag{53}$$

Then

$$\frac{dE}{dt} \text{ is always negative in the backward path} \tag{54}$$

Therefore, combining the forward and backward path, the energy function E of Eqn.31 is a Lyapunov function if and only if all weights are symmetric.

The proposed RHN is a dynamic system. When an input vector is presented to the input nodes, and the input vector is in a specific basin of attraction, the proposed network sends signals back and forth between the hidden and output nodes until the network reaches an equilibrium state or the corresponding attractor.

IV. TRAINING OF PROPOSED RHN

The proposed network can be trained using either the modified SPSA or BPTT algorithms to ensure that all the weights are symmetric, as described in the following.

a) SPSA Algorithm

As mentioned earlier (Equations 3 and 4), the conventional Hebbian rule is not suitable for training the proposed network because the outputs of the hidden nodes are unknown, and the equations cannot handle analog quantities.

The simultaneous perturbation stochastic approximation (SPSA) algorithm uses a gradient approximation that requires only 2N objective function measurements over all N iterations regardless of the optimization network's dimension [4, 9]. Therefore, the SPSA algorithm, as shown in the following formulae, is suited for a high-dimensional optimization problem of minimizing an objective function dependent on multiple adjustable symmetric weights.

$$\Delta W_{ij} = \frac{J(W(k) + c(k)\Delta(k)) - J(W(k) - c(k)\Delta(k))}{2c(k)\Delta_{ij}(k)} \qquad (55)$$

$$W_{ij}(k+1) = W_{ji}(k+1) = W_{ij}(k) - a(k)\Delta W_{ij}(k)$$

At each iteration, a simultaneous perturbation delta vector with mutually independent zero-mean random variables is generated; each element $\Delta_{ij}(k)$ in $\Delta(k)$ matrix is generated with a probability of 0.5 of being either +1 or 1. Two weight matrices $W+$ and W are calculated by adding and subtracting the $\Delta(k)$ matrix scaled by gain sequence $c(k)$ to/from the current weight matrix $W(k)$ to compute their respective contributions $J(W+)$ and $J(W)$ to the objective function. Dependent on the outcome of the evaluation and scaled by gain sequences $a(k)$ and $c(k)$, the current weight matrix W is updated accordingly. The gain sequences $a(k)$ and $c(k)$ decrease as the number of iterations k increases, will converge to 0 as k approaches ∞.

The objective function J used for the optimization of the proposed RHN is:

$$J = \sum_{i=1}^{P}\sum_{j=1}^{B}(\hat{D}_{ij} - V_{ij}^{O}(k))^2 \qquad (56)$$

Where $\widehat{D}_{ij}$ is the jth element of the desired output vector i, $V_{ij}^{O}(k)$ is the output value of the jth output node when training pattern i is presented, B is the number of output nodes, and P is the number of training patterns.

b) Backward Propagation Through Time (BPTT) Algorithm

For simplicity and the ability to apply BPTT training algorithm, the proposed network in Figure 3 can be transformed into a discrete-time system and unfolded in time, as shown in Figure 4.
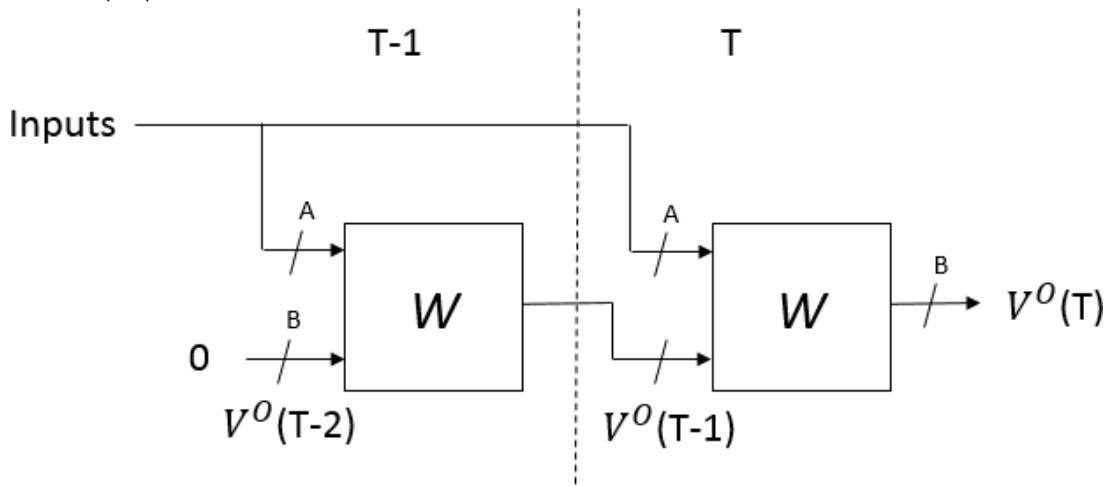
Figure 4: Unfolded RHN in 2-time steps

W represents all the weights in the proposed RHN. $V^{O}(T)$ and $V^{O}(T-1)$ are the outputs of the output nodes at T and $T-1$, respectively. The structure of the block is presented in Figure 5.

The error function J used for the optimization of the proposed RHN is:

$$J = \frac{1}{2}\sum_{p=1}^{P}\sum_{j=1}^{B}(\hat{D}_{pj} - V_{pj}^{O}(T))^2 \qquad (57)$$

Where $\widehat{D}_{pj}$ is the jth element of the desired output vector k, $V^{O}(T)$ is the output value of the jth output node when training pattern p is presented, B is the number of output nodes, and P is the number of training patterns.

Applying the BPTT algorithm,

$$\Delta W_{ji}^{O} = \varepsilon(\delta_{pj}^{O} V_{pj}^{H}(T) + \delta_{pj}^{H2} V_{i}^{H}(T-1))$$ (58)

For $j = 1 \ldots A$:

$$\Delta W_{ij}^{H} = \varepsilon(\delta_{pi}^{H1} + \delta_{pi}^{H3}) I_{pj}^{O}$$ (59)

For $j = A + 1 \ldots A + B, k = 1 \ldots B$:

$$\Delta W_{ij}^{H} = \varepsilon(\delta_{pi}^{H1} V_{pk}^{O}(T-1) + \delta_{pi}^{H3} V_{pk}^{O}(T-2))$$ (60)
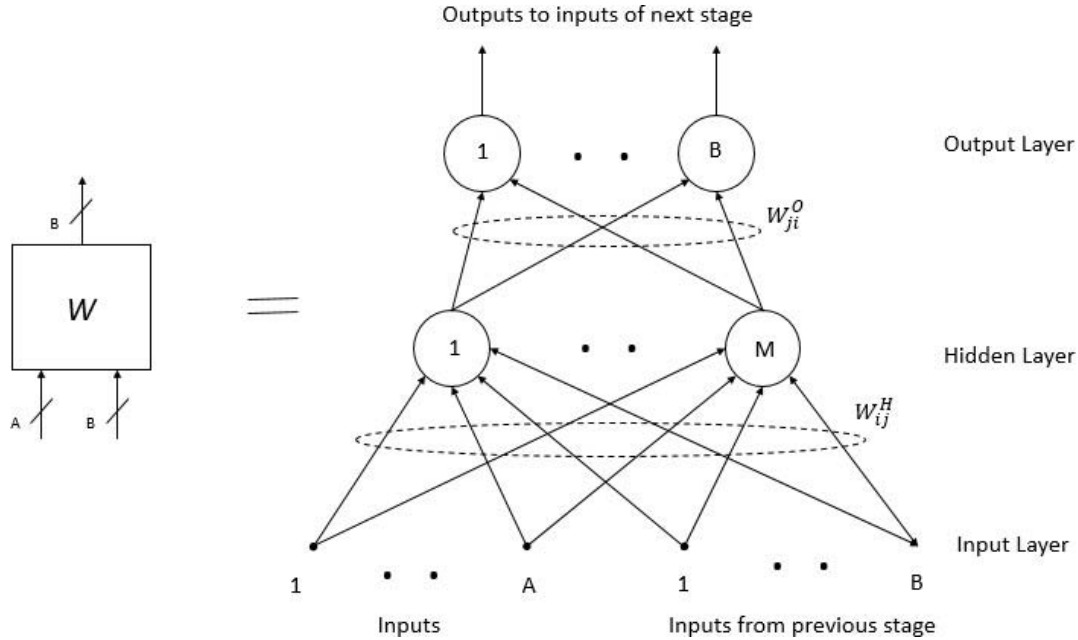
Figure 5: Structure of block W in Figure 4

Where the deltas are:

$$\delta_{pj}^{O} = g'(u_{pj}^{O}(T))(\hat{D}_{pj} - V_{pj}^{O}(T))$$

$$\delta_{pi}^{H1} = g'(u_{pi}^{H}(T)) \sum_{j=1}^{B} \delta_{pj}^{O} W_{ji}^{O}$$

$$\delta_{pj}^{H2} = g'(u_{pj}^{O}(T-1)) \sum_{i=1}^{M} \delta_{pj}^{H1} W_{ij}^{H}$$ (61)

$$\delta_{pi}^{H3} = g'(u_{pj}^{H}(T-1)) \sum_{i=1}^{B} \delta_{pj}^{H2} W_{ji}^{O}$$

Since the weights are symmetric, then:

$$W_{ji}^{O}(T+1) = w_{ij}^{H}(T+1) = w_{ji}^{O}(T) + \Delta W_{ji}^{O} + \Delta W_{ij}^{H}$$ (62)

V. SIMULATION RESULTS

a) Comparison of Hopfield Network and RHN

Let us consider storing 3 vectors ([1100], [0110], [0101]) in a Hopfield network. Hopfield network can be programmed to memorize these three vector patterns using Hebbian Rule, and the weight matrix is:

$$
\begin{bmatrix} 0 & 1 & -1 & -1 \\ 1 & 0 & -1 & -1 \\ -1 & -1 & 0 & 1 \\ -1 & -1 & 1 & 0 \end{bmatrix} + \begin{bmatrix} 0 & -1 & -1 & 1 \\ -1 & 0 & 1 & -1 \\ -1 & 1 & 0 & -1 \\ 1 & -1 & -1 & 0 \end{bmatrix} + \begin{bmatrix} 0 & -1 & 1 & -1 \\ -1 & 0 & -1 & 1 \\ 1 & -1 & 0 & -1 \\ -1 & 1 & -1 & 0 \end{bmatrix} = \begin{bmatrix} 0 & -1 & -1 & -1 \\ -1 & 0 & -1 & -1 \\ -1 & -1 & 0 & -1 \\ -1 & -1 & -1 & 0 \end{bmatrix}
$$

The weight matrix will generate the correct output vector when the corresponding input vector with noise is provided.

Let us consider storing the fourth vector [1111] in the network. The weight matrix to store vector [1111] is:

$$
\begin{bmatrix} 0 & 1 & 1 & 1 \\ 1 & 0 & 1 & 1 \\ 1 & 1 & 0 & 1 \\ 1 & 1 & 1 & 0 \end{bmatrix}
$$

$$
\begin{bmatrix} 0 & -1 & -1 & -1 \\ -1 & 0 & -1 & -1 \\ -1 & -1 & 0 & -1 \\ -1 & -1 & -1 & 0 \end{bmatrix} + \begin{bmatrix} 0 & 1 & 1 & 1 \\ 1 & 0 & 1 & 1 \\ 1 & 1 & 0 & 1 \\ 1 & 1 & 1 & 0 \end{bmatrix} = \begin{bmatrix} 0 & 0 & 0 & 0 \\ 0 & 0 & 0 & 0 \\ 0 & 0 & 0 & 0 \\ 0 & 0 & 0 & 0 \end{bmatrix}
$$

Adding this new weight matrix to the previous weight matrix of the Hopfield network programmed to store 3 vectors ([1100], [0110], [0101]) yields a weight matrix with zero elements, erasing all the previous programming, as shown in the following. Therefore, the Hopfield network cannot be programmed to remember all four vectors ([1100], [0110], [0101], [1111]) using Hebbian rule.

However, by introducing five hidden nodes in the proposed RHN, all the vectors can be easily stored and recalled correctly. The simulation shows that it is possible to increase the Hopfield network's memory capacity by using more hidden nodes. By increasing the number of hidden nodes to 50, the proposed network can remember all 16 binary vectors.

b)   EXOR Problem

The EXOR or exclusive-or problem is a classical problem in neural network research. It is a problem of using a neural network to predict EXOR logic gates' outputs given two binary inputs. The network should return a "1" if the two inputs are not equal and a "0" if they are similar. The EXOR problem appears to be simple. However, Minksy and Papert in 1969 showed that this was a big problem for neural network architectures of the 1960s, providing a good test for the proposed network [18].

Using an RHN with input and output nodes, as shown in Figure 3, is used. An RHN with 2 input nodes, one output node, and four hidden nodes was created. It was trained to learn the EXOR problem. Figure 6 shows the training curve of the network using the SPSA algorithm described earlier. The network is trained after 1000 training iterations.
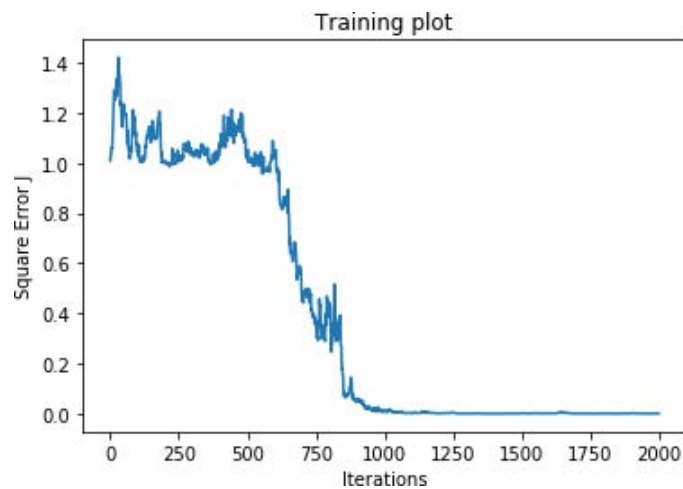
Figure 6: The training plot of square error J

Figures 7 and 8 show the basin of attraction and the network's energy profile, indicating four attractors, one attractor for each input pair.
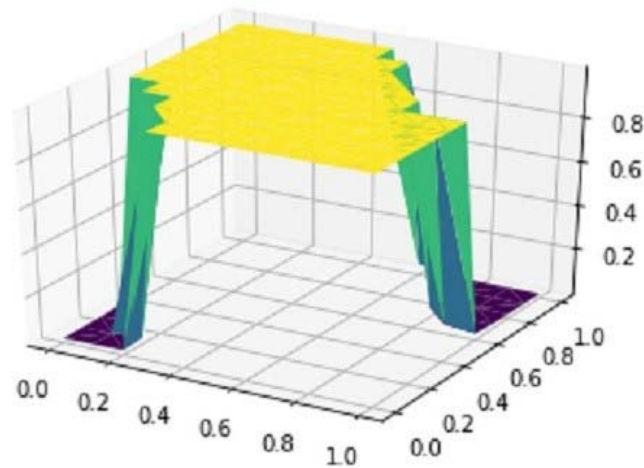
Figure 7: Basin of attraction of an RHN implementing EXOR function

Table 1 illustrates the effect of feedback as the output of an RHN network evolves when an initial input is presented. The EXOR output takes 3 to 4 feedback iterations to settle on the correct result.
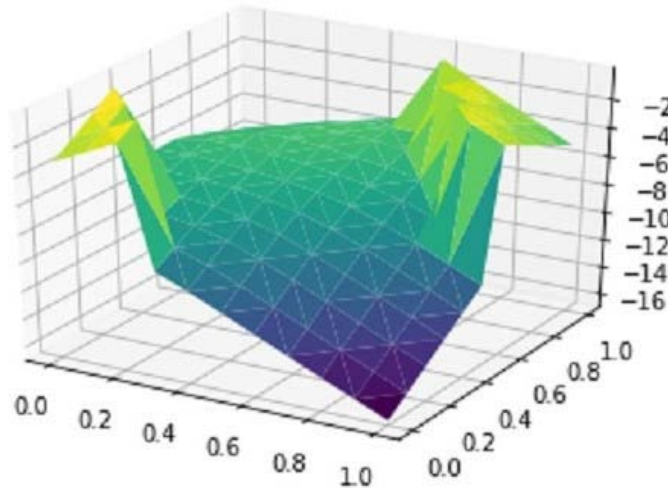
Figure 8: The energy function of an RHN implementing EXOR function

Table 1: The evolution of the RHN's output

Input		Output at each iteration					
		T = 0	T = 1	T = 2	T = 3	T = 5	T = 6
0	0	0	0.004	0.004	0.004	0.004	0.004
0	1	0	0.258	0.510	0.638	0.847	0.997
1	0	0	0.316	0.521	0.851	0.990	0.995
1	1	0	0.003	0.003	0.003	0.003	0.003

c) Associative Memory Problem

An RHN with 35 input nodes, 35 output nodes, and ten hidden nodes is created. The network is then trained to perform auto-encoding of *A, U, T, S* characters, each with 5 7 pixels. The input characters are distorted by changing some of the pixels to test the network's ability to re-create the characters in the presence of noise.

In Figure 9, the distorted images of *A, U, T, S* are on the left and re-created images are on the right. The figure shows that the network can perform perfect re-creation of these images even when distorted images with the Hamming distance of 13 are presented.
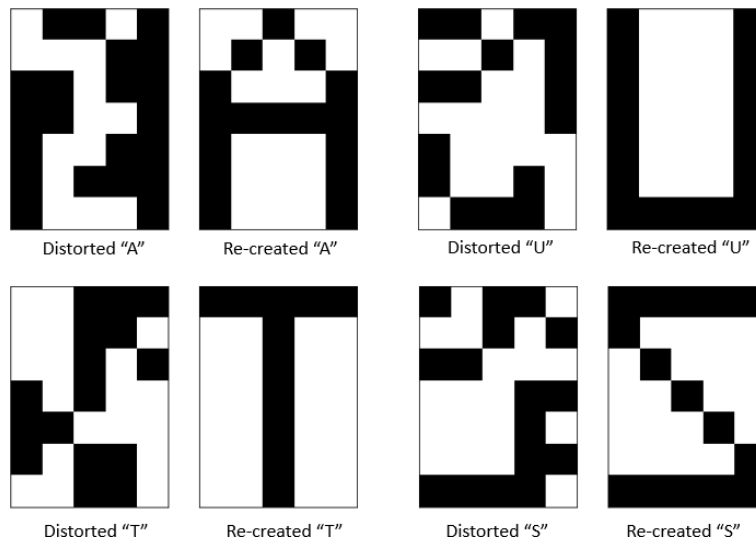
Figure 9: Distorted and re-created images of A, U, T, and S

As shown in Figure 10, an RHN trained with the BPTT algorithm can re-create the images with an average error rate of 2.4% when the Hamming distance is 5. The result is significantly improved compared with the RHN trained with the SPSA algorithm resulting in an error pattern of more than 4.4% for the same input. The classical Hopfield network and RBM can only achieve an error rate of 22.6% and 13.4%, respectively, for input vectors with the same Hamming distance. The RHN performs better compared to the Hopfield network and RBM.

d) Creating an Associative Memory Model of Hand Written Digits

The MNIST handwritten digit classification problem is a standard dataset used in computer vision

and deep learning. The dataset contains 60,000 images, typically split into 50,000 training images and 10,000 validation images.

In this example, instead of performing handwritten classification, some of the 50,000 MNIST images are used as training inputs to associate with 3 5 pixel models representing handwritten digits, as shown in Figure 11. All 10,000 validation MNIST images will be used as test images to verify the network's associative function

Figure 10: Performance comparison of the Hopfield Network and RBM with RHN

14
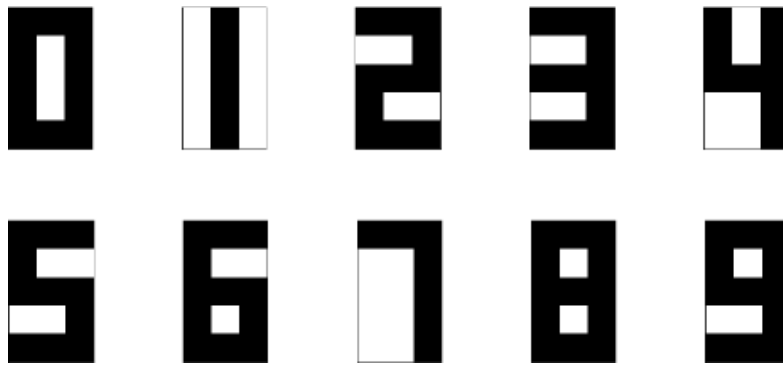
Figure 11: 3 × 5 pixel model of digits

The architecture to process MNIST images is inspired by a Convolution Neural Network architecture [19, 20], as shown in Figure 12. It consists of several layers: Input, 2D-Convolution, ReLU (Rectified Linear Unit), Max-pooling, Matrix to Vector, and RHN. The function of each layer in more detail is presented as follows:

- The Input layer will hold the raw pixel values of the image, in this case, an image of width 28, height 28;
- The 2D-Convolution layer will compute the output of nodes that are connected to local re- gions in the input image, each computing a dot product between their weights and a small area they are connected to in the input. Since four filters (horizontal line, vertical line, 45-degree line, and 135-degree line detection) are used in the architecture, this results in a volume equal to [26 × 26 × 4];
- The ReLU layer will apply an elementwise activation function, max(0,x), thresholding at zero. The layer leaves the size of the volume unchanged ([26 × 26 × 4]).
- The Max-pooling layer will perform a downsampling operation along the spatial dimensions (width, height), resulting in a smaller volume of [7 × 7 × 4].
- The Matrix to Vector layer will convert a volume of data (in this case [7 × 7 × 4] elements) into a linear vector of 196 elements.
- An RHN with 196 input nodes, 100 hidden nodes, and 15 output nodes will be trained using the BPTT algorithm to associate an input image with a digit model of 3 × 5 pixels.

The network architecture was inspired by the visual cortex's organization, having a similar connectivity pattern of the retina, ganglion cells, and neurons in a human brain. Individual neurons respond to stimuli only in a restricted region of the visual field known as the receptive field. A collection of such fields overlap to cover the entire image area.
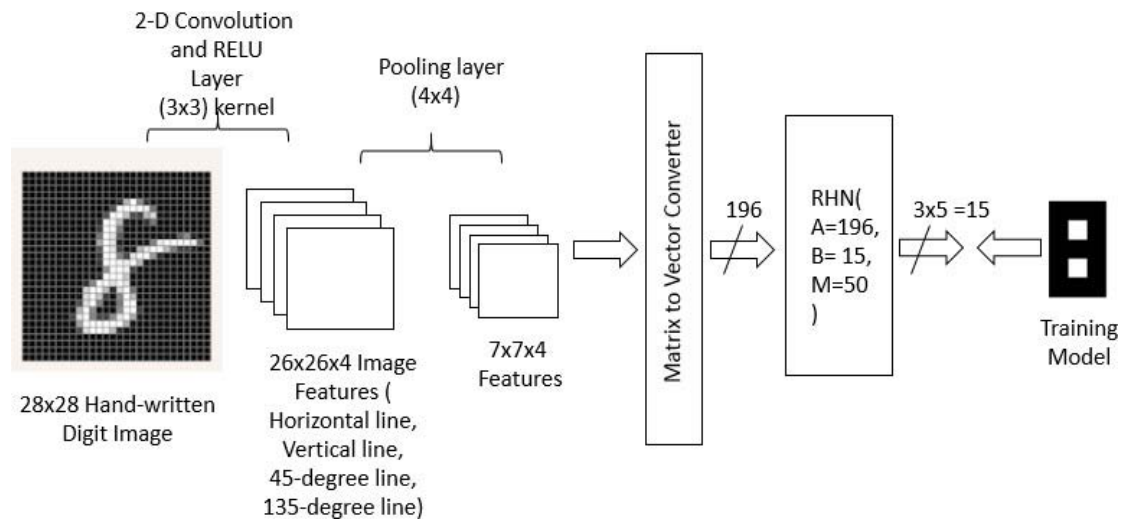
Figure 12: Image Processing and RHN

An RHN was trained with 1 percent of the 50,000 training images. Figure 13 shows the responses of an RHN when different input images are presented at zero, one, and two feedback iterations.

An RHN with zero feedback iteration is a feed-forward multilayer perceptron (MLP) acting as a mapping function. When input images "0" and "4" are presented, models of "0" and "4" with 1-bit error were

created as outputs at iteration 0. The network generated correct models of "0" and "4" after the first iteration. When input image "1" is presented, it takes two feedback iterations to generate the correct model of "1".

When input image "6" is presented, the network first generated a wrong model of "5" and then corrected its output to generate the correct model of "6" after the first feedback iteration.
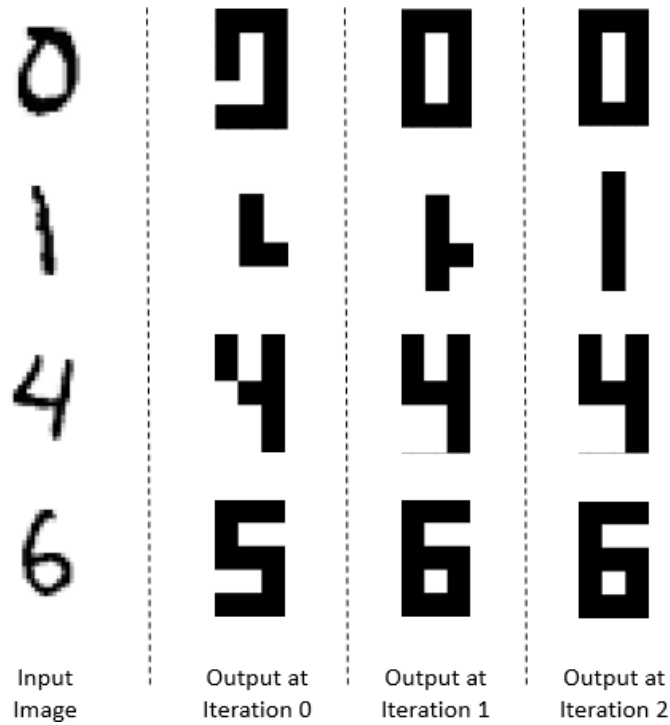
Figure 13: RHN's sample output at different iterations

The effect of feedback iterations on the performance of an RHN is illustrated in Figure 14. The figure shows that the network can re-create half of the models correctly without any feedback iteration. However, the network's performance can be improved by applying one or more feedback iterations. This result illustrates the importance of feedback iteration in implementing an associative memory using the proposed RHN.

Figure 15 shows a network's performance after being trained using only 500 and 5000 training images. The graph shows that the network could re-create 6674 of the images perfectly when 500 training images were used, while the network can re-create 7849 of the images perfectly when 5000 training images were used.
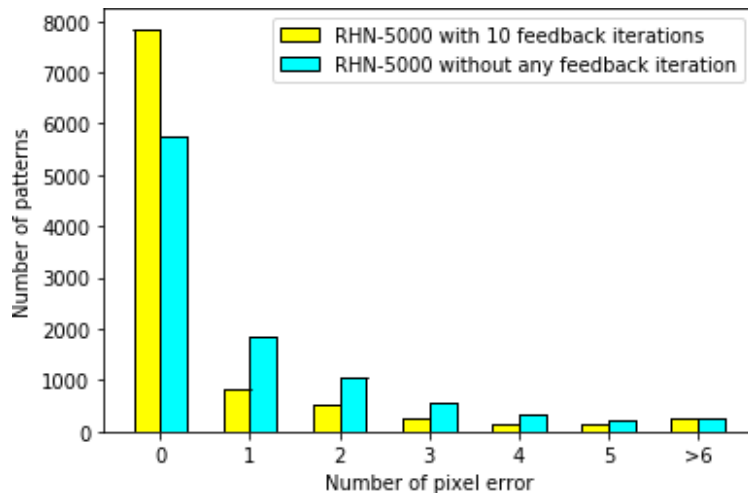
Figure 14: Effect of feedback iterations on the performance of an RHN
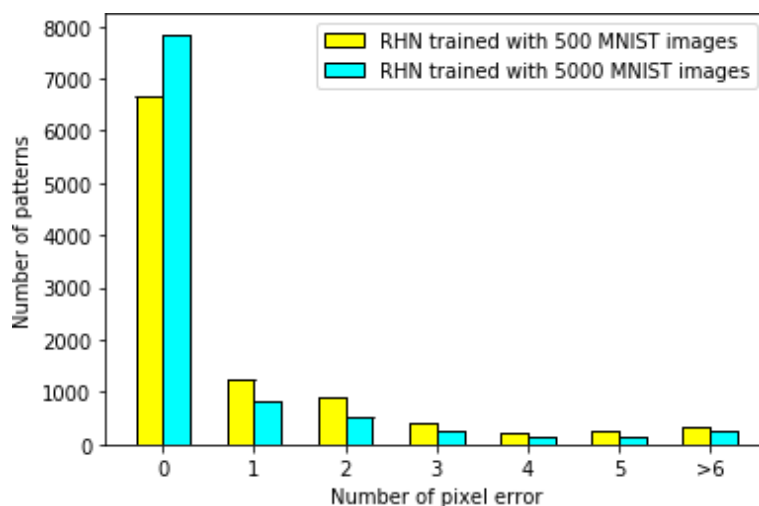
Figure 15: Performance of RHNs trained with 500 and 5000 MNIST training images

VI. CONCLUSION

A trainable analog Restricted Hopfield Network is presented in this paper. An energy or Lyapunov function was derived to show that the proposed network will converge to stable states when an input vector is introduced. The proposed network can be trained using either the modified SPSA or BPTT algorithms to ensure that all the weights are symmetric. Simulation results show that the presence of hidden nodes increases the network's memory capacity. Using A, U, T, S as training characters, the network can be trained to be an associative memory. Simulation results show that the network can perform perfect re-creation of noisy images and perform better than the standard Hopfield Network and RBM. Simulation results also illustrate the importance of feedback iteration in implementing associative memory to re-create from noisy images.

REFERENCES RÉFÉRENCES REFERENCIAS

1. John J Hopfield. Neural networks and physical systems with emergent collective computational abilities. *Proceedings of the national academy of sciences*, 79(8):2554–2558, 1982.
2. John J Hopfield and David W Tank. "neural" computation of decisions in optimization problems. *Biological cybernetics*, 52(3):141–152, 1985.
3. John J Hopfield and David W Tank. Computing with neural circuits: A model. *Science*, 233(4764):625–633, 1986.
4. ROBERTJ McEliece, Edwardc Posner, EUGENER Rodemich, and SANTOSHS Venkatesh. The capacity of the hopfield associative memory. *IEEE transactions on Information Theory*, 33(4):461–482, 1987.
5. Amos J Storkey and Romain Valabregue. The basins of attraction of a new hopfield learning rule. *Neural Networks*, 12(6):869–876, 1999.
6. Elizabeth Gardner. Maximum storage capacity in neural networks. *EPL (Europhysics Letters)*, 4(4):481, 1987.
7. Elizabeth Gardner. The space of interactions in neural network models. *Journal of physics A: Mathematical and general*, 21(1):257, 1988.
8. Elizabeth Gardner and Bernard Derrida. Optimal storage properties of neural network models. *Journal of Physics A: Mathematical and general*, 21(1):271, 1988.
9. David H Ackley, Geoffrey E Hinton, and Terrence J Sejnowski. A learning algorithm for boltzmann machines. *Cognitive science*, 9(1):147–169, 1985.
10. Ruslan Salakhutdinov and Geoffrey Hinton. Deep boltzmann machines. In *Artificial intelligence and statistics*, pages 448–455. PMLR, 2009.
11. Geoffrey E Hinton. A practical guide to training restricted boltzmann machines. In *Neural networks: Tricks of the trade*, pages 599–619. Springer, 2012.
12. Ilya Sutskever, Geoffrey E Hinton, and Graham W Taylor. The recurrent temporal restricted boltzmann machine. In *Advances in neural information processing systems*, pages 1601–1608, 2009.
13. Ruslan Salakhutdinov, Andriy Mnih, and Geoffrey Hinton. Restricted boltzmann machines for collaborative filtering. In *Proceedings of the 24th international conference on Machine learning*, pages 791–798, 2007.
14. James C Spall et al. Multivariate stochastic approximation using a simultaneous perturbation gradient approximation. *IEEE transactions on automatic control*, 37(3):332–341, 1992.
15. James C Spall. An overview of the simultaneous perturbation method for efficient optimization. *Johns Hopkins apl technical digest*, 19(4):482–492, 1998.
16. Paul J Werbos. Backpropagation through time: what it does and how to do it. *Proceedings of the IEEE*, 78(10): 1550–1560, 1990.

17. Simon Haykin. N*eural networks and learning machines, 3/E*. Pearson Education India, 2010.
18. Marvin Minsky and Seymour A Papert. *Perceptrons: An introduction to computational geometry*. MIT press, 2017.
19. Yann LeCun, Bernhard Boser, John S Denker, Donnie Henderson, Richard E Howard, Wayne Hubbard, and Lawrence D Jackel. Back propagation applied to handwritten zip code recognition. *Neural computation*, 1(4): 541–551, 1989.
20. Yann LeCun, Yoshua Bengio, et al. Convolutional networks for images, speech, and time series. *The handbook of brain theory and neural networks*, 3361(10):1995, 1995.

A Novel Approach for the Characterization of Triangular Modulated Frequency Modulated Continuous Wave Low Probability of Intercept Radar Signals via Application of the Wigner-Ville Distribution and the Reassigned Smoothed Pseudo Wigner-Ville Distribution

By Daniel L. Stevens

Abstract- Digital intercept receivers are changing from Fourier-based analysis to classical time-frequency analysis techniques for analyzing low probability of intercept radar signals. This paper presents a novel approach of characterizing low probability of intercept triangular modulated frequency modulated continuous wave radar signals through utilization and direct comparison of the signal processing techniques Wigner-Ville Distribution versus the Reassigned Smooth Pseudo Wigner-Ville Distribution. The following metrics were used for evaluation: percent error of: carrier frequency, modulation bandwidth, modulation period, chirp rate, and time-frequency localization (x and y direction). Also used were: percent detection, lowest signal-to-noise ratio for signal detection, and plot (processing) time. Experimental results demonstrate that overall, the Reassigned Smooth Pseudo Wigner-Ville Distribution signal processing technique produced more accurate characterization metrics than the Wigner-Ville Distribution signal processing technique.

An improvement in performance may equate to an increase in personnel safety.

GJRE-F Classification: FOR Code: 290901

A Novel Approach for the Characterization of Triangular Modulated Frequency Modulated Continuous Wave Low Probability of Intercept Radar Signals via Application of the Wigner-Ville Distribution and the Reassigned Smoothed Pseudo Wigner-Ville Distribution[1]

Daniel L. Stevens

Abstract- Digital intercept receivers are changing from Fourier-based analysis to classical time-frequency analysis techniques for analyzing low probability of intercept radar signals. This paper presents a novel approach of characterizing low probability of intercept triangular modulated frequency modulated continuous wave radar signals through utilization and direct comparison of the signal processing techniques Wigner-Ville Distribution versus the Reassigned Smooth Pseudo Wigner-Ville Distribution. The following metrics were used for evaluation: percent error of: carrier frequency, modulation bandwidth, modulation period, chirp rate, and time-frequency localization (x and y direction). Also used were: percent detection, lowest signal-to-noise ratio for signal detection, and plot (processing) time. Experimental results demonstrate that overall, the Reassigned Smooth Pseudo Wigner-Ville Distribution signal processing technique produced more accurate characterization metrics than the Wigner-Ville Distribution signal processing technique.

An improvement in performance may equate to an increase in personnel safety.

I. INTRODUCTION

The Low Probability of Intercept (LPI) signal used for this paper is the Frequency Modulated Continuous Wave (FMCW) signal, which is commonly used in modern radar systems [WAN10], [WON09], [WAJ08]. The frequency modulation spreads the transmitted energy over a large modulation bandwidth ΔF, providing good range resolution that is essential for discriminating targets from clutter. The power spectrum of the FMCW signal is nearly rectangular over the modulation bandwidth, so non-cooperative interception can be challenging. Since the transmit waveform is deterministic, the form of the return signals can be predicted. This gives it the added advantage of being

resistant to interference (such as jamming), since any signal not matching this form can be suppressed [WIL06]. Consequently, it is problematic for an intercept receiver to detect the FMCW waveform and measure the parameters accurately enough to match the jammer waveform to the radar waveform [PAC09].

The most prevalent linear modulation utilized is the triangular FMCW emitter [LIA09], since it can measure the target's range and Doppler [MIL02], [LIW08]. Triangular modulated FMCW is the waveform that is employed for this paper.

Time-frequency signal analysis involves the analysis and processing of signals with time-varying frequency content. These signals are best represented by a time-frequency distribution [PAP95], [HAN00], which shows how the energy of the signal is distributed over the two-dimensional time-frequency plane [WEI03], [LIX08], [OZD03]. Processing of the signal can exploit the features produced by the concentration of signal energy in two dimensions (time and frequency), instead of in one dimension (time or frequency) [BOA03], [LIY03]. Noise tends to spread out evenly over the time-frequency domain, whereas signals concentrate their energies within limited time intervals and frequency bands; therefore the local SNR of a 'noisy' signal can be improved simply by using time-frequency analysis [XIA99]. In addition, the intercept receiver can increase its processing gain simply by implementing time-frequency signal analysis [GUL08].

Time-frequency representations are valuable for the visual interpretation of signal dynamics [RAN01]. An experienced operator can more easily detect a signal and extract the signal parameters by analyzing a time-frequency representation, vice a time representation, or a frequency representation [ANJ09].

One of the members of the time-frequency analysis techniques family is the Wigner-Ville Distribution (WVD). The WVD has a number of desirable

Author: Air Force Research Laboratory, Rome, NY 13441.
e-mail: daniel.stevens.7@us.af.mil

---

[1] Approved for Public Release; Distribution Unlimited: Case Number: AFRL-2021-1236 20210421

mathematical properties: it is always real-valued, it preserves time and frequency shifts, and it satisfies marginal properties [QIA02]. The WVD is computed by correlating the signal with a time and frequency translated version of itself, making it bilinear. The WVD has the highest signal energy concentration in the time-frequency plane [WIL06]. By using the WVD, an intercept receiver can come close to having a processing gain near the LPI radar's matched filter processing gain [PAC09]. The WVD, however, contains cross term interference between each pair of signal components, which may limit its applications [GUL07], [STE96], and which can make the WVD time-frequency representation hard to read, especially if the components are numerous or close to each other, and the more so in the presence of noise [BOA03]. This lack of readability may equate to less accurate signal detection and parameter extraction metrics, potentially placing the intercept receiver signal analyst's platform in harm's way.

The WVD of a signal x(t) is given in equation (1) as:

$$W_x(t,f) = \int_{-\infty}^{+\infty} x\left(t+\frac{\tau}{2}\right) x^*\left(t-\frac{\tau}{2}\right) e^{-j2\pi f\tau}\, d\tau \qquad (1)$$

or equivalently in equation (2) as:

$$W_x(t,f) = \int_{-\infty}^{+\infty} X\left(f+\frac{\xi}{2}\right) X^*\left(f-\frac{\xi}{2}\right) e^{j2\pi\xi t}\, d\xi \qquad (2)$$

A lack of readability must be overcome in order to obtain time-frequency distributions that can be easily read by operators and easily included in a signal processing application [BOA03].

Some efforts have been made recently in that direction, and in particular, a general methodology referred to as reassignment.

The original idea of reassignment was introduced in an attempt to improve the Spectrogram [OZD03]. As with any other bilinear energy distribution, the Spectrogram is faced with an unavoidable trade-off between the reduction of misleading interference terms and a sharp localization of the signal components.

We can define the Spectrogram as a two-dimensional convolution of the WVD of the signal by the WVD of the analysis window, as in equation (3):

$$S_x(t,f;h) = \iint_{-\infty}^{+\infty} W_x(s,\xi)W_h(t-s,f-\xi)\,ds\,d\xi \qquad (3)$$

Therefore, the distribution reduces the interference terms of the signal's WVD, but at the expense of time and frequency localization. However, a closer look at equation (3) shows that $W_h(t-s,f-\xi)$ delimits a time-frequency domain at the vicinity of the (t,f) point, inside which a weighted average of the signal's WVD values is performed. The key point of the reassignment principle is that these values have no

reason to be symmetrically distributed around (t,f), which is the geometrical center of this domain. Therefore, their average should not be assigned at this point, but rather at the center of gravity of this domain, which is much more representative of the local energy distribution of the signal [AUG94]. Reasoning with a mechanical analogy, the local energy distribution $W_h(t-s,f-\xi)W_x(s,\xi)$ (as a function of s and ξ) can be considered as a mass distribution, and it is much more accurate to assign the total mass (i.e. the Spectrogram value) to the center of gravity of the domain rather than to its geometrical center. Another way to look at it is this: the total mass of an object is assigned to its geometrical center, an arbitrary point which except in the very specific case of a homogeneous distribution, has no reason to suit the actual distribution. A much more meaningful choice is to assign the total mass of an object, as well as the Spectrogram value, to the center of gravity of their respective distribution [BOA03].

This is precisely how the reassignment method proceeds: it moves each value of the Spectrogram computed at any point (t,f) to another point $(\hat{t},\hat{f})$ which is the center of gravity of the signal energy distribution around (t,f) (see equations (4) and (5)) [LIX08]:

$$\hat{t}(x;t,f) = \frac{\iint_{-\infty}^{+\infty} s\, W_h(t-s,f-\xi)W_x(s,\xi)ds\,d\xi}{\iint_{-\infty}^{+\infty} W_h(t-s,f-\xi)W_x(s,\xi)ds\,d\xi} \qquad (4)$$

$$\hat{f}(x;t,f) = \frac{\iint_{-\infty}^{+\infty} \xi\, W_h(t-s,f-\xi)W_x(s,\xi)ds\,d\xi}{\iint_{-\infty}^{+\infty} W_h(t-s,f-\xi)W_x(s,\xi)ds\,d\xi} \qquad (5)$$

And thus leads to a reassigned Spectrogram (equation (6)), whose value at any point (t',f') is the sum of all the Spectrogram values reassigned to this point:

$$S_x^{(r)}(t',f';h) = \iint_{-\infty}^{+\infty} S_x(t,f;h)\delta\big(t'-\hat{t}(x;t,f)\big)\delta$$

$$\big(f'-\hat{f}(x;t,f)\big)dt\,df \qquad (6)$$

One of the most interesting properties of this new distribution is that it also uses the phase information of the STFT, and not only its squared modulus as in the Spectrogram. It uses this information from the phase spectrum to sharpen the amplitude estimates in time and frequency. This can be seen from the following expressions of the reassignment operators:

$$\hat{t}(x;t,f) = -\frac{d\Phi_x(t,f;h)}{df} \qquad (7)$$

$$\hat{f}(x;t,f) = f + \frac{d\Phi_x(t,f;h)}{dt} \qquad (8)$$

where $\Phi_x(t,f;h)$ is the phase of the STFT of x: $\Phi_x(t,f;h) = \arg(F_x(t,f;h))$. However, these expressions (equations (7) and (8)) do not lead to an

efficient implementation, and have to be replaced by equations (9) (local group delay) and (10) (local instantaneous frequency):

$$\hat{t}(x;t,f) = t - \Re\left\{\frac{F_x(t,f;T_h)F_x^*(t,f;h)}{|F_{x(t,f;h)}|^2}\right\} \quad (9)$$

$$\hat{f}(x;t,f) = f - \Im\left\{\frac{F_x(t,f;D_h)F_x^*(t,f;h)}{|F_{x(t,f;h)}|^2}\right\} \quad (10)$$

Where $T_h(t) = t \times h(t)$ and $D_h(t) = \frac{dh}{dt}(t)$. This leads to an efficient implementation for the Reassigned Spectrogram without explicitly computing the partial derivatives of phase. The Reassigned Spectrogram may thus be computed by using 3 STFTs, each having a different window (the window function h; the same window with a weighted time ramp t*h; the derivative of the window function h with respect to time (dh/dt)). Reassigned Spectrograms are therefore very computationally efficient to implement.

Since time-frequency reassignment is not a bilinear operation, it does not permit a stable reconstruction of the signal. In addition, once the phase information has been used to reassign the amplitude coefficients, it is no longer available for use in reconstruction. For this reason, the reassignment method has received limited attention from engineers, and its greatest potential seems to be where reconstruction is not necessary, that is, where signal analysis is an end unto itself.

One of the most important properties of the reassignment method is that the application of the reassignment process to any distribution of Cohen's class theoretically yields perfectly localized distributions for chirp signals, frequency tones, and impulses. This is one of the reasons that the reassignment method was chosen for this paper as a signal processing technique for analyzing LPI radar waveforms such as the triangular modulated FMCW waveforms (which can be viewed as back-to-back chirps).

In order to rectify the classical time-frequency analysis deficiency of cross-term interference, a method needs to be utilized that reduces cross-terms, which the reassignment method does.

The reassignment principle for the Spectrogram allows for a straight-forward extension of its use for other distributions as well [HIP00], including the WVD. If we consider the general expression of a distribution of the Cohen's class as a two-dimensional convolution of the WVD, as in equation (11):

$$C_x(t,f;\Pi) = \iint\limits_{-\infty}^{+\infty} \Pi(t-s,f-\xi)W_x(s,\xi)ds\,d\xi \quad (11)$$

Replacing the particular smoothing kernel $W_h(u,\xi)$ by an arbitrary kernel $\Pi(s,\xi)$ simply defines the

reassignment of any member of Cohen's class (equations (12) through (14)):

$$\hat{t}(x;t,f) = \frac{\iint_{-\infty}^{+\infty} s\,\Pi(t-s,f-\xi)W_x(s,\xi)ds\,d\xi}{\iint_{-\infty}^{+\infty} \Pi(t-s,f-\xi)W_x(s,\xi)ds\,d\xi} \quad (12)$$

$$\hat{f}(x;t,f) = \frac{\iint_{-\infty}^{+\infty} \xi\,\Pi(t-s,f-\xi)W_x(s,\xi)ds\,d\xi}{\iint_{-\infty}^{+\infty} \Pi(t-s,f-\xi)W_x(s,\xi)ds\,d\xi} \quad (13)$$

$$C_x^{(r)}(t',f';\Pi) = \iint\limits_{-\infty}^{+\infty} C_x(t,f;\Pi)\delta\big(t'-\hat{t}(x;t,f)\big)\delta$$
$$\big(f'-\hat{f}(x;t,f)\big)dt\,df \quad (14)$$

The resulting reassigned distributions (which includes the RSPWVD) efficiently produce a reduction of the interference terms provided by a well adapted smoothing kernel. In addition, the reassignment operators $\hat{t}(x;t,f)$ and $\hat{f}(x;t,f)$ are very computationally efficient [AUG95].

II. Methodology

The methodologies detailed in this section describe the processes involved in obtaining and comparing metrics between the WVD signal processing technique and the RSPWVD signal processing technique for the detection and characterization of low probability of intercept triangular modulated FMCW radar signals.

The tools used for this testing were: MATLAB (version 8.3), Signal Processing Toolbox (version 6.21), and Time-Frequency Toolbox (version 1.0) (http://tftb. nongnu.org/).

All testing was accomplished on a desktop computer (Dell Precision T1700; Processor -Intel Xeon CPU E3-1226 v3 3.30GHz; Installed RAM - 32.0GB; System type - 64-bit operating system, x64-based processor).

Testing was performed for the triangular modulated FMCW waveform, whose parameters were chosen for academic validation of signal processing techniques. Due to computer processing resources they were not meant to represent real-world values. The number of samples was chosen to be 256, which seemed to be optimum size for the desktop computer. Testing was performed at three different SNR levels: 10dB, 0dB, and the lowest SNR at which the signal could be detected. The noise added was white Gaussian noise, which best reflects the thermal noise present in the IF section of an intercept receiver [PAC09]. Kaiser windowing was used, where windowing was applicable. 250 runs were performed for each test, for statistical purposes. The plots included in this paper were done at a threshold of 5% of the maximum intensity and were linear scale (not dB) of analytic (complex) signals; the color bar represented intensity.

The signal processing techniques used for each task were the WVD and the RSPWVD.

The triangular modulated FMCW signal (most prevalent LPI radar waveform [LIA09]) used had the following parameters: sampling frequency=4KHz; carrier frequency=1KHz; modulation bandwidth= 500Hz; modulation period=.02sec.

After each individual run for each individual test, metrics were extracted from the time-frequency representation. The metrics that were extracted were as follows:

Relative processing time: The relative processing time for each time-frequency representation.

Percent detection: Percent of time signal was detected - signal was declared a detection if any portion of each of the signal components (4 chirp components for triangular modulated FMCW) exceeded a set threshold (a certain percentage of the maximum intensity of the time-frequency representation).

Threshold percentages were determined based on visual detections of low SNR signals (lowest SNR at which the signal could be visually detected in the time-frequency representation) (see Figure 1).
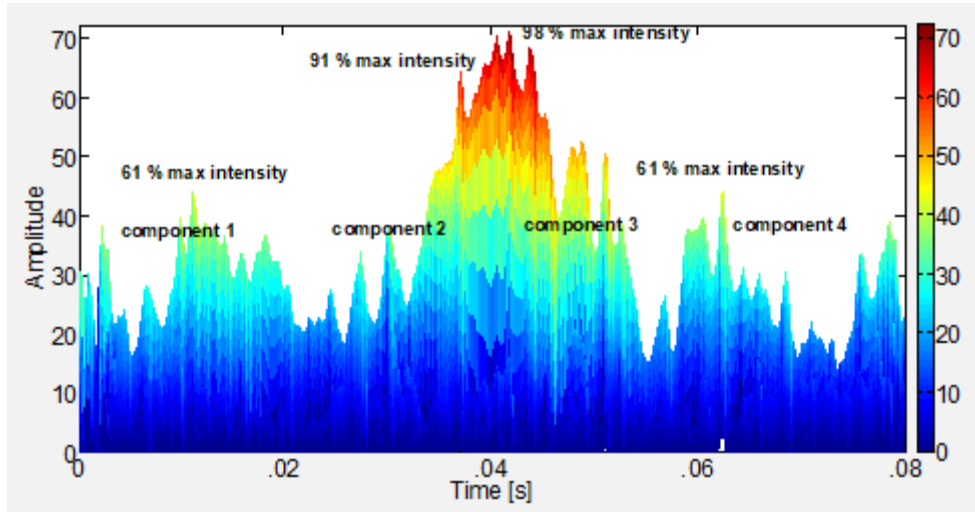
Figure 1: Threshold percentage determination. This plot is a time vs. amplitude (x-z view) of a signal processing technique of a triangular modulated FMCW signal (256 samples, with SNR= -3dB). For visually detected low SNR plots (like this one), the percent of max intensity for the peak z-value of each of the signal components (the 2 legs for each of the 2 triangles of the triangular modulated FMCW) was noted (here 61%, 91%, 98%, 61%), and the lowest of these 4 values was recorded (61%). Ten test runs were performed for this waveform for each of the signal processing techniques that were used. The average of these recorded low values was determined and then assigned as the threshold for that particular signal processing technique.

Based on the above methodology, thresholds were assigned as follows for the signal processing techniques used for this paper: WVD (50%); RSPWVD (50%)

For percent detection determination, these threshold values were included for each of the signal processing technique algorithms so that the thresholds could be applied automatically during the plotting process. From the time-frequency representation threshold plot, the signal was declared a detection if any portion of each of the signal components was visible (see Figure 2).

Figure 2: Percent detection (time-frequency). This plot is a time vs. frequency (x-y view) of a signal processing technique of a triangular modulated FMCW signal (256 samples, with SNR= 10dB) with threshold value automatically set to 60%. From this threshold plot, the signal was declared a (visual) detection because at least a portion of each of the 4 signal components (the 2 legs for each of the 2 triangles of the triangular modulated FMCW) was visible.

Carrier frequency: The frequency corresponding to the maximum intensity of the time-frequency representation (see Figure 3).
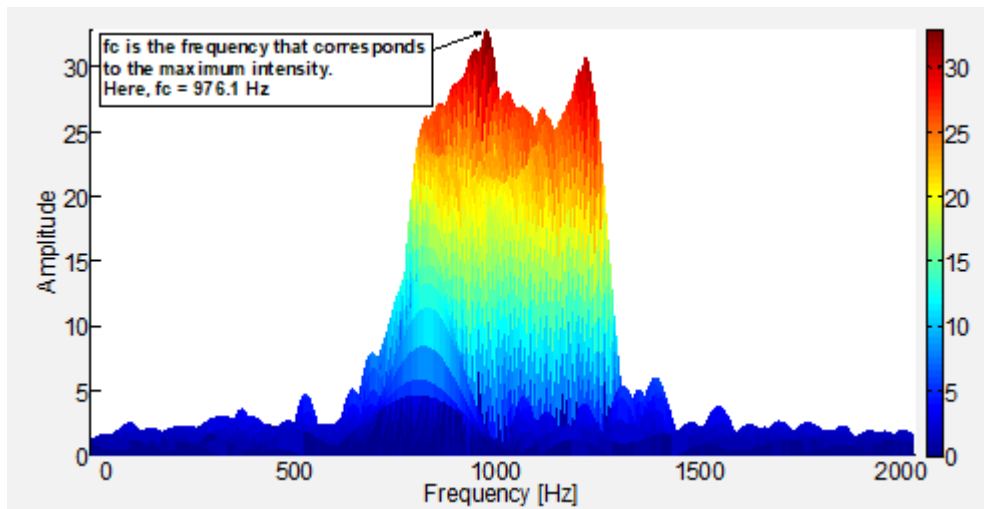
Figure 3: Determination of carrier frequency. Plot of a signal processing technique of a triangular modulated FMCW signal (256 samples, SNR=10dB). From the frequency vs. amplitude (y-z view), the maximum intensity value is manually determined. The frequency corresponding to the max intensity value is the carrier frequency (here $fc=976.1$Hz).

Modulation bandwidth: Distance from highest frequency value of signal (at a threshold of 20% maximum intensity) to lowest frequency value of signal (at same threshold) in Y-direction (frequency).

The threshold percentage was determined based on manual measurement of the modulation bandwidth of the signal in the time-frequency representation. This was accomplished for ten test runs for each of the signal processing techniques that were used, for the triangular modulated FMCW waveform. During each manual measurement, the max intensity of the high and low measuring points was recorded. The average of the max intensity values for these test runs was 20%. This was adopted as the threshold value, and is representative of what is obtained when performing manual measurements. This 20% threshold was also adapted for determining the modulation period and the time-frequency localization (both are described below).

For modulation bandwidth determination, the 20% threshold value was included for each the signal processing technique algorithms so that the threshold could be applied automatically during the plotting process. From the threshold plot, the modulation bandwidth was manually measured (see Figure 4).

24
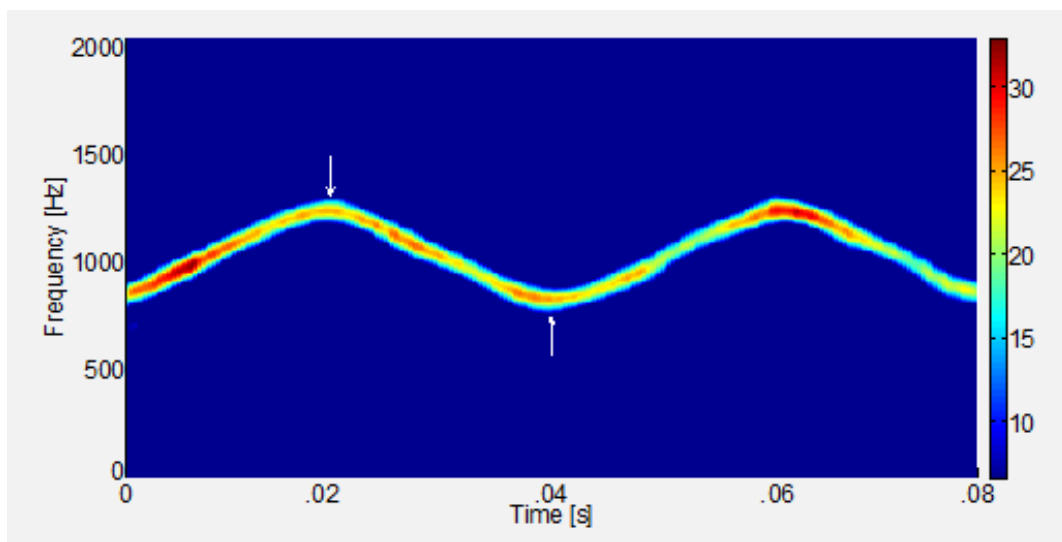
Figure 4: Modulation bandwidth determination. This plot is a time vs. frequency (x-y view) of a signal processing technique of a triangular modulated FMCW signal (256 samples, SNR=10dB) with threshold value automatically set to 20%. From this threshold plot, the modulation bandwidth was measured manually from the highest frequency value of the signal (top white arrow) to the lowest frequency value of the signal (bottom white arrow) in the y-direction (frequency).

Modulation period: Distance from highest frequency value of signal (at a threshold of 20% maximum intensity) to lowest frequency value of signal (at same threshold) in X-direction (time).

For modulation period determination, the 20% threshold value was included for each of the signal processing technique algorithms so that the threshold could be applied automatically during the plotting process. From the threshold plot, the modulation period was manually measured (see Figure 5).
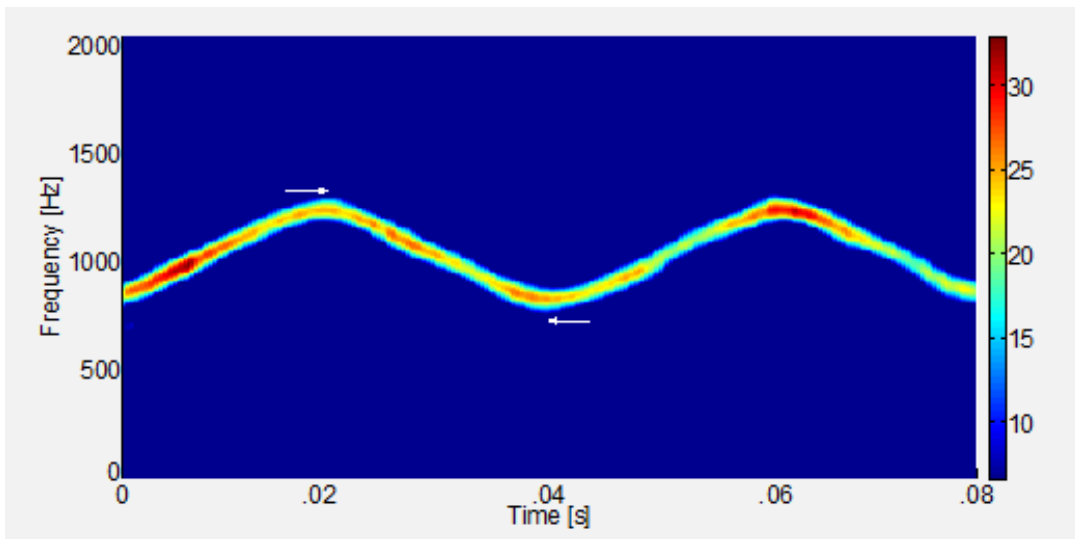
Figure 5: Modulation period determination. This plot is a time vs. frequency (x-y view) of a signal processing technique of a triangular modulated FMCW signal (256 samples, SNR=10dB) with threshold value automatically set to 20%. From this threshold plot, the modulation period was measured manually from the highest frequency value of the signal (top white arrow) to the lowest frequency value of the signal (bottom white arrow) in the x-direction (time).

Time-frequency localization: Measure of the thickness of a signal component (at a threshold of 20% maximum intensity on each side of the component) – converted to % of entire X-Axis, and % of entire Y-Axis.

For time-frequency localization determination, the 20% threshold value was included for each of the signal processing technique algorithms so that the threshold could be applied automatically during the plotting process. From the threshold plot, the time-frequency localization was manually measured (see Figure 6).

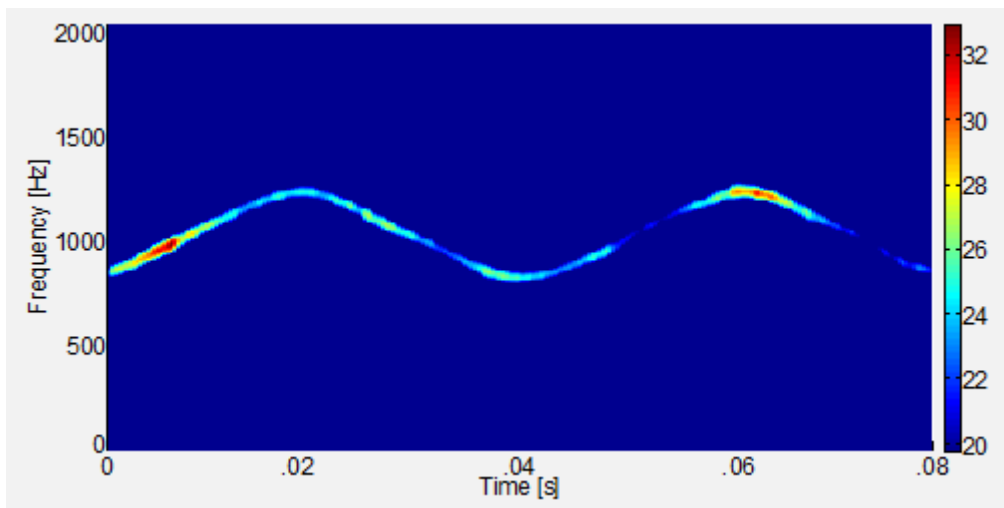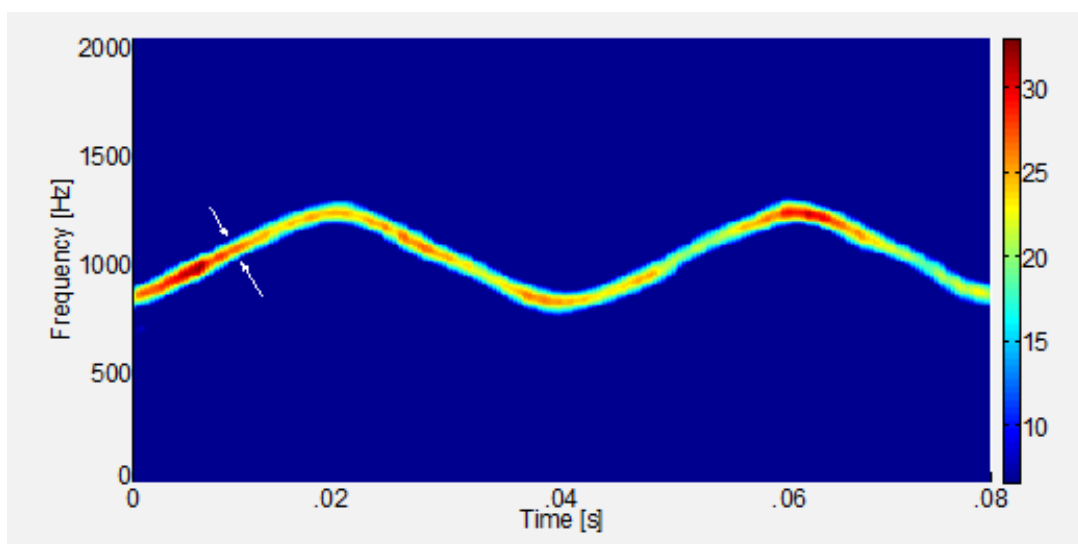*Figure 6:* Time-frequency localization determination. This plot is a time vs. frequency (x-y view) of a signal processing technique of a triangular modulated FMCW signal (256 samples, SNR=10dB) with threshold value automatically set to 20%. From this threshold plot, the time-frequency localization was measured manually from the left side of the signal (left white arrow) to the right side of the signal (right white arrow) in both the x-direction (time) and the y-direction (frequency). Measurements were made at the center of each of the 4 'legs', and the average values were determined. Average time and frequency 'thickness' values were then converted to: % of entire x-axis and % of entire y-axis.

Chirp rate: (modulation bandwidth)/(modulation period)

Lowest detectable SNR: The lowest SNR level at which at least a portion of each of the signal components exceeded the set threshold listed in the percent detection section above.

For lowest detectable SNR determination, these threshold values were included for each of the signal

processing technique algorithms so that the thresholds could be applied automatically during the plotting process. From the threshold plot, the signal was declared a detection if any portion of each of the signal components was visible. The lowest SNR level for which the signal was declared a detection is the lowest detectable SNR (see Figure 7).
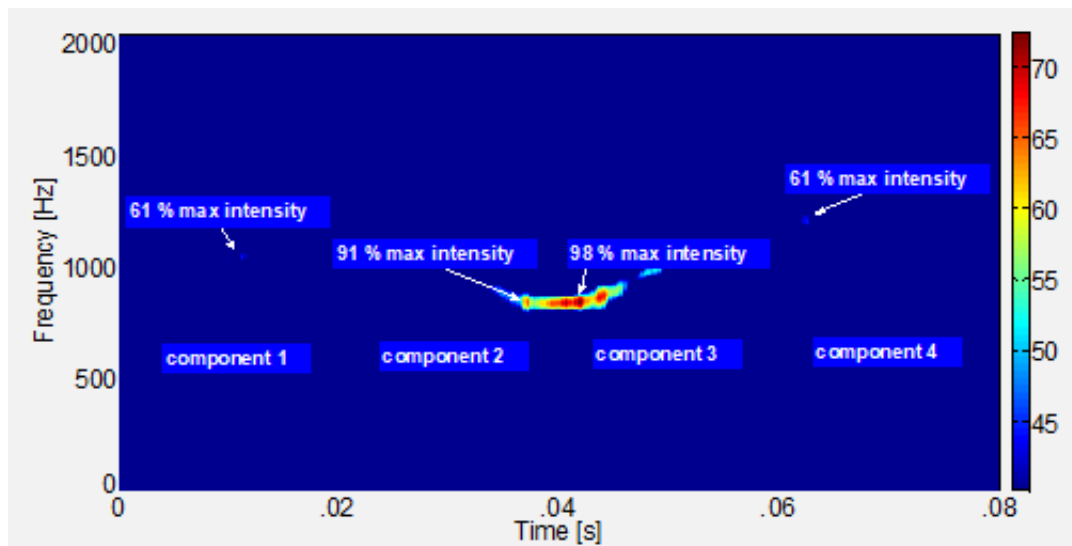
Figure 7: Lowest detectable SNR. This plot is a time vs. frequency (x-y view) of a signal processing technique of a triangular modulated FMCW signal (256 samples, with SNR= -3dB) with threshold value automatically set to 60%. From this threshold plot, the signal was declared a (visual) detection because at least a portion of each of the 4 signal components (the 2 legs for each of the 2 triangles of the triangular modulated FMCW) was visible. Note that the signal portion for the two 61% max intensities are barely visible, because the threshold for this particular signal processing technique is 60%. For this case, any lower SNR than -3dB would have been a non-detect.

The data from all 250 runs for each test was used to produce the actual, error, and percent error for each of the metrics listed above.

The metrics for the WVD signal processing technique were then compared to the metrics for the RSPWVD signal processing technique. By and large, the RSPWVD signal processing technique outperformed

the WVD signal processing technique, as will be shown in the results section.

III. RESULTS

Table 1 presents the overall test metrics for the two signal processing techniques used for this testing (RSPWVD versus WVD).

Table 1: Overall test metrics (average percent error: carrier frequency, modulation bandwidth, modulation period, chirp rate; average: percent detection, lowest detectable snr, plot time, time-frequency localization (as a percent of x axis and y axis) for the two signal processing techniques (RSPWVD versus WVD).

Parameters	RSPWVD	WVD
carrier frequency	2.07%	2.46%
modulation bandwidth	3.33%	5.63%
modulation period	2.44%	4.51%
chirp rate	4.57%	7.77%
percent detection	95.6%	74.6%
lowest detectable snr	-3.11db	-2.23db
relative processing time	0.0177s	0.443s
time-frequency localization-x	0.57%	1.68%
time-frequency localization-y	1.64%	4.04%

From Table 1, the RSPWVD outperformed the WVD in average percent error: carrier frequency (2.07% vs. 2.46%), modulation bandwidth (3.33% vs. 5.63%), modulation period (2.44% vs. 4.51%), and chirp rate (4.57% vs. 7.77%). The RSPWVD also outperformed the WVD in average: percent detection (95.6% vs. 74.6%), lowest detectable SNR (-3.11db vs. -2.23db), relative processing time (0.0177s vs. 0.443s), time-frequency

localization (x-direction) (0.57% vs. 1.68%), and time-frequency localization (y-direction) (1.64% vs. 4.04%).

Figure 8 shows comparative plots of the RSPWVD (left) vs. the WVD (right) (triangular modulated FMCW signal) at SNRs of 10dB (top row), 0dB (middle row), and lowest detectable SNR (-3dB for RSPWVD and -2dB for WVD) (bottom row).
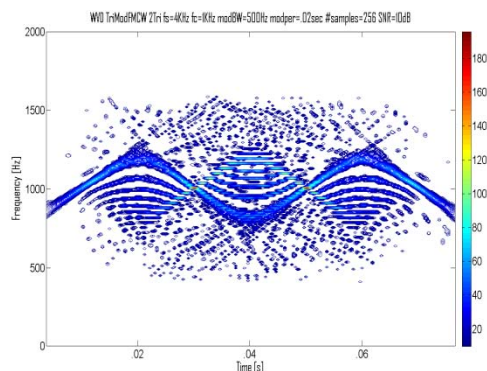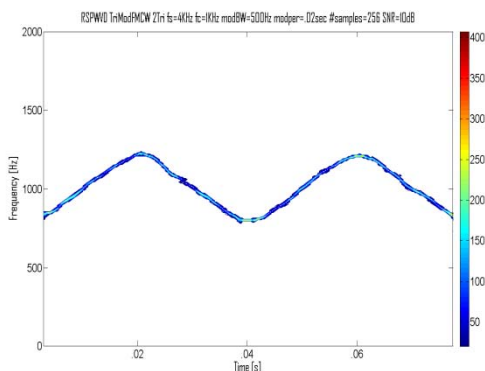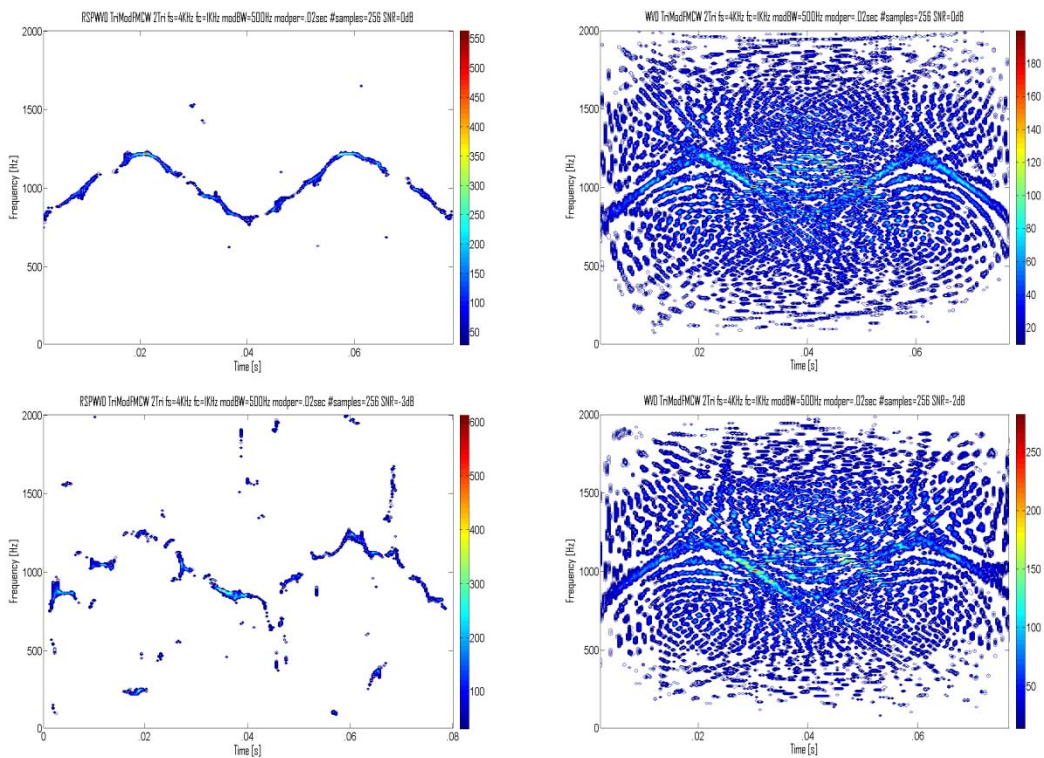
Figure 8: Comparative plots of the triangular modulated FMCW low probability of intercept radar signals (RSPWVD (left-hand side) vs. the WVD (right-hand side)). The SNR for the top row is 10dB, for the middle row is 0dB, and for the bottom row is the lowest detectable SNR(-3dB for RSPWVD; -2 dB for WVD).In general, the RSPWVD signal appears more localized ('thinner') than does the WVD signal, and has no cross-term interference, compared to the WVD.

IV. Discussion

This section will elaborate on the results from the previous section.

From Table 1, the RSPWVD outperformed the WVD in average percent error: carrier frequency (2.07% vs. 2.46%), modulation bandwidth (3.33% vs. 5.63%), modulation period (2.44% vs. 4.51%), and chirp rate (4.57% vs. 7.77%). The RSPWVD also outperformed the WVD in average: percent detection (95.6% vs. 74.6%), lowest detectable SNR (-3.11db vs. -2.23db), relative processing time (0.0177s vs. 0.443s), time-frequency localization (x-direction) (0.57% vs. 1.68%), and time-frequency localization (y-direction) (1.64% vs. 4.04%).

The cross-term interference of the WVD accounts for its: slower relative processing time, lower percent detection, and poorer lowest detectable SNR.

The RSPWVD reduces cross-term interference and has a more localized ('tighter') signal, accounting for its lower average percent error for: carrier frequency, modulation bandwidth, modulation period, and chirp rate – and accounting for its better time-frequency localization (x and y direction).

V. Conclusions

Digital intercept receivers, whose main job is to detect and extract parameters from low probability of intercept radar signals, are currently moving away from Fourier-based analysis and towards classical time-frequency analysis techniques, such as the WVD. Though classical time-frequency analysis techniques are an improvement over Fourier-based analysis techniques, classical time-frequency analysis techniques, in particular the WVD, suffer from cross-term interference, which can make the time-frequency representation hard to read, especially if the components are numerous or close to each other, and the more so in the presence of noise. This lack of readability may equate to less accurate signal detection and parameter extraction metrics, potentially placing the intercept receiver signal analyst's platform in harm's way. This paper examined a potential solution to this problem: the reassignment method, in particular, the RSPWVD signal processing technique, which was found to reduce cross-term interference, making the time-frequency representation much easier to read, leading to more accurate signal detection and parameter extraction metrics. The RSPWVD signal processing technique by-and-large outperformed the WVD signal processing technique in every metrics category. More accurate characterization metrics could well translate into saved equipment and lives.

Future plans include continuing to analyze low probability of intercept radar waveforms (such as the

frequency hopping and the triangular modulated FMCW), using additional signal processing techniques.

References Références Referencias

1. [ANJ09] Anjaneyulu, L., Murthy, N., Sarma, N., A Novel Method for Recognition of Modulation Code of LPI Radar Signals. International Journal of Recent Trends in Engineering, Vol. 1, No. 3, pp. 176-180, May 2009.
2. [AUG94] Auger, F., Flandrin, P., The Why and How of Time-Frequency Reassignment. IEEE International Symposium on Time-Frequency and Time-Scale Analysis, pp. 197-200, 1994.
3. [AUG95] Auger, F., Flandrin, P., Improving the Readability of Time-Frequency and Time-Scale Representations by the Reassignment Method. IEEE Transactions on Signal Processing, 43(5):1068-1089, 1995.
4. [BOA03] Boashash, B., Time Frequency Signal Analysis and Processing: A Comprehensive Reference. Elsevier, Oxford, England, 2003.
5. [GUL07] Gulum, T., Autonomous Non-Linear Classifications of LPI Radar Signal Modulations. Thesis, Naval Postgraduate School, Monterey, CA, 2007.
6. [GUL08] Gulum, T., Pace, P., Cristi, R., Extraction of Polyphase Radar Modulation Parameters Using a Wigner-Ville Distribution-Radon Transform. IEEE International Conference on Acoustics, Speech, and Signal Processing, Las Vegas, NV, April 2008.
7. [HAN00] Han, S., Hong, H., Seo, D., Choi, J., Target Position Extraction Based on Instantaneous Frequency Estimation in a Fixed-Reticle Seeker. Opt. Eng., Vol. 39, pp. 2568-2573, September 2000.
8. [HIP00] Hippenstiel, R., Fargues, M., Moraitakis, I., Williams, C., Detection and Parameter Estimation of Chirped Radar Signals. Final Report, Naval Postgraduate School, Monterey, CA, Jan. 10, 2000.
9. [LIA09] Liang, Y., Zhang, L., Xing, M., Bao, Z., High-Speed Ground Moving Target Detection Research Using Triangular Modulation FMCW. Front. Electr. Electron. Eng., China, 4(2), pp. 127-133, 2009.
10. [LIW08] Li, W., Dan, M., Wang, X., Li, D., Wang, G., Fast Estimation Method and Performance Analysis of Frequency Modulation Rate Via RAT. Proceedings of the 2008 IEEE International Conference on Information and Automation, Zhangjiajie, China, pp. 144-147, June 20-23, 2008.
11. [LIX08] Li, X., Bi, G., A New Reassigned Time-Frequency Representation. 16th European Signal Processing Conference, Lausanne, Switzerland, pp. 1-4, August 25-29, 2008.
12. [LIY03] Li, Y., Xiao, X., Recursive Filtering Radon-Ambiguity Transform Algorithm for Detecting Multi-LFM Signals. Journal of Electronics (China), Vol. 20, No. 3, pp. 161-166, May 2003.
13. [MIL02] Milne, P., Pace, P., Wigner Distribution Detection and Analysis of FMCW and P-4 Polyphase LPI Waveforms. Proceedings of ICASSP, Orlando, FL, pp. 3944-3947, 2002.
14. [OZD03] Ozdemir, A., Time-Frequency Component Analyzer. Dissertation, Bilkent University, Ankara, Turkey, Sept. 2003.
15. [PAC09] Pace, P., Detecting and Classifying Low Probability of Intercept Radar. Artech House, Norwood, MA, 2009.
16. [PAP95] Papandreou, A., Boudreaux-Bartels, G.F., Kay, S., Detection and Estimation of Generalized Chirps Using Time-Frequency Representations. 1994 Conference Record of the Twenty-Eighth Asilomar Conference on Signals, Systems and Computers, pp. 50-54, 1994.
17. [QIA02] Qian, S., Introduction To Time-Frequency and Wavelet Transforms. Prentice Hall, Upper River, NJ, 2002.
18. [RAN01] Rangayyan, R., Krishnan, S., Feature Identification in the Time-Frequency Plane by Using the Hough-Radon Transform. Pattern Recognition, Vol. 34, pp. 1147-1158, 2001.
19. [STE96] Stephens, J., Advances in Signal Processing Technology for Electronic Warfare. IEEE AES Systems Magazine, pp. 31-38, November 1996.
20. [WAJ08] Wang, Y., Jiang, Y., Detection and Parameter Estimation of Multi component LFM Signal Based on the Cubic Phase Function. EURASIP Journal on Advances in Signal Processing, Vol. 2008, Article ID 743985, pp. 1-7, 2008
21. [WAN10] Wang, P., Li, H., Djurovic, I., Himed, B., Integrated Cubic Phase Function for Linear FM Signal Analysis. IEEE Transactions on Aerospace and Electronic Systems, to appear, 2010.
22. [WEI03] Wei, G., Wu, S., Mao, E., Analysis of Multicomponent LFM Signals Using Time-Frequency and The Gray-Scale Inverse Hough Transform. IEEE Workshop on Statistical Signal Processing, pp. 190-193, September 28 – October 1, 2003.
23. [WIL06] Wiley, R., ELINT: The Interception and Analysis of Radar Signals. Artech House, Norwood, MA, 2006.
24. [WON09] Wong, K., Davidson, T., Abelkader, S., Detection of Low Probability of Intercept Radar Signals. Defence R&D Canada – Ottawa Contract Report 2009-142, September 2009.
25. [XIA99] Xia, X., Chen, V., A Quantitative SNR Analysis for the Pseudo Wigner-Ville Distribution. IEEE Transactions on Signal Processing, Vol. 47, No. 10, pp. 2891-2894, October, 1999.

Design of a Solar Charging Station for Electric Vehicles in Shopping Malls

By C Peña & M Céspedes

Universidad Nacional del Centro del Perú

Abstract- In this article, we present the design, sizing and modeling of a grid-connected solar charging station for recharging electric vehicles in shopping malls. The applied method consists of an analysis of the solar resource available at the location of the shopping mall, as well as the analysis, evaluation and selection of the components of the grid-connected photovoltaic system with the support of simulation software such as PVsyst and Helioscope, as well as analysis, evaluation and selection of the components of the charging points of electric vehicles and finally the economic analysis of the solar charging station in the shopping mall.

GJRE-F Classification: FOR Code: 090699

DESIGNOFASOLARCHARGINGSTATIONFORELECTRICVEHICLESINSHOPPINGMALLS

Strictly as per the compliance and regulations of:

Design of a Solar Charging Station for Electric Vehicles in Shopping Malls

C Peña[α] & M Céspedes[σ]

Abstract- In this article, we present the design, sizing and modeling of a grid-connected solar charging station for recharging electric vehicles in shopping malls. The applied method consists of an analysis of the solar resource available at the location of the shopping mall, as well as the analysis, evaluation and selection of the components of the grid-connected photovoltaic system with the support of simulation software such as PVsyst and Helioscope, as well as analysis, evaluation and selection of the components of the charging points of electric vehicles and finally the economic analysis of the solar charging station in the shopping mall.

I. Introduction

There are two alternatives to mitigate greenhouse gas emissions, the first is the electrification of transport and the second is the generation of electricity using renewable energy.

For electro mobility to be successful, it is necessary that the used energy comes from renewable energies such as solar, wind or biomass.

This article proposes the design of a solar charging station for electric vehicles in shopping malls. Which consists of the dimensioning of a grid-connected photovoltaic system and analysis, evaluation and selection of the charging components for electric vehicles.

In this sense, one of the ways to charge the energy of the batteries of electric vehicles is to use the recharging points that the shopping mall install in their parking lots, all this while users come to make purchases or spend their leisure time in the malls.

II. Methodology

a) Background
i. Current situation of electric vehicles

Currently the battery of new versions of electric vehicles has a capacity that varies between 38 and 64 kWh, except for high-end cars such as the Taycan by Porsche and the Model S by Tesla, whose capacity varies between 70 and 100 kWh. In most electric cars the internal charger is 7.2 kW except for Tesla which is 10 kW. Figure 1 shows the electric vehicle charging system [1].
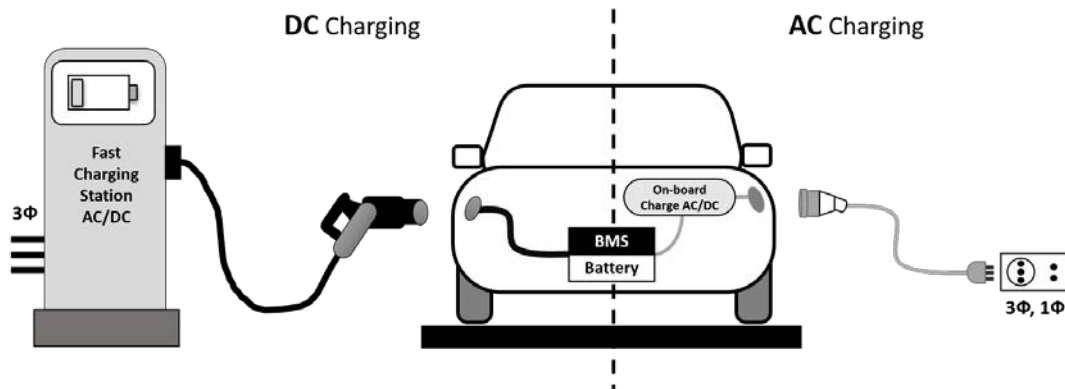
Figure 1: Electric vehicle charging system

The time (hours) of charging in AC of the battery (kWh) of the electric vehicle will depend on the power of the internal charger (kW) of the electric vehicle.
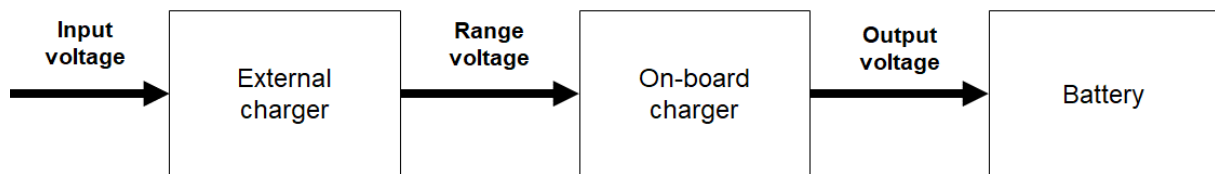
Figure 2: Charging an electric vehicle with an external charger

Author α: Faculty of Electrical Engineering, Universidad Nacional del Centro del Perú, Huancayo, Peru. e-mail: cpena.ugsa@gmail.com
Author σ: Faculty of Mechanical-Electrical Engineering, Universidad Nacional Pedro Ruiz Gallo, Lambayeque, Peru.

Below are the technical data of 2019's electric vehicles.

Table 1: Technical data of electric vehicles

Make and Model of the Car	Hyundai Ioniq Eléctrico	Kia eSoul Standard	Kia eSoul Autonomía Extendida	Nissan Leaf S	Nissan Leaf S Plus	BYD E5-400
Type	EV	EV	EV	EV	EV	EV
Year of production	2019	2019	2019	2019	2019	2019
Maximum speed (km/h)	165	155	167	144	157	130
Battery capacity (kWh)	38.3	39.2	64	40	62	60.5
Autonomy (km)	293	277	452	270	385	400
Motor power (kW)	100	100	150	110	160	160
Torque (N.m.)	295	395	395	320	340	310
Internal charger power (kW)	7.2	7.2	7.2	6.6	6.6	7
Fast charge time from 100 kW to 80% (min)	54	42	42	40 (50kW)	45 y 60 (50 kW)	
Price (USD.)	38639.00	40121.00	47320.00	29990.00	36550.00	34760.00

Table 2: Battery capacity and autonomy for one hour of charge

Brand and model of the car	Battery capacity for one hour of charge (kWh)	Autonomy for one hour of charge (km)
Hyundai Ioniq Eléctrico	7.2	55.08
Kia eSoul Standard	7.2	50.88
Kia eSoul Autonomía Extendida	7.2	50.85
Nissan Leaf S	6.6	44.55
Nissan Leaf S Plus	6.6	40.98
ByD E5-400	7.0	46.28
Porsche Taycan 4S	9.6	49.33
Porsche Taycan Turbo	9.6	46.25
Tesla Model S - Perfomance	10	56.00
Average	8.00	49.00

ii. *Current situation of charging stations with renewable energies*

In Spain, the SIRVE project (Integrated Systems for Recharging Electric Vehicles) was developed, the objective of which is to desaturate the electrical network in LV, if the aggregate demand for fast charging and moderate charging systems exceeds the capacity of the line or of the transformation malls from which it is supplying. The SIRVE project is made up of a 1kWp photovoltaic system, which provides power to the 30 kWh lithium batteries. [2]

In 2017, Shanghai launched its first solar-powered charging station for electric vehicles as a test. It is made up of 40 solar panels on the roof of the building. In addition, it had backup batteries and was connected to the electrical network. In half an hour with fast charge the battery was charged with 70% and around two hours to completely fill the electric vehicle. [3]

b) *Descriptive memory*

i. *Description of the study area*

For the study analysis of the project, the "Molina Plaza" shopping mall was selected, located in the La Molina district, Lima, Peru.

The Molina Plaza shopping mall was selected for two reasons. The first is that it is located in an area of considerable solar radiation during the year. According to the Global Solar Atlas, the specific output photovoltaic energy is 1435 kWh/kWp [4]. The second reason is because the residents of the district have enough purchasing power to buy electric vehicles.

Table 3: Geographical data of the study area

Geographical data	
South latitude	12° 05' 28"
West longitude	76° 57' 01"
Medium altitude	234 m

Table 4: Temperature data of the study area

Temperature Data	
Maximum temperature	28 °C
Medium temperature	18 °C
Minimum temperature	11 °C

ii. *Objectives*

- Dimension the grid-connected photovoltaic system to provide 50% of the energy needed by electric vehicle batteries during the hours that the solar resource is available.

- Encourage and spread the use of renewable energy for electrified transport.

c) *Memory of Justifying Calculations*
   i. *Solar irradiation*

   With geographic coordinates and using NASA's Power Data Access Viewer application. Monthly global horizontal mean irradiance is obtained from the NASA database (1983– 2005) and NASA (1984-2013).

Table 5: NASA Monthly Weather Values

	Jan.	Feb.	Mar.	Apr.	May.	Jun.	Jul.	Aug.	Sep.	Oct.	Nov.	Dec.	
Hor. global	6.48	6.32	6.72	6.17	5.04	3.86	3.73	4.09	4.83	5.84	6.31	6.52	kWh/m^2.day

The optimal inclination is determined using the following formula:

$$\beta_{opt} = 3.7 + 0.69\phi \qquad (1)$$

Where:

β_{opt} : optimal tilt angle in degrees.

ϕ : latitude of unsigned place in degrees.

The optimal inclination of the photovoltaic modules is approximately 12°, using NASA's Power Data Access Viewer application the monthly global mean irradiation on a surface tilted at its optimal angle, facing north.

Table 6: Monthly average global irradiation on a 12° inclined surface

	Jan.	Feb.	Mar.	Apr.	May.	Jun.	Jul.	Aug.	Sep.	Oct.	Nov.	Dec.	Año	
Global Average Monthly Irradiation in a 12° angle	6.63	6.33	6.79	6.62	5.87	4.53	4.24	4.37	4.90	5.84	6.41	6.72	5.77	kWh/m^2.day

The month that has the least irradiation according to the previous table, is the month of July [5][6]. If the irradiance is considered equal to 1000 W/m^2, then the peak solar hours (HSP) equals 4.24 h.

ii. *Calculation of the energy consumed by charging electric vehicles*

To calculate the energy consumed, the following should be considered:

- Eight Wallbox chargers [7] 11 kW are being taken into account for charging electric vehicles.
- According to Table 2, the average battery capacity per 1 hour of charge is equivalent to 8 kWh. Thus, if the charging time is 1 hour, 8 vehicles can be charged simultaneously every hour.
- The energy consumed from 9:00 a.m. until 06:00 p.m. is 576 kWh, while the energy consumed from 06:00 p.m. until 09:00 p.m. is 192 kWh.
- The grid-connected photovoltaic system will be dimensioned to provide 50% of the energy consumed during 09:00 a.m. until 06:00 p.m. which is equivalent to 288 kWh.
- The chargers will be available from 09:00 a.m. until 09:00 p.m. Being 12 hours the available time considering the 37.5% supplied by the photovoltaic system and 62.5% by the electrical network.

The energy consumed during the day is estimated to be 768 kWh. If the charging time increases and considering the number of cars constant for the respective charging time (1, 2, 3 or 4), the energy consumed is the same, the only thing that changes is the number of cars supplied per day.

Table 7: Energy consumed by charging electric vehicles

Loading time (h)	1		2		3		4	
Hours available	Quantity EV (und.)	Energy EV (kWh)	Quantity EV (und.)	Energy EV (kWh)	Quantity EV (und.)	Energy EV (kWh)	Quantity EV (und.)	Energy EV (kWh)
09:00 a.m. – 10:00 a.m.	8	64	8	128	8	192	8	256
10:00 a.m. – 11:00 a.m.	8	64						
11:00 a.m. – 12:00 p.m.	8	64	8	128				
12:00 p.m. – 01:00 p.m.	8	64						
01:00 p.m. – 02:00 p.m.	8	64	8	128	8	192		
02:00 p.m. – 03:00 p.m.	8	64					8	256
03:00 p.m. – 04:00 p.m.	8	64	8	128				
04:00 p.m. –05:00 p.m.	8	64			8	192		
05:00 p.m. –06:00 p.m.	8	64	8	128				
06:00 p.m. –07:00 p.m.	8	64					8	256
07:00 p.m. –08:00 p.m.	8	64	8	128	8	192		
08:00 p.m. –09:00 p.m.	8	64						
Total	96	768	48	768	32	768	24	768

Table 8: Technical specifications Wallbox charger

Technical specifications Wallbox charger 11 kW	
Brand and model	EV Box
Charging mode	Mode 3
Connector load capacity	11 kW
Number of connectors	1
CE certification	Yes
Output values	1 phase o 3 phases, 230 V - 400 V, 16 A - 32 A
Temperature range	Since -25°C until 60°C
Cable length	4 m.
RH	0.95
Activation / Identification	Automatic start / card or keychain RFID
Status indicator	Ring LED

iii. *Calculation of the power of the photovoltaic generator*

The power of the photovoltaic generator is determined using the following formula:

$$P_G = \frac{1.11\, W_d}{HSP.PR} \qquad (2)$$

Where:

P_G : Photovoltaic generator power in Wp.

W_d : Daily energy consumption for the calculation of the PV generator in kWh, which is equivalent to 288 kWh.

HSP: Peak solar hours in h, which equals 4.24 h.

PR : Energy performance of the installation, which is equivalent to 80%.

03 photovoltaic generators will be required whose power amounts to 31415.09 Wp. Considering 330 Wp polycrystalline photovoltaic modules, from the manufacturer Amerisolar [8]. Thus, the power of each real photovoltaic generator is 31350 Wp. Each one will be made up of 95 photovoltaic modules, distributed in 5 chains of 19330 Wp polycrystalline photovoltaic modules.

Table 9: Technical specifications of the photovoltaic module

Technical Specifications of the Selected Photovoltaic Module	
Type	Policristalino
Power	330 Wp
Imp	8.85 A
Vmp	37.3 V

Isc	9.26 A
Voc	45.9 V
β	-0.14229 V/°C
α	0.00463 A/°C

Table 10: Technical characteristics of the photovoltaic generator

Technical characteristics of the photovoltaic generator	
Generator power PV	31350 Wp
Module power PV	330 Wp
Number of chains	5
Number of PV modules, by serie	19
Number of PV modules	95
Isc, by chain	9.26 A
Voc , by chain	872.10 V

iv. *Selection of grid interconnect inverters*

Each photovoltaic generator will be connected to a grid interconnection inverter [9]. The following parameters must be taken into account when selecting the Inverter:

- Inverter nominal power, must be between 80% and 90% of the power of the photovoltaic generator.

$$P_{Inv} = 0.8 \dots 0.9\, P_G \qquad (3)$$

Where:

P_{inv} : Inverter power in W.
P_G : Photovoltaic generator power in Wp.

- Inverter MPP follower voltage range($U_{inv.min}$ … $U_{inv.máx}$):

This range must contain the maximum and minimum values that the photovoltaic generator can supply at the point of maximum power specified for a cell temperature of -10° C and 70° C respectively($U_{Gmpp\,(70°C)}$ y $U_{Gmpp\,(-10°C)}$).In both cases with an irradiance of 1000 W/m².

$$\boldsymbol{U_{inv.mín} \leq U_{Gmpp\,(70°C)}} \qquad (4)$$

$$U_{Gmpp\,(70°C)} = N_S \cdot U_{mpp\,(70°C)} \qquad (5)$$

$$U_{mpp\,(70°C)} = U_{mpp} + \beta \cdot (T - 25) \qquad (6)$$

$$\boldsymbol{U_{inv.máx} \geq U_{Gmpp\,(-10°C)}} \qquad (7)$$

$$U_{Gmpp\,(-10°C)} = N_S \cdot U_{mpp\,(-10°C)} \qquad (8)$$

$$U_{mpp\,(-10°C)} = U_{mpp} + \beta \cdot (T - 25) \qquad (9)$$

Where:

U_{Gmpp} : Voltage of the photovoltaic generator at its maximum power point (V) at a certain temperature.
U_{mpp} : Voltage of the photovoltaic module at its maximum power point (V) at standard measurement conditions.
N_S: Number of panels in series.
β: Voltage coefficient - module temperature (V/°C).
T: Temperature (°C).

- Inverter maximum voltage ($U_{máx.\,vacío}$):

The inverter must withstand the maximum voltage that the open-circuit photovoltaic generator can produce with a cell temperature of -10° C and an irradiance of 1000 W/m².

$$U_{máx.vacío} \geq U_{Goc\,(-10°C)} \qquad (10)$$

$$U_{Goc\,(-10°C)} = N_S \cdot U_{Goc\,(-10°C)} \qquad (11)$$

$$U_{oc\,(-10°C)} = U_{oc} + \beta \cdot (T - 25) \qquad (12)$$

Where:

U_{Goc}: It is the voltage of the photovoltaic generator in vacuum (V) at a certain temperature.
U_{oc} : It is the voltage of the photovoltaic module in vacuum (V) at standard measurement conditions.

- Maximum intensity ($I_{inv.\,máx}$):

The inverter must withstand the short-circuit current of the generator with a cell temperature of 70 ° C and an irradiance of 1000 W / m².

$$I_{máx.vacío} \geq I_{Gsc\,(-10°C)} \qquad (13)$$

$$I_{Gsc\,(70°C)} = N_P \cdot I_{sc\,(70°C)} \qquad (14)$$

$$I_{sc\,(70°C)} = I_{sc} + \alpha \cdot (T - 25) \qquad (15)$$

Where:

I_{Gsc}: It is the maximum short-circuit current intensity of the photovoltaic generator in (A) at a given temperature.
I_{sc}: It is the short circuit current intensity of the photovoltaic module (A) or string at standard measurement conditions.
N_P: Parallel panel chain number.
α: Current coefficient - module temperature (A/°C).
T: Temperature (°C).

Taking into account the above, 03 three-phase inverters for grid interconnection of 27 kW - 380/220 VAC, from the Fronius brand [10] with their respective Smart Meter 50kA-3 are selected.

Table 11: Parameters calculated to select the inverter

Parameters calculated to select the grid interconnect inverters	
Inverter power	25080 … 28215 W
Minimum value of the MPP voltage range	587.10 V
Maximum value of MPP voltage range	803.32 V
Maximum no-load voltage	966.72 V
Maximum intensity	47.35 A

Table 12: Main technical specifications of the inverter

Main technical specifications of the inverter	
Brand and model	Fronius Eco 27.0-3-S
Inverter power	27 kW
MPP voltage range (Ucc min - Ucc max.)	580 V – 850V
Maximum no-load voltage	1000 V
Maximum PV input intensity	47.7 A
Maximum short-circuit current per PV series	71.6 A
Number of MPP followers	1
Number of DC inputs	6
Maximum PV generator output	37.8 kWp
Link to the network	3~ NPE 400/230, 3~ NPE 380/220 V
Frequency	50/60 Hz
Nominal output current at 400 V	39 A

v. *Selection of protection devices*

PV generator protection: For each photovoltaic generator, 1 string box will be installed to connect 5 chains in parallel with 19 photovoltaic modules connected in series. Each string box must have at least 10 cylindrical rifle bases for 10 x 38 mm fuses.

- The fuse rating is determined with the following formula:

$$I_F = 1.5 \ ... \ 2I_{SC} \qquad (16)$$

Where:

I_{sc}: It is the short circuit current intensity of the photovoltaic module (A) or string at standard measurement conditions.

I_F: It is the current intensity (A) that the fuse supports.

- The assigned voltage is determined with the following formula:

$$U_F \geq 1.2 \ U_{GOC'} \qquad (17)$$

Where:

$U_{GOC'}$: It is the voltage of the photovoltaic generator in vacuum (V).

U_F: It is the rated voltage (V) that the fuse supports.

- In the string box, for each chain there must be two 16 A (gR) fuses with a rated voltage of 1000 VDC cylindrical 10 x 38 mm. One will be connected to the positive pole and the other to the negative pole of each chain.

Investor Protection: A thermomagnetic switch will be placed at the output of each inverter, having to meet the output characteristics of the inverter.:

- Nominal intensity: $I_n \geq 48.26 \ A$
- Nominal working voltage: $U_n = 380 \ VAC$

Wallbox charger protection: A thermomagnetic switch will be placed in each circuit of each 11 kW Wallbox charger.:

- Nominal intensity: $I_n \geq 19.66 \ A$
- Nominal working voltage: $U_n = 380 \ VAC$

vi. *Network connection*

For the connection of the electric chargers and the grid interconnection inverters, a new MV power supply (10 kV or 22.9 kV) and a new primary network will be necessary. The conventional three-phase substation must have a 250 kVA encapsulated dry transformer - 10-22.9 / 0.38-0.22 kV.

For the analysis, the inverters are considered as a load, and a power factor of 0.85.

Table 13: Load chart

Load	Pot.unit (kW)	I. currents total (A)	Quantity(Und.)	P. total (kW)	I. currentstotal (A)	Pot. transformer (kVA)
Grid connection inverter - de 27 kW. 380/220 V- Fronius	27	48.26	3	81	144.78	
Wallbox charger 11Kw – 380/220 V	11	19.66	8	88	157.28	250
Street lighting luminaires	0.07	0.00040	8	0.56	0.0032	
	Total			169.56	302.0632	250

d) Estimated annual energy produced per year
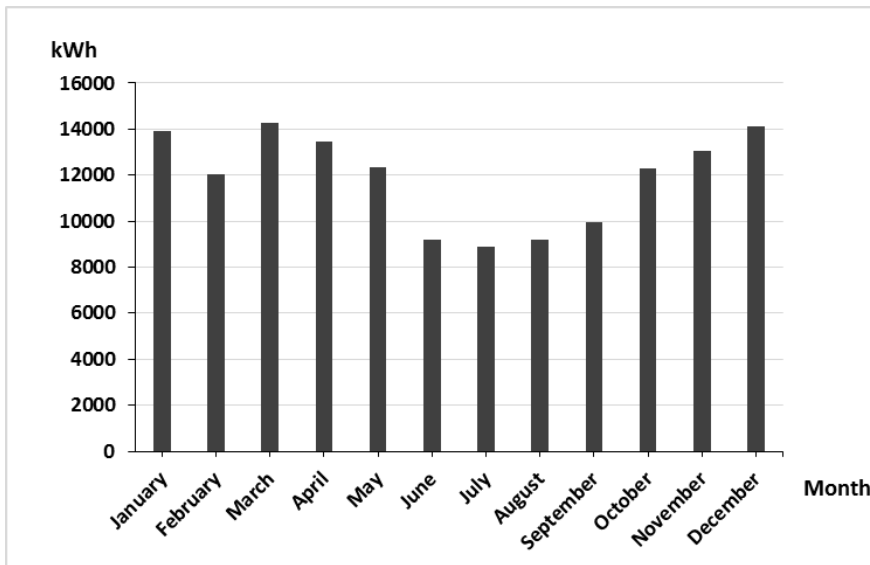
Figure 3: Estimated annual energy produced per year

With the data in Table 6 and 10, the annual energy produced by the grid-connected photovoltaic system is calculated. Which amounts to 142705 kWh.

The plant factor is 17.32%. According to the Global Solar Atlas [11], the energy produced is 135675 kWh and the specific production 1443 kWh / kWp.

Table 14: Energy produced annually

Month	Monthly energy (kWh)
January	13932
February	12014
March	14268
April	13462
May	12335
June	9212
July	8910
August	9183
September	9964
October	12272
November	13035
December	14121
Annual (kWh)	142708

The solar charging station will be available from 09:00 a.m. until 09:00 p.m. Being a total period of 12 hours. The energy produced by the photovoltaic system during the first hours of the morning may be used for other uses such as refrigeration, ventilation or any other auxiliary circuit. With the information obtained from the report generated by the Global Solar Atlas. The energy produced by the photovoltaic system in the early hours of the day destined for others would be 14666 kWh per year.
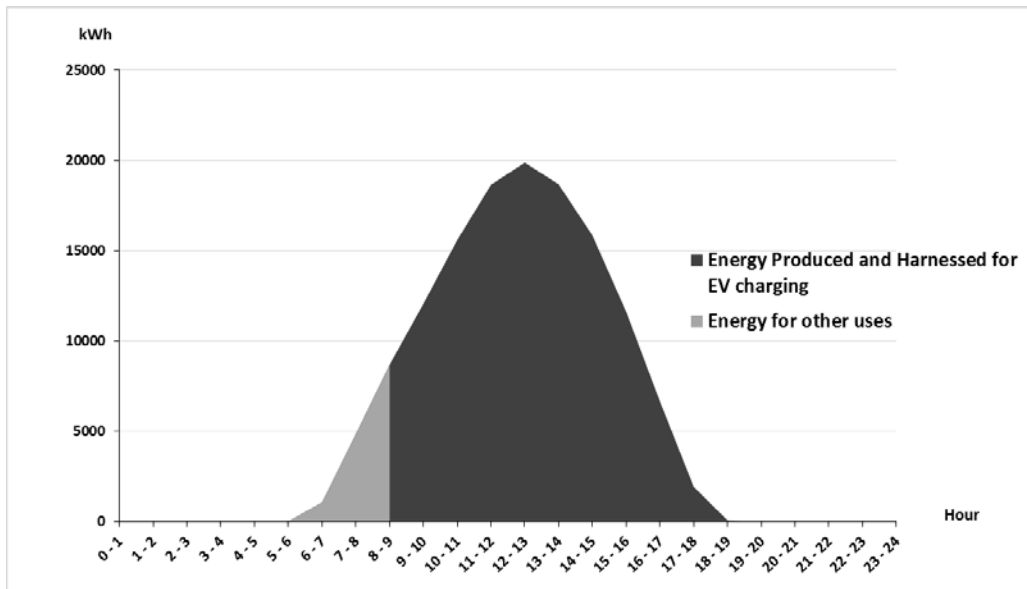
Figure 4: Estimated annual energy produced per year

e) Estimation of the reduction of CO_2 emissions

According to the Peruvian Ministry of Energy and Mines, the emission reduction factor [12] for 2016 is 0.4082 tCO_2/MWh. They consider a degradation factor of 0.5% of the photovoltaic modules. It is estimated that 1111.33 tCO_2 would no longer be emitted.

Table 15: Reduced CO_2 emissions

Period	Energy produced (kWh)	Emission factor (tCO_2/MWh)	CO_2 emissions (tCO_2)
1	142708	0.4082	58.25
2	141994	0.4082	57.96
3	141284	0.4082	57.67
4	140578	0.4082	57.38
5	139875	0.4082	57.10
6	139176	0.4082	56.81
7	138480	0.4082	56.53
8	137788	0.4082	56.25
9	137099	0.4082	55.96
10	136413	0.4082	55.68
11	135731	0.4082	55.41
12	135052	0.4082	55.13
13	134377	0.4082	54.85
14	133705	0.4082	54.58
15	133037	0.4082	54.31
16	132372	0.4082	54.03
17	131710	0.4082	53.76
18	131051	0.4082	53.50
19	130396	0.4082	53.23
20	129744	0.4082	52.96
Total			**1111.35**

f) Simulation with PVsyst software and Helioscope

  i. *Simulation with the software PVsyst*

To perform the simulation in the PVsyst software, the Typical Meteorological Year (TMY) was selected, which the software obtains from the PVGIS platform data. The PVGIS platform works with the 2005-2015 database, provided by the National Renewable Energy Laboratory (NREL).The main parameters of the system and the main results of the simulation with the PVsyst software are as follows:

Table 16: Main parameters for the PVsyst simulation

Main parameters for the PVsyst simulation	
PV field orientation and inclination	Azimuth 0° y 12° tilt
PV modules	Model AS6P33-330 Pnom.330 Wp
PV set	285 modules Pnom total 94.05 kWp
Investor	Model Fronius Eco 27.0-3-S
Amount of Investors	3 units Pnom. Total 81 kW AC

Table 17: Main simulation results in PVsyst

Main simulation results in PVsyst 6.8.1.	
Energy produced	138.3 MWh/year
Specific production	1471 kWh/kWp/year
Performance index (PR)	86.58%

ii. *Simulation with Helioscope software*

The Helioscope software performs the simulation with the Typical Meteorological Year (TMY), which it obtains from the data from Meteonorm. In addition, it distributes the photovoltaic modules on the roof of the Molina Plaza shopping mall.

Table 18: Main results of the simulation in Helioscope

Main results of the simulation in Helioscope	
Energy produced	144.4 MWh/year
Specific Production	1535.5 kWh/kWp/year
Performance Index (PR)	78.2%
Investors	3 Fronius Eco 27.0-3-S. Total 81 kW AC
Chains	15
PV modules	285, Amerisolar, AS-6P-330. Total 94.1 kWp
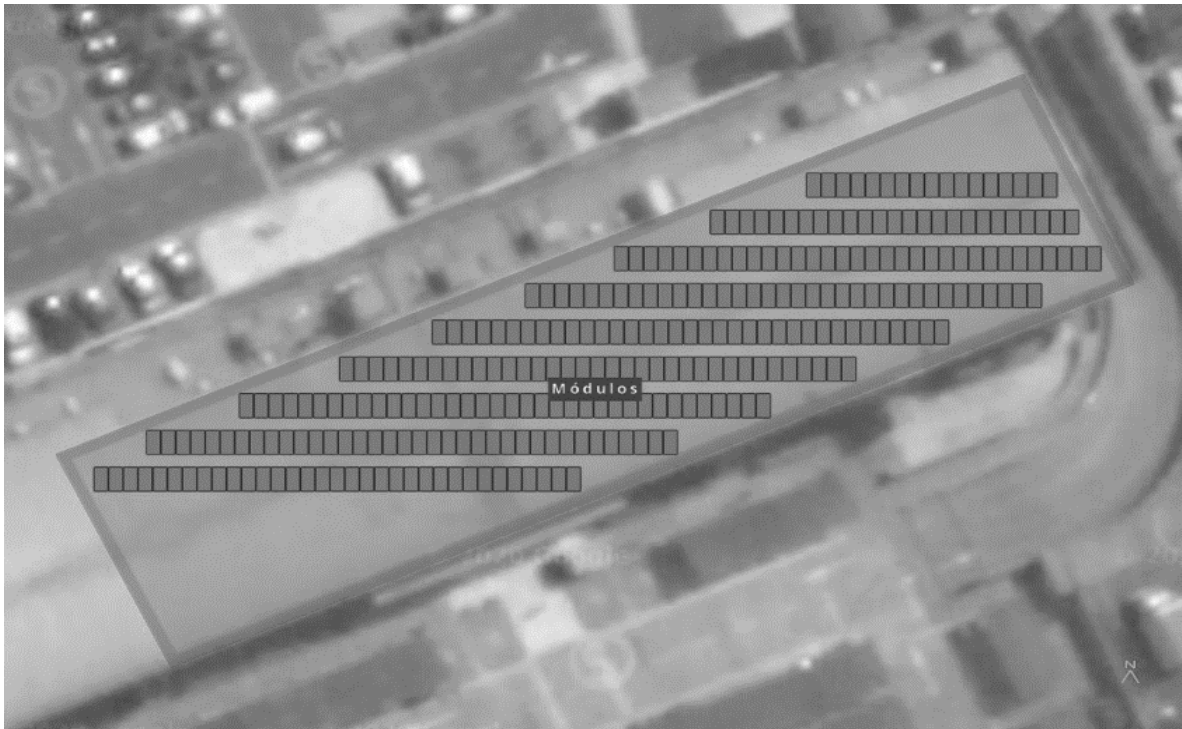
Figure 5: Distribution of photovoltaic modules with Helioscope
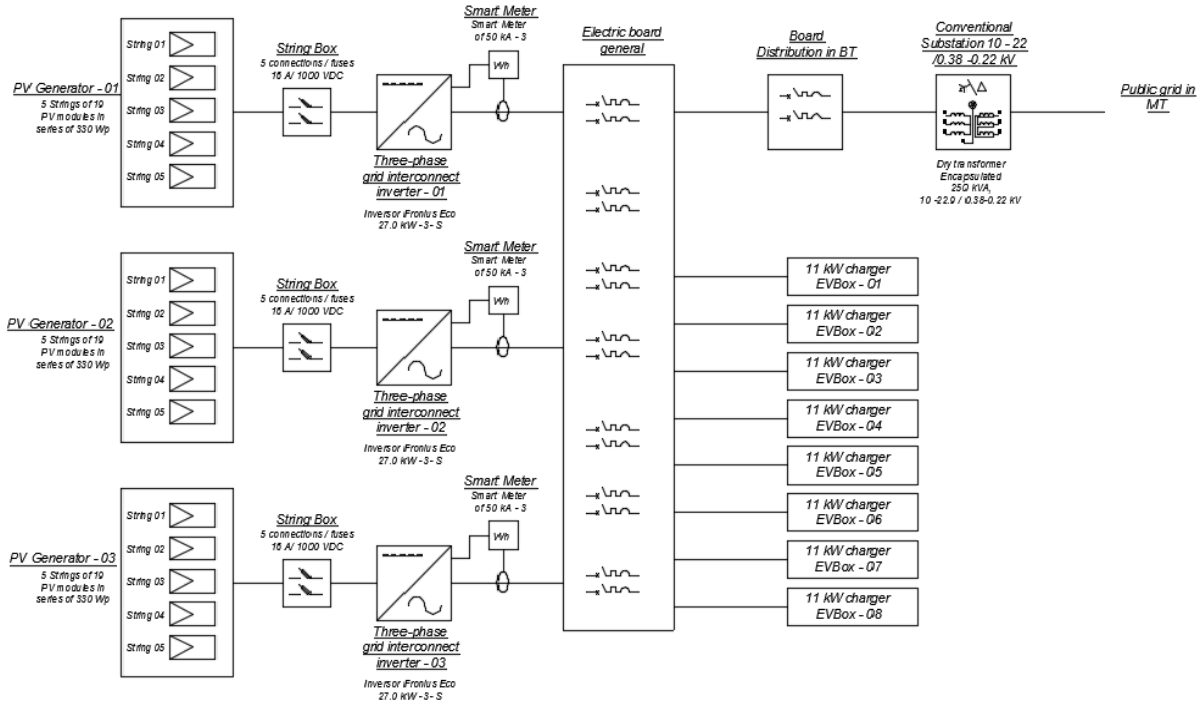
Figure 6: Blocks diagram

g) *Materials supply*

Table 19: Materials supply

Ítem	Description	Und.	Qty.	Price Unit.	Total
1.00	**Components of the photovoltaic system**				
	Polycrystalline photovoltaic modules330 Wp	und	285.00	563.90	160711.50
	Mains connection inverter 27 kW - three-phase - 380/220 VAC	und	3.00	19666.57	58999.71
	Aluminum fixing bracket for 19 panels	und	15.00	6090.48	91357.20
					S/.311068.41
2.00	**Additional components of the photovoltaic system**				
	Supply of electrical boards, string box, conductors and hardware, grounding.	glb	1.00	46660.26	S/.46660.26
3.00	**Wallbox chargers**				
	WallBox Charger - 11 kW. - 230 V a 230/400 V three phase - 50/60 Hz. - Connector Type 2 o Mennekes - Cable length 4m.	und	8.00	5252.12	S/.42016.96
4.00	Materials for medium voltage pipes and networks	und	1.00	7207.76	S/.7207.76
5.00	Materials of the conventional substation of 250 kVA 22.9-10 / 0.38-0.22 kV	glb	1.00	96056.18	S/.96056.18
6.00	Protective and sectional structure materials	glb	1.00	60684.36	S/.60684.36
	Total				S/.563693.93

Table 20: Total budget

Ítem	Detalle	Total
A	Suministro de materiales	563693.93
B	Montaje electromecánico	121329.17
C	Gastos adicionales aproximados	28252.20
D	Gastos administrativos	34870.00
	Total	S/.748145.30

h) Economic evaluation

To perform the investment valuation, it was necessary to determine the FC (Cash Flow). For this, it is necessary to determine the net operating flow, thus we consider the following parameters:

Table 21: Parameters to determine the operational cash flow

Parameters		
Item	Detail	Total
r	Discount rate	7.5%
d	Degradation rate	0.5%
e	Energy cost as a free client	0.1510 S/./kWh
i	Rate of inflation	2.0 %
s	Hourly rental price of each parking space	2.54 soles
p	Project period	20 years

Once the net operating flow has been determined, the net financial flow of the project is determined:

Table 22: Financial cash flow

Values		
Item	Detail	Total
NPV	Net present value	S/. 161113.86
IRR	Internal rate of return	10.04%
PRI	Return on investment period	8 years

For this project, the NPV is: S /. 161113.86, which indicates that the project is financially viable since the NPV is> 0.

In this case the IRR is 10.04%, compared to the discount rate, it is feasible to invest in a project under these conditions.

It is evident that the PRI period of time to recover the investment is up to about 8 years, which determines that it would make viable the start-up of the project under the proposed scenario.

III. Conclusions

- The project is economically viable, as the NPV and IRR are viable, and the return on investment time is around 8 years.
- The project is technically feasible, current technology would allow this project to be carried out.
- With this project, 1111.35 tCO2 would no longer be emitted, contributing to the environment and demonstrating that the use of renewable energy is the solution to environmental pollution.
- According to the simulations and calculations, the proposed objectives will be able to meet. More than 50% of the energy consumed by the charge of electric vehicles would be covered during the hours of 9:00 am - 6:00 pm.
- Interconnection inverters will be configured so that they do not inject energy into the public grid and are only used for self-consumption.
- The interconnect inverter will stop working if there is a grid disconnection. It is because the inverter needs to be synchronized with the frequency of the public electrical network.
- In order for the grid interconnection inverters to work with a backup system such as a generator set in the event of a disconnection from the public grid. It is recommended to make a modification and change the Smart Meter 50kA-3, for a Fronius PV system controller with its two accessories to optimize the operation of the photovoltaic system with the

generator set. The technical specifications of the generator set will be required. This solution is called Fronius Fronius PV - Genset Easy.

References Références Referencias

1. López Redondo, N. (June 11, 2020). Electric cars with the best price-to-autonomy ratio of the market with which car is most economical each kilometer of cargo[online]. Retrieved June 2020, 13, from Web site Electric Mobility: https://movilidadelectrica.com/coches-electricos-mejor-relacion-precio-autonomia/

2. Urbener. (2015). Project Serves, Integrated Systems for Recharging Electric Vehicles [online]. Retrieved May 25, 2020, from Urbener Web site: https://www.urbener.com/sirve

3. El País. (October 25, 2017). Shanghai debuts its first solar station to charge electric vehicles [online]. Retrieved May 20, 2020, from El País Web site: https://negocios.elpais.com.uy/shanghai-estrena-primera-estacion-solar-cargar-vehiculoselectricos.html

4. Global Solar Atlas. (February 2020). Global Solar Atlas [online]. Retrieved May 20, 2020, from Global Solar Atlas Web site: https://globalsolaratlas.info/map?c=12.097403,76.935883,11&s=%2012.090977,76.95035&m=site

5. González Pinzón, C. L., Ponce Corral, C., Valenzuela Nájera, R. A., & Atayde Campos, D. (2013).Selecting a solar photovoltaic system for an electric vehicle[online]. (U. A. Juárez, Ed.). Scientific and Technological Culture, 10(Extra 50 ,2), 11-26. Retrieved May 25, 2020, fromhttp://erevistas.uacj.mx/ojs/index.php/culcyt/article/view/927/863

6. Pereira Micena, R., Llerena P., O. R., de Queiróz Lamas, W., & Luz Silveira, J. (June 30, 2018). Technical study of the use of solar energy and biogas in electric vehicles in Ilhabela - Brazil[online]. Ingenius. Journal of Science and Technology (20), 58-69. Retrieved May 26, 2020, from https://ingenius.ups.edu.ec/index.php/ingenius/article/view/20.2018.06

7. EVBox. (s.f.). Technical specifications of electric vehicle chargers [online]. Retrieved May 20, 2020, from EVBox Web site: https://evbox.com/en/products/business-chargers/businessline

8. Amerisolar (s.f). AS-6P Module Technical Specifications [online]. Retrieved May 20, 2020, from Amerisolar Web site: http://www.weamerisolar.com/english/product/pro1/255.html

9. Castejón, A., & Santamaría, G. (2010). Photovoltaic solar installations. Madrid: Editorial Editex.

10. Fronius (2014). Fronius Eco Inverter Technical Specifications 27.0-3-S [online]. Retrieved May 20, 2020, from Amerisolar Web site: https://www.fronius.com/es-es/spain/energia-solar/productos/todos-losproductos/inversor/fronius-eco/fronius-eco-27-0-3-s.

11. Global Solar Atlas. (February 2020). Global Solar Atlas Report[online]. Retrieved Jun 7, 2020, from Global Solar Atlas Web site: https://globalsolaratlas.info/map?c=-12.091024,-76.950302,11&s=-12.090977,-76.95035&m=site&pv=ground,0,12,94.05.

12. Directorate-General for Energy Efficiency - Ministry of Energy and Mines, Peru (2018). Monthly Renewable Energy Bulletin (2018) [power point slides].

New Type of Unipolar Generator

By F. F. Mende

Abstract- Application in the unipolar engines of samariumcobalt magnets opens the new prospects of creating the engines with the large rotational moment, since. such magnets possess the great magnetic field, which cannot they will reach in other magnets. However, the creation of engines are connected with the need of using the brushes, friction against the external rim of the revolving disk and against its axis. Since the speed of rotation of the rim of disk is great, brushes rapidly are worn out, what is an essential drawback in this construction.

In the article is represented the construction and the experimental mock-up of the unipolar generator, in which there are no brushes. This is achieved by the use of two ball bearings of those inserted in each other.

Keywords: unipolar generator, unipolar engine, magnet, brush, ball bearing.

GJRE-F Classification: FOR Code: 090699

NEWTYPEOFUNIPOLARGENERATOR

Strictly as per the compliance and regulations of:

New Type of Unipolar Generator

F. F. Mende

Abstract- Application in the unipolar engines of samarium-cobalt magnets opens the new prospects of creating the engines with the large rotational moment, since. such magnets possess the great magnetic field, which cannot they will reach in other magnets. However, the creation of engines are connected with the need of using the brushes, friction against the external rim of the revolving disk and against its axis. Since the speed of rotation of the rim of disk is great, brushes rapidly are worn out, what is an essential drawback in this construction.

In the article is represented the construction and the experimental mock-up of the unipolar generator, in which there are no brushes. This is achieved by the use of two ball bearings of those inserted in each other.

Keywords: unipolar generator, unipolar engine, magnet, brush, ball bearing.

I. Introduction

The unipolar electric motor is a kind of DC electric machines. Contains a conductive disk, a constant magnetic field parallel to the axis of rotation of the disk, the 1st collector on the axis of the disk and the 2nd collector at the edge of the disk [1].
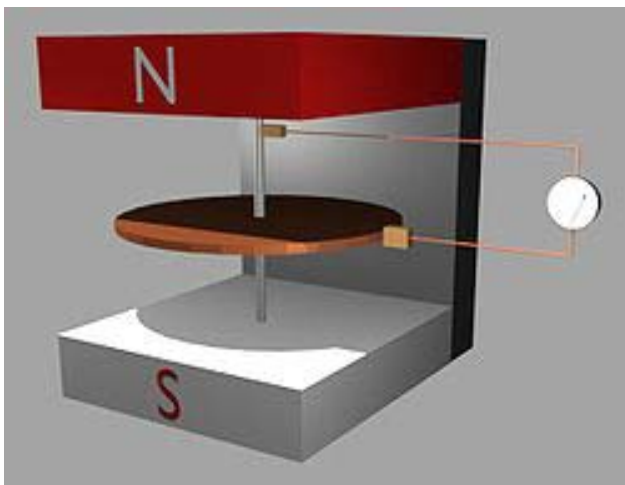
Fig. 1: Conducting disk in the magnetic field

In Fig.1 the operating principle of unipolar engine is shown. If there is a conducting disk, located in magnetic field, then during the supplying stress on the axis of disk and on its edge through the disk flows current, which leads to its rotation. This rotation is caused by the influence of Lorentz force on the moving charges.

The first unipolar engine, the wheel of Barlow, created Peter by Barlow, after describing him in the

Author: e-mail: fedormende@gmail.com

book "study of the magnetic attractions", published in 1824.

Barlow's wheel was two copper gears, which are located on one axis. As a result interaction of current, passing through wheels, with the magnetic field of permanent magnets, wheels they revolve. Barlow explained that with change in contacts or position of magnetic poles the replacement of the direction of rotation of wheels to the opposite occurs. Barlow's engine in the inverted version presents direct-current generator.

It is evident from semy of generator that it contains two brushes, one of which tert against the axis engine, and the second of tert against the external rim disk. The presence of two brushes worsens the parameters of engine, since they rapidly are worn out.

II. Use of Ball Bearings in the Unipolar Generator

In sharikopodshipntke during its rotation galvanic contact between the external and internal rim ensure the moving balls or rollers. This fact can be used for creating unipolar genratora, in which there are no brushes. For this slebuet to use composite bearing, as shown in Fig. 2
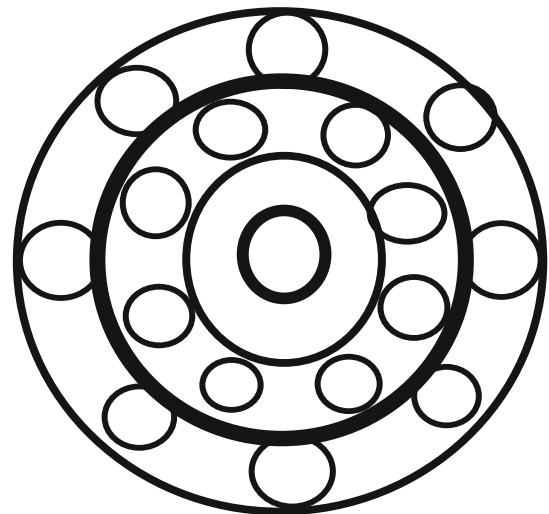
Fig. 2: Composite bearing

Composite bearing consists of two bearings of those inserted in each other, when the diameter of the external rim of inner bearing is equal to the diameter of the internal rim of outboard bearing, and they are combined. In the figure the combined rims they are shown by heavy line and present united cartridge clip.

During the rotation of this cartridge clip the balls will move in one direction, while the external cartridge clip of outboard bearing and the internal cartridge clip of inner bearing they will remain fixed.

In this case moving of ball or the rollers present the moving disk of unipolar generator, if we with one or from its two sides place permanent magnets. In this case the fixed cartridge clip of outboard bearing and the fixed internal cartridge clip of inner bearing are slip rings.

Experimental layoutthe generator examined it is represented in Fig. 3. In it they are used two inserted in each other of bearing, under which they are located six samarium-cobalt magnets, located symmetrically relative to rotational axis.
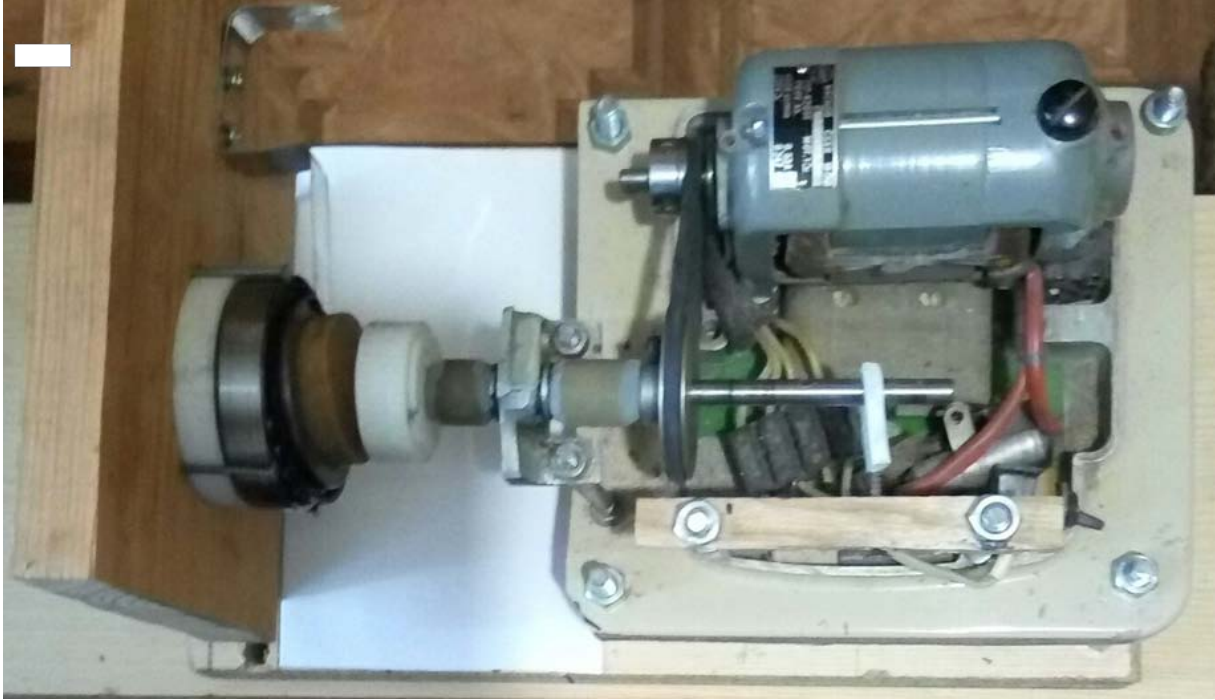
Fig. 3: Experimental layout the generator

III. Conclusion

Application in the unipolar engines of samarium-cobalt magnets opens the new prospects of creating the engines with the large rotational moment, since. such magnets possess the great magnetic field, which cannot they will reach in other magnets. However, the creation of engines are connected with the need of using the brushes, friction against the external rim of the revolving disk and against its axis. Since the speed of rotation of the rim of disk is great, brushes rapidly are worn out, what is an essential drawback in this construction. In the article is represented the construction and the experimental layoutof the unipolar generator, in which there are no brushes. This is achieved by the use of two ball bearings of those inserted in each other.

References Références Referencias

1. Тамм И. Е. Основы теории электричества. Учебное пособие для вузов. – М. Наука. Гл. ред. Физ. Мат. лит. 1960.- 504 с.
.

Global Journals Guidelines Handbook 2021

www.GlobalJournals.org

Memberships
fellows/associates of engineering research council
ferc/aerc memberships

Introduction

FERC/AERC is the most prestigious membership of Global Journals accredited by Open Association of Research Society, U.S.A (OARS). The credentials of Fellow and Associate designations signify that the researcher has gained the knowledge of the fundamental and high-level concepts, and is a subject matter expert, proficient in an expertise course covering the professional code of conduct, and follows recognized standards of practice. The credentials are designated only to the researchers, scientists, and professionals that have been selected by a rigorous process by our Editorial Board and Management Board.

Associates of FERC/AERC are scientists and researchers from around the world are working on projects/researches that have huge potentials. Members support Global Journals' mission to advance technology for humanity and the profession.

FERC

fellow of engineering research council

FELLOW OF ENGINEERING RESEARCH COUNCIL is the most prestigious membership of Global Journals. It is an award and membership granted to individuals that the Open Association of Research Society judges to have made a 'substantial contribution to the improvement of computer science, technology, and electronics engineering.

The primary objective is to recognize the leaders in research and scientific fields of the current era with a global perspective and to create a channel between them and other researchers for better exposure and knowledge sharing. Members are most eminent scientists, engineers, and technologists from all across the world. Fellows are elected for life through a peer review process on the basis of excellence in the respective domain. There is no limit on the number of new nominations made in any year. Each year, the Open Association of Research Society elect up to 12 new Fellow Members.

To the institution
Get letter of appreciation

Global Journals sends a letter of appreciation of author to the Dean or CEO of the University or Company of which author is a part, signed by editor in chief or chief author.

Exclusive Network
Get access to a closed network

A FERC member gets access to a closed network of Tier 1 researchers and scientists with direct communication channel through our website. Fellows can reach out to other members or researchers directly. They should also be open to reaching out by other.

Career	Credibility	Exclusive	Reputation

Certificate
Certificate, LoR and Laser-Momento

Fellows receive a printed copy of a certificate signed by our Chief Author that may be used for academic purposes and a personal recommendation letter to the dean of member's university.

Career	Credibility	Exclusive	Reputation

Designation
Get honored title of membership

Fellows can use the honored title of membership. The "FERC" is an honored title which is accorded to a person's name viz. Dr. John E. Hall, Ph.D., FERC or William Walldroff, M.S., FERC.

Career	Credibility	Exclusive	Reputation

Recognition on the Platform
Better visibility and citation

All the Fellow members of FERC get a badge of "Leading Member of Global Journals" on the Research Community that distinguishes them from others. Additionally, the profile is also partially maintained by our team for better visibility and citation. All fellows get a dedicated page on the website with their biography.

Career	Credibility	Reputation

Future Work

Get discounts on the future publications

Fellows receive discounts on the future publications with Global Journals up to 60%. Through our recommendation programs, members also receive discounts on publications made with OARS affiliated organizations.

Career   Financial

GJ Account

Unlimited forward of Emails

Fellows get secure and fast GJ work emails with unlimited storage of emails that they may use them as their primary email. For example, john [AT] globaljournals [DOT] org.

Career   Credibility   Reputation

Premium Tools

Access to all the premium tools

To take future researches to the zenith, fellows receive access to all the premium tools that Global Journals have to offer along with the partnership with some of the best marketing leading tools out there.

Financial

Conferences & Events

Organize seminar/conference

Fellows are authorized to organize symposium/seminar/conference on behalf of Global Journal Incorporation (USA). They can also participate in the same organized by another institution as representative of Global Journal. In both the cases, it is mandatory for him to discuss with us and obtain our consent. Additionally, they get free research conferences (and others) alerts.

Career   Credibility   Financial

Early Invitations

Early invitations to all the symposiums, seminars, conferences

All fellows receive the early invitations to all the symposiums, seminars, conferences and webinars hosted by Global Journals in their subject.

Exclusive

Publishing Articles & Books

Earn 60% of sales proceeds

Fellows can publish articles (limited) without any fees. Also, they can earn up to 70% of sales proceeds from the sale of reference/review books/literature/publishing of research paper. The FERC member can decide its price and we can help in making the right decision.

| Exclusive | Financial |

Reviewers

Get a remuneration of 15% of author fees

Fellow members are eligible to join as a paid peer reviewer at Global Journals Incorporation (USA) and can get a remuneration of 15% of author fees, taken from the author of a respective paper.

| Financial |

Access to Editorial Board

Become a member of the Editorial Board

Fellows may join as a member of the Editorial Board of Global Journals Incorporation (USA) after successful completion of three years as Fellow and as Peer Reviewer. Additionally, Fellows get a chance to nominate other members for Editorial Board.

| Career | Credibility | Exclusive | Reputation |

And Much More

Get access to scientific museums and observatories across the globe

All members get access to 5 selected scientific museums and observatories across the globe. All researches published with Global Journals will be kept under deep archival facilities across regions for future protections and disaster recovery. They get 10 GB free secure cloud access for storing research files.

AERC

ASSOCIATE OF ENGINEERING RESEARCH COUNCIL

ASSOCIATE OF ENGINEERING RESEARCH COUNCIL is the membership of Global Journals awarded to individuals that the Open Association of Research Society judges to have made a 'substantial contribution to the improvement of computer science, technology, and electronics engineering.

> The primary objective is to recognize the leaders in research and scientific fields of the current era with a global perspective and to create a channel between them and other researchers for better exposure and knowledge sharing. Members are most eminent scientists, engineers, and technologists from all across the world. Associate membership can later be promoted to Fellow Membership. Associates are elected for life through a peer review process on the basis of excellence in the respective domain. There is no limit on the number of new nominations made in any year. Each year, the Open Association of Research Society elect up to 12 new Associate Members.

To the institution

Get letter of appreciation

Global Journals sends a letter of appreciation of author to the Dean or CEO of the University or Company of which author is a part, signed by editor in chief or chief author.

Exclusive Network

Get access to a closed network

A AERC member gets access to a closed network of Tier 1 researchers and scientists with direct communication channel through our website. Associates can reach out to other members or researchers directly. They should also be open to reaching out by other.

| Career | Credibility | Exclusive | Reputation |

Certificate

Certificate, LoR and Laser-Momento

Associates receive a printed copy of a certificate signed by our Chief Author that may be used for academic purposes and a personal recommendation letter to the dean of member's university.

| Career | Credibility | Exclusive | Reputation |

Designation

Get honored title of membership

Associates can use the honored title of membership. The "AERC" is an honored title which is accorded to a person's name viz. Dr. John E. Hall, Ph.D., AERC or William Walldroff, M.S., AERC.

| Career | Credibility | Exclusive | Reputation |

Recognition on the Platform

Better visibility and citation

All the Associate members of AERC get a badge of "Leading Member of Global Journals" on the Research Community that distinguishes them from others. Additionally, the profile is also partially maintained by our team for better visibility and citation. All associates get a dedicated page on the website with their biography.

| Career | Credibility | Reputation |

Future Work

Get discounts on the future publications

Associates receive discounts on the future publications with Global Journals up to 60%. Through our recommendation programs, members also receive discounts on publications made with OARS affiliated organizations.

Career   Financial
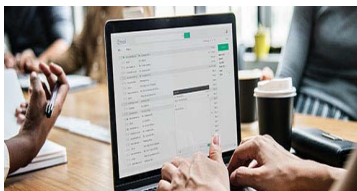
GJ Account

Unlimited forward of Emails

Associates get secure and fast GJ work emails with unlimited storage of emails that they may use them as their primary email. For example, john [AT] globaljournals [DOT] org..

Career   Credibility   Reputation

Premium Tools

Access to all the premium tools

To take future researches to the zenith, associates receive access to all the premium tools that Global Journals have to offer along with the partnership with some of the best marketing leading tools out there.

Financial

Conferences & Events

Organize seminar/conference

Associates are authorized to organize symposium/seminar/conference on behalf of Global Journal Incorporation (USA). They can also participate in the same organized by another institution as representative of Global Journal. In both the cases, it is mandatory for him to discuss with us and obtain our consent. Additionally, they get free research conferences (and others) alerts.

Career   Credibility   Financial

Early Invitations

Early invitations to all the symposiums, seminars, conferences

All associates receive the early invitations to all the symposiums, seminars, conferences and webinars hosted by Global Journals in their subject.

Exclusive

Publishing Articles & Books

Earn 30-40% of sales proceeds

Associates can publish articles (limited) without any fees. Also, they can earn up to 30-40% of sales proceeds from the sale of reference/review books/literature/publishing of research paper.

<div align="right">

Exclusive	Financial

</div>

Reviewers

Get a remuneration of 15% of author fees

Associate members are eligible to join as a paid peer reviewer at Global Journals Incorporation (USA) and can get a remuneration of 15% of author fees, taken from the author of a respective paper.

<div align="right">

Financial

</div>

And Much More

Get access to scientific museums and observatories across the globe

All members get access to 2 selected scientific museums and observatories across the globe. All researches published with Global Journals will be kept under deep archival facilities across regions for future protections and disaster recovery. They get 5 GB free secure cloud access for storing research files.

Associate	Fellow	Research Group	Basic
$4800	$6800	$12500.00	APC
lifetime designation	lifetime designation	organizational	per article
Certificate, LoR and Momento	**Certificate,** LoR and Momento	**Certificates,** LoRs and Momentos	GJ Community Access
2 discounted publishing/year	**Unlimited** discounted publishing/year	**Unlimited** free publishing/year	
Gradation of Research	**Gradation** of Research	**Gradation** of Research	
10 research contacts/day	**Unlimited** research contacts/day	**Unlimited** research contacts/day	
1 GB Cloud Storage	**5 GB** Cloud Storage	**Unlimited** Cloud Storage	
GJ Community Access	**Online Presense** Assistance	**Online Presense** Assistance	
	GJ Community Access	GJ Community Access	

We accept the manuscript submissions in any standard (generic) format.

We typeset manuscripts using advanced typesetting tools like Adobe In Design, CorelDraw, TeXnicCenter, and TeXStudio. We usually recommend authors submit their research using any standard format they are comfortable with, and let Global Journals do the rest.

Alternatively, you can download our basic template from https://globaljournals.org/Template.zip

Authors should submit their complete paper/article, including text illustrations, graphics, conclusions, artwork, and tables. Authors who are not able to submit manuscript using the form above can email the manuscript department at submit@globaljournals.org or get in touch with chiefeditor@globaljournals.org if they wish to send the abstract before submission.

Before and during Submission

Authors must ensure the information provided during the submission of a paper is authentic. Please go through the following checklist before submitting:

1. Authors must go through the complete author guideline and understand and *agree to Global Journals' ethics and code of conduct,* along with author responsibilities.
2. Authors must accept the privacy policy, terms, and conditions of Global Journals.
3. Ensure corresponding author's email address and postal address are accurate and reachable.
4. Manuscript to be submitted must include keywords, an abstract, a paper title, co-author(s') names and details (email address, name, phone number, and institution), figures and illustrations in vector format including appropriate captions, tables, including titles and footnotes, a conclusion, results, acknowledgments and references.
5. Authors should submit paper in a ZIP archive if any supplementary files are required along with the paper.
6. Proper permissions must be acquired for the use of any copyrighted material.
7. Manuscript submitted *must not have been submitted or published elsewhere* and all authors must be aware of the submission.

Declaration of Conflicts of Interest

It is required for authors to declare all financial, institutional, and personal relationships with other individuals and organizations that could influence (bias) their research.

Policy on Plagiarism

Plagiarism is not acceptable in Global Journals submissions at all.

Plagiarized content will not be considered for publication. We reserve the right to inform authors' institutions about plagiarism detected either before or after publication. If plagiarism is identified, we will follow COPE guidelines:

Authors are solely responsible for all the plagiarism that is found. The author must not fabricate, falsify or plagiarize existing research data. The following, if copied, will be considered plagiarism:

- Words (language)
- Ideas
- Findings
- Writings
- Diagrams
- Graphs
- Illustrations
- Lectures

- Printed material
- Graphic representations
- Computer programs
- Electronic material
- Any other original work

AUTHORSHIP POLICIES

Global Journals follows the definition of authorship set up by the Open Association of Research Society, USA. According to its guidelines, authorship criteria must be based on:

1. Substantial contributions to the conception and acquisition of data, analysis, and interpretation of findings.
2. Drafting the paper and revising it critically regarding important academic content.
3. Final approval of the version of the paper to be published.

Changes in Authorship

The corresponding author should mention the name and complete details of all co-authors during submission and in manuscript. We support addition, rearrangement, manipulation, and deletions in authors list till the early view publication of the journal. We expect that corresponding author will notify all co-authors of submission. We follow COPE guidelines for changes in authorship.

Copyright

During submission of the manuscript, the author is confirming an exclusive license agreement with Global Journals which gives Global Journals the authority to reproduce, reuse, and republish authors' research. We also believe in flexible copyright terms where copyright may remain with authors/employers/institutions as well. Contact your editor after acceptance to choose your copyright policy. You may follow this form for copyright transfers.

Appealing Decisions

Unless specified in the notification, the Editorial Board's decision on publication of the paper is final and cannot be appealed before making the major change in the manuscript.

Acknowledgments

Contributors to the research other than authors credited should be mentioned in Acknowledgments. The source of funding for the research can be included. Suppliers of resources may be mentioned along with their addresses.

Declaration of funding sources

Global Journals is in partnership with various universities, laboratories, and other institutions worldwide in the research domain. Authors are requested to disclose their source of funding during every stage of their research, such as making analysis, performing laboratory operations, computing data, and using institutional resources, from writing an article to its submission. This will also help authors to get reimbursements by requesting an open access publication letter from Global Journals and submitting to the respective funding source.

PREPARING YOUR MANUSCRIPT

Authors can submit papers and articles in an acceptable file format: MS Word (doc, docx), LaTeX (.tex, .zip or .rar including all of your files), Adobe PDF (.pdf), rich text format (.rtf), simple text document (.txt), Open Document Text (.odt), and Apple Pages (.pages). Our professional layout editors will format the entire paper according to our official guidelines. This is one of the highlights of publishing with Global Journals—authors should not be concerned about the formatting of their paper. Global Journals accepts articles and manuscripts in every major language, be it Spanish, Chinese, Japanese, Portuguese, Russian, French, German, Dutch, Italian, Greek, or any other national language, but the title, subtitle, and abstract should be in English. This will facilitate indexing and the pre-peer review process.

The following is the official style and template developed for publication of a research paper. Authors are not required to follow this style during the submission of the paper. It is just for reference purposes.

Manuscript Style Instruction (Optional)

- Microsoft Word Document Setting Instructions.
- Font type of all text should be Swis721 Lt BT.
- Page size: 8.27" x 11'", left margin: 0.65, right margin: 0.65, bottom margin: 0.75.
- Paper title should be in one column of font size 24.
- Author name in font size of 11 in one column.
- Abstract: font size 9 with the word "Abstract" in bold italics.
- Main text: font size 10 with two justified columns.
- Two columns with equal column width of 3.38 and spacing of 0.2.
- First character must be three lines drop-capped.
- The paragraph before spacing of 1 pt and after of 0 pt.
- Line spacing of 1 pt.
- Large images must be in one column.
- The names of first main headings (Heading 1) must be in Roman font, capital letters, and font size of 10.
- The names of second main headings (Heading 2) must not include numbers and must be in italics with a font size of 10.

Structure and Format of Manuscript

The recommended size of an original research paper is under 15,000 words and review papers under 7,000 words. Research articles should be less than 10,000 words. Research papers are usually longer than review papers. Review papers are reports of significant research (typically less than 7,000 words, including tables, figures, and references)

A research paper must include:

a) A title which should be relevant to the theme of the paper.
b) A summary, known as an abstract (less than 150 words), containing the major results and conclusions.
c) Up to 10 keywords that precisely identify the paper's subject, purpose, and focus.
d) An introduction, giving fundamental background objectives.
e) Resources and techniques with sufficient complete experimental details (wherever possible by reference) to permit repetition, sources of information must be given, and numerical methods must be specified by reference.
f) Results which should be presented concisely by well-designed tables and figures.
g) Suitable statistical data should also be given.
h) All data must have been gathered with attention to numerical detail in the planning stage.

Design has been recognized to be essential to experiments for a considerable time, and the editor has decided that any paper that appears not to have adequate numerical treatments of the data will be returned unrefereed.

i) Discussion should cover implications and consequences and not just recapitulate the results; conclusions should also be summarized.
j) There should be brief acknowledgments.
k) There ought to be references in the conventional format. Global Journals recommends APA format.

Authors should carefully consider the preparation of papers to ensure that they communicate effectively. Papers are much more likely to be accepted if they are carefully designed and laid out, contain few or no errors, are summarizing, and follow instructions. They will also be published with much fewer delays than those that require much technical and editorial correction.

The Editorial Board reserves the right to make literary corrections and suggestions to improve brevity.

FORMAT STRUCTURE

It is necessary that authors take care in submitting a manuscript that is written in simple language and adheres to published guidelines.

All manuscripts submitted to Global Journals should include:

Title

The title page must carry an informative title that reflects the content, a running title (less than 45 characters together with spaces), names of the authors and co-authors, and the place(s) where the work was carried out.

Author details

The full postal address of any related author(s) must be specified.

Abstract

The abstract is the foundation of the research paper. It should be clear and concise and must contain the objective of the paper and inferences drawn. It is advised to not include big mathematical equations or complicated jargon.

Many researchers searching for information online will use search engines such as Google, Yahoo or others. By optimizing your paper for search engines, you will amplify the chance of someone finding it. In turn, this will make it more likely to be viewed and cited in further works. Global Journals has compiled these guidelines to facilitate you to maximize the web-friendliness of the most public part of your paper.

Keywords

A major lynchpin of research work for the writing of research papers is the keyword search, which one will employ to find both library and internet resources. Up to eleven keywords or very brief phrases have to be given to help data retrieval, mining, and indexing.

One must be persistent and creative in using keywords. An effective keyword search requires a strategy: planning of a list of possible keywords and phrases to try.

Choice of the main keywords is the first tool of writing a research paper. Research paper writing is an art. Keyword search should be as strategic as possible.

One should start brainstorming lists of potential keywords before even beginning searching. Think about the most important concepts related to research work. Ask, "What words would a source have to include to be truly valuable in a research paper?" Then consider synonyms for the important words.

It may take the discovery of only one important paper to steer in the right keyword direction because, in most databases, the keywords under which a research paper is abstracted are listed with the paper.

Numerical Methods

Numerical methods used should be transparent and, where appropriate, supported by references.

Abbreviations

Authors must list all the abbreviations used in the paper at the end of the paper or in a separate table before using them.

Formulas and equations

Authors are advised to submit any mathematical equation using either MathJax, KaTeX, or LaTeX, or in a very high-quality image.

Tables, Figures, and Figure Legends

Tables: Tables should be cautiously designed, uncrowned, and include only essential data. Each must have an Arabic number, e.g., Table 4, a self-explanatory caption, and be on a separate sheet. Authors must submit tables in an editable format and not as images. References to these tables (if any) must be mentioned accurately.

Figures

Figures are supposed to be submitted as separate files. Always include a citation in the text for each figure using Arabic numbers, e.g., Fig. 4. Artwork must be submitted online in vector electronic form or by emailing it.

PREPARATION OF ELETRONIC FIGURES FOR PUBLICATION

Although low-quality images are sufficient for review purposes, print publication requires high-quality images to prevent the final product being blurred or fuzzy. Submit (possibly by e-mail) EPS (line art) or TIFF (halftone/ photographs) files only. MS PowerPoint and Word Graphics are unsuitable for printed pictures. Avoid using pixel-oriented software. Scans (TIFF only) should have a resolution of at least 350 dpi (halftone) or 700 to 1100 dpi (line drawings). Please give the data for figures in black and white or submit a Color Work Agreement form. EPS files must be saved with fonts embedded (and with a TIFF preview, if possible).

For scanned images, the scanning resolution at final image size ought to be as follows to ensure good reproduction: line art: >650 dpi; halftones (including gel photographs): >350 dpi; figures containing both halftone and line images: >650 dpi.

Color charges: Authors are advised to pay the full cost for the reproduction of their color artwork. Hence, please note that if there is color artwork in your manuscript when it is accepted for publication, we would require you to complete and return a Color Work Agreement form before your paper can be published. Also, you can email your editor to remove the color fee after acceptance of the paper.

TIPS FOR WRITING A GOOD QUALITY ENGINEERING RESEARCH PAPER

Techniques for writing a good quality engineering research paper:

1. Choosing the topic: In most cases, the topic is selected by the interests of the author, but it can also be suggested by the guides. You can have several topics, and then judge which you are most comfortable with. This may be done by asking several questions of yourself, like "Will I be able to carry out a search in this area? Will I find all necessary resources to accomplish the search? Will I be able to find all information in this field area?" If the answer to this type of question is "yes," then you ought to choose that topic. In most cases, you may have to conduct surveys and visit several places. Also, you might have to do a lot of work to find all the rises and falls of the various data on that subject. Sometimes, detailed information plays a vital role, instead of short information. Evaluators are human: The first thing to remember is that evaluators are also human beings. They are not only meant for rejecting a paper. They are here to evaluate your paper. So present your best aspect.

2. Think like evaluators: If you are in confusion or getting demotivated because your paper may not be accepted by the evaluators, then think, and try to evaluate your paper like an evaluator. Try to understand what an evaluator wants in your research paper, and you will automatically have your answer. Make blueprints of paper: The outline is the plan or framework that will help you to arrange your thoughts. It will make your paper logical. But remember that all points of your outline must be related to the topic you have chosen.

3. Ask your guides: If you are having any difficulty with your research, then do not hesitate to share your difficulty with your guide (if you have one). They will surely help you out and resolve your doubts. If you can't clarify what exactly you require for your work, then ask your supervisor to help you with an alternative. He or she might also provide you with a list of essential readings.

4. Use of computer is recommended: As you are doing research in the field of research engineering then this point is quite obvious. Use right software: Always use good quality software packages. If you are not capable of judging good software, then you can lose the quality of your paper unknowingly. There are various programs available to help you which you can get through the internet.

5. Use the internet for help: An excellent start for your paper is using Google. It is a wondrous search engine, where you can have your doubts resolved. You may also read some answers for the frequent question of how to write your research paper or find a model research paper. You can download books from the internet. If you have all the required books, place importance on reading, selecting, and analyzing the specified information. Then sketch out your research paper. Use big pictures: You may use encyclopedias like Wikipedia to get pictures with the best resolution. At Global Journals, you should strictly follow here.

6. Bookmarks are useful: When you read any book or magazine, you generally use bookmarks, right? It is a good habit which helps to not lose your continuity. You should always use bookmarks while searching on the internet also, which will make your search easier.

7. Revise what you wrote: When you write anything, always read it, summarize it, and then finalize it.

8. Make every effort: Make every effort to mention what you are going to write in your paper. That means always have a good start. Try to mention everything in the introduction—what is the need for a particular research paper. Polish your work with good writing skills and always give an evaluator what he wants. Make backups: When you are going to do any important thing like making a research paper, you should always have backup copies of it either on your computer or on paper. This protects you from losing any portion of your important data.

9. Produce good diagrams of your own: Always try to include good charts or diagrams in your paper to improve quality. Using several unnecessary diagrams will degrade the quality of your paper by creating a hodgepodge. So always try to include diagrams which were made by you to improve the readability of your paper. Use of direct quotes: When you do research relevant to literature, history, or current affairs, then use of quotes becomes essential, but if the study is relevant to science, use of quotes is not preferable.

10. Use proper verb tense: Use proper verb tenses in your paper. Use past tense to present those events that have happened. Use present tense to indicate events that are going on. Use future tense to indicate events that will happen in the future. Use of wrong tenses will confuse the evaluator. Avoid sentences that are incomplete.

11. Pick a good study spot: Always try to pick a spot for your research which is quiet. Not every spot is good for studying.

12. Know what you know: Always try to know what you know by making objectives, otherwise you will be confused and unable to achieve your target.

13. Use good grammar: Always use good grammar and words that will have a positive impact on the evaluator; use of good vocabulary does not mean using tough words which the evaluator has to find in a dictionary. Do not fragment sentences. Eliminate one-word sentences. Do not ever use a big word when a smaller one would suffice.

Verbs have to be in agreement with their subjects. In a research paper, do not start sentences with conjunctions or finish them with prepositions. When writing formally, it is advisable to never split an infinitive because someone will (wrongly) complain. Avoid clichés like a disease. Always shun irritating alliteration. Use language which is simple and straightforward. Put together a neat summary.

14. Arrangement of information: Each section of the main body should start with an opening sentence, and there should be a changeover at the end of the section. Give only valid and powerful arguments for your topic. You may also maintain your arguments with records.

15. Never start at the last minute: Always allow enough time for research work. Leaving everything to the last minute will degrade your paper and spoil your work.

16. Multitasking in research is not good: Doing several things at the same time is a bad habit in the case of research activity. Research is an area where everything has a particular time slot. Divide your research work into parts, and do a particular part in a particular time slot.

17. Never copy others' work: Never copy others' work and give it your name because if the evaluator has seen it anywhere, you will be in trouble. Take proper rest and food: No matter how many hours you spend on your research activity, if you are not taking care of your health, then all your efforts will have been in vain. For quality research, take proper rest and food.

18. Go to seminars: Attend seminars if the topic is relevant to your research area. Utilize all your resources.

19. Refresh your mind after intervals: Try to give your mind a rest by listening to soft music or sleeping in intervals. This will also improve your memory. Acquire colleagues: Always try to acquire colleagues. No matter how sharp you are, if you acquire colleagues, they can give you ideas which will be helpful to your research.

20. Think technically: Always think technically. If anything happens, search for its reasons, benefits, and demerits. Think and then print: When you go to print your paper, check that tables are not split, headings are not detached from their descriptions, and page sequence is maintained.

21. Adding unnecessary information: Do not add unnecessary information like "I have used MS Excel to draw graphs." Irrelevant and inappropriate material is superfluous. Foreign terminology and phrases are not apropos. One should never take a broad view. Analogy is like feathers on a snake. Use words properly, regardless of how others use them. Remove quotations. Puns are for kids, not grunt readers. Never oversimplify: When adding material to your research paper, never go for oversimplification; this will definitely irritate the evaluator. Be specific. Never use rhythmic redundancies. Contractions shouldn't be used in a research paper. Comparisons are as terrible as clichés. Give up ampersands, abbreviations, and so on. Remove commas that are not necessary. Parenthetical words should be between brackets or commas. Understatement is always the best way to put forward earth-shaking thoughts. Give a detailed literary review.

22. Report concluded results: Use concluded results. From raw data, filter the results, and then conclude your studies based on measurements and observations taken. An appropriate number of decimal places should be used. Parenthetical remarks are prohibited here. Proofread carefully at the final stage. At the end, give an outline to your arguments. Spot perspectives of further study of the subject. Justify your conclusion at the bottom sufficiently, which will probably include examples.

23. Upon conclusion: Once you have concluded your research, the next most important step is to present your findings. Presentation is extremely important as it is the definite medium though which your research is going to be in print for the rest of the crowd. Care should be taken to categorize your thoughts well and present them in a logical and neat manner. A good quality research paper format is essential because it serves to highlight your research paper and bring to light all necessary aspects of your research.

INFORMAL GUIDELINES OF RESEARCH PAPER WRITING

Key points to remember:

- Submit all work in its final form.
- Write your paper in the form which is presented in the guidelines using the template.
- Please note the criteria peer reviewers will use for grading the final paper.

Final points:

One purpose of organizing a research paper is to let people interpret your efforts selectively. The journal requires the following sections, submitted in the order listed, with each section starting on a new page:

The introduction: This will be compiled from reference matter and reflect the design processes or outline of basis that directed you to make a study. As you carry out the process of study, the method and process section will be constructed like that. The results segment will show related statistics in nearly sequential order and direct reviewers to similar intellectual paths throughout the data that you gathered to carry out your study.

The discussion section:

This will provide understanding of the data and projections as to the implications of the results. The use of good quality references throughout the paper will give the effort trustworthiness by representing an alertness to prior workings.

Writing a research paper is not an easy job, no matter how trouble-free the actual research or concept. Practice, excellent preparation, and controlled record-keeping are the only means to make straightforward progression.

General style:

Specific editorial column necessities for compliance of a manuscript will always take over from directions in these general guidelines.

To make a paper clear: Adhere to recommended page limits.

Mistakes to avoid:

- Insertion of a title at the foot of a page with subsequent text on the next page.
- Separating a table, chart, or figure—confine each to a single page.
- Submitting a manuscript with pages out of sequence.
- In every section of your document, use standard writing style, including articles ("a" and "the").
- Keep paying attention to the topic of the paper.

- Use paragraphs to split each significant point (excluding the abstract).
- Align the primary line of each section.
- Present your points in sound order.
- Use present tense to report well-accepted matters.
- Use past tense to describe specific results.
- Do not use familiar wording; don't address the reviewer directly. Don't use slang or superlatives.
- Avoid use of extra pictures—include only those figures essential to presenting results.

Title page:

Choose a revealing title. It should be short and include the name(s) and address(es) of all authors. It should not have acronyms or abbreviations or exceed two printed lines.

Abstract: This summary should be two hundred words or less. It should clearly and briefly explain the key findings reported in the manuscript and must have precise statistics. It should not have acronyms or abbreviations. It should be logical in itself. Do not cite references at this point.

An abstract is a brief, distinct paragraph summary of finished work or work in development. In a minute or less, a reviewer can be taught the foundation behind the study, common approaches to the problem, relevant results, and significant conclusions or new questions.

Write your summary when your paper is completed because how can you write the summary of anything which is not yet written? Wealth of terminology is very essential in abstract. Use comprehensive sentences, and do not sacrifice readability for brevity; you can maintain it succinctly by phrasing sentences so that they provide more than a lone rationale. The author can at this moment go straight to shortening the outcome. Sum up the study with the subsequent elements in any summary. Try to limit the initial two items to no more than one line each.

Reason for writing the article—theory, overall issue, purpose.

- Fundamental goal.
- To-the-point depiction of the research.
- Consequences, including definite statistics—if the consequences are quantitative in nature, account for this; results of any numerical analysis should be reported. Significant conclusions or questions that emerge from the research.

Approach:

o Single section and succinct.
o An outline of the job done is always written in past tense.
o Concentrate on shortening results—limit background information to a verdict or two.
o Exact spelling, clarity of sentences and phrases, and appropriate reporting of quantities (proper units, important statistics) are just as significant in an abstract as they are anywhere else.

Introduction:

The introduction should "introduce" the manuscript. The reviewer should be presented with sufficient background information to be capable of comprehending and calculating the purpose of your study without having to refer to other works. The basis for the study should be offered. Give the most important references, but avoid making a comprehensive appraisal of the topic. Describe the problem visibly. If the problem is not acknowledged in a logical, reasonable way, the reviewer will give no attention to your results. Speak in common terms about techniques used to explain the problem, if needed, but do not present any particulars about the protocols here.

The following approach can create a valuable beginning:

o Explain the value (significance) of the study.
o Defend the model—why did you employ this particular system or method? What is its compensation? Remark upon its appropriateness from an abstract point of view as well as pointing out sensible reasons for using it.
o Present a justification. State your particular theory(-ies) or aim(s), and describe the logic that led you to choose them.
o Briefly explain the study's tentative purpose and how it meets the declared objectives.

Approach:

Use past tense except for when referring to recognized facts. After all, the manuscript will be submitted after the entire job is done. Sort out your thoughts; manufacture one key point for every section. If you make the four points listed above, you will need at least four paragraphs. Present surrounding information only when it is necessary to support a situation. The reviewer does not desire to read everything you know about a topic. Shape the theory specifically—do not take a broad view.

As always, give awareness to spelling, simplicity, and correctness of sentences and phrases.

Procedures (methods and materials):

This part is supposed to be the easiest to carve if you have good skills. A soundly written procedures segment allows a capable scientist to replicate your results. Present precise information about your supplies. The suppliers and clarity of reagents can be helpful bits of information. Present methods in sequential order, but linked methodologies can be grouped as a segment. Be concise when relating the protocols. Attempt to give the least amount of information that would permit another capable scientist to replicate your outcome, but be cautious that vital information is integrated. The use of subheadings is suggested and ought to be synchronized with the results section.

When a technique is used that has been well-described in another section, mention the specific item describing the way, but draw the basic principle while stating the situation. The purpose is to show all particular resources and broad procedures so that another person may use some or all of the methods in one more study or referee the scientific value of your work. It is not to be a step-by-step report of the whole thing you did, nor is a methods section a set of orders.

Materials:

Materials may be reported in part of a section or else they may be recognized along with your measures.

Methods:

- Report the method and not the particulars of each process that engaged the same methodology.
- Describe the method entirely.
- To be succinct, present methods under headings dedicated to specific dealings or groups of measures.
- Simplify—detail how procedures were completed, not how they were performed on a particular day.
- If well-known procedures were used, account for the procedure by name, possibly with a reference, and that's all.

Approach:

It is embarrassing to use vigorous voice when documenting methods without using first person, which would focus the reviewer's interest on the researcher rather than the job. As a result, when writing up the methods, most authors use third person passive voice.

Use standard style in this and every other part of the paper—avoid familiar lists, and use full sentences.

What to keep away from:

- Resources and methods are not a set of information.
- Skip all descriptive information and surroundings—save it for the argument.
- Leave out information that is immaterial to a third party.

Results:

The principle of a results segment is to present and demonstrate your conclusion. Create this part as entirely objective details of the outcome, and save all understanding for the discussion.

The page length of this segment is set by the sum and types of data to be reported. Use statistics and tables, if suitable, to present consequences most efficiently.

You must clearly differentiate material which would usually be incorporated in a study editorial from any unprocessed data or additional appendix matter that would not be available. In fact, such matters should not be submitted at all except if requested by the instructor.

Content:

- Sum up your conclusions in text and demonstrate them, if suitable, with figures and tables.
- In the manuscript, explain each of your consequences, and point the reader to remarks that are most appropriate.
- Present a background, such as by describing the question that was addressed by creation of an exacting study.
- Explain results of control experiments and give remarks that are not accessible in a prescribed figure or table, if appropriate.
- Examine your data, then prepare the analyzed (transformed) data in the form of a figure (graph), table, or manuscript.

What to stay away from:

- Do not discuss or infer your outcome, report surrounding information, or try to explain anything.
- Do not include raw data or intermediate calculations in a research manuscript.
- Do not present similar data more than once.
- A manuscript should complement any figures or tables, not duplicate information.
- Never confuse figures with tables—there is a difference.

Approach:

As always, use past tense when you submit your results, and put the whole thing in a reasonable order.

Put figures and tables, appropriately numbered, in order at the end of the report.

If you desire, you may place your figures and tables properly within the text of your results section.

Figures and tables:

If you put figures and tables at the end of some details, make certain that they are visibly distinguished from any attached appendix materials, such as raw facts. Whatever the position, each table must be titled, numbered one after the other, and include a heading. All figures and tables must be divided from the text.

Discussion:

The discussion is expected to be the trickiest segment to write. A lot of papers submitted to the journal are discarded based on problems with the discussion. There is no rule for how long an argument should be.

Position your understanding of the outcome visibly to lead the reviewer through your conclusions, and then finish the paper with a summing up of the implications of the study. The purpose here is to offer an understanding of your results and support all of your conclusions, using facts from your research and generally accepted information, if suitable. The implication of results should be fully described.

Infer your data in the conversation in suitable depth. This means that when you clarify an observable fact, you must explain mechanisms that may account for the observation. If your results vary from your prospect, make clear why that may have happened. If your results agree, then explain the theory that the proof supported. It is never suitable to just state that the data approved the prospect, and let it drop at that. Make a decision as to whether each premise is supported or discarded or if you cannot make a conclusion with assurance. Do not just dismiss a study or part of a study as "uncertain."

Research papers are not acknowledged if the work is imperfect. Draw what conclusions you can based upon the results that you have, and take care of the study as a finished work.

- You may propose future guidelines, such as how an experiment might be personalized to accomplish a new idea.
- Give details of all of your remarks as much as possible, focusing on mechanisms.
- Make a decision as to whether the tentative design sufficiently addressed the theory and whether or not it was correctly restricted. Try to present substitute explanations if they are sensible alternatives.
- One piece of research will not counter an overall question, so maintain the large picture in mind. Where do you go next? The best studies unlock new avenues of study. What questions remain?
- Recommendations for detailed papers will offer supplementary suggestions.

Approach:

When you refer to information, differentiate data generated by your own studies from other available information. Present work done by specific persons (including you) in past tense.

Describe generally acknowledged facts and main beliefs in present tense.

The Administration Rules

Administration Rules to Be Strictly Followed before Submitting Your Research Paper to Global Journals Inc.

Please read the following rules and regulations carefully before submitting your research paper to Global Journals Inc. to avoid rejection.

Segment draft and final research paper: You have to strictly follow the template of a research paper, failing which your paper may get rejected. You are expected to write each part of the paper wholly on your own. The peer reviewers need to identify your own perspective of the concepts in your own terms. Please do not extract straight from any other source, and do not rephrase someone else's analysis. Do not allow anyone else to proofread your manuscript.

Written material: You may discuss this with your guides and key sources. Do not copy anyone else's paper, even if this is only imitation, otherwise it will be rejected on the grounds of plagiarism, which is illegal. Various methods to avoid plagiarism are strictly applied by us to every paper, and, if found guilty, you may be blacklisted, which could affect your career adversely. To guard yourself and others from possible illegal use, please do not permit anyone to use or even read your paper and file.

Criterion for Grading a Research Paper (Compilation)
by Global Journals

Please note that following table is only a Grading of "Paper Compilation" and not on "Performed/Stated Research" whose grading solely depends on Individual Assigned Peer Reviewer and Editorial Board Member. These can be available only on request and after decision of Paper. This report will be the property of Global Journals.

Topics	Grades		
	A-B	**C-D**	**E-F**
Abstract	Clear and concise with appropriate content, Correct format. 200 words or below	Unclear summary and no specific data, Incorrect form Above 200 words	No specific data with ambiguous information Above 250 words
Introduction	Containing all background details with clear goal and appropriate details, flow specification, no grammar and spelling mistake, well organized sentence and paragraph, reference cited	Unclear and confusing data, appropriate format, grammar and spelling errors with unorganized matter	Out of place depth and content, hazy format
Methods and Procedures	Clear and to the point with well arranged paragraph, precision and accuracy of facts and figures, well organized subheads	Difficult to comprehend with embarrassed text, too much explanation but completed	Incorrect and unorganized structure with hazy meaning
Result	Well organized, Clear and specific, Correct units with precision, correct data, well structuring of paragraph, no grammar and spelling mistake	Complete and embarrassed text, difficult to comprehend	Irregular format with wrong facts and figures
Discussion	Well organized, meaningful specification, sound conclusion, logical and concise explanation, highly structured paragraph reference cited	Wordy, unclear conclusion, spurious	Conclusion is not cited, unorganized, difficult to comprehend
References	Complete and correct format, well organized	Beside the point, Incomplete	Wrong format and structuring

INDEX

save our planet

Global Journal of Researches in Engineering

9   2

70116 58698   61427>